11-15-2019

Hierarchical Conjugated Polymer Systems Prepared by Controlled Chain-Growth Polymerization

Chunwa Peter Kei
Louisiana State University and Agricultural and Mechanical College

HIERARCHICAL CONJUGATED POLYMER SYSTEMS PREPARED BY CONTROLLED CHAIN-GROWTH POLYMERIZATION

A Dissertation

Submitted to the Graduate Faculty of the
Louisiana State University and
Agricultural and Mechanical College
in partial fulfillment of the
requirements for the degree of
Doctor of Philosophy

in

The Department of Chemistry

by
Chunwa Peter Kei
B.S., Bridgewater State University, 2014
December 2019

ACKNOWLEDGEMENTS

I would like to thank Prof. Evgueni Nesterov for his advice, mentorship and support throughout my Ph.D. studies. Prof. Nesterov has always guided his students towards the utmost excellence, including me. I am sincerely grateful to have learned great science, virtues, and patience from him. He always encouraged me to do further experiments and to explore original ideas. Eventually, this led me to the exciting discoveries that many scientists seek after. I am very grateful to have these experiences. I would also like to thank my committee Prof. Justin Ragains, Prof. Donghui Zhang and Prof. Sibel Bargu Ates for their time and willingness to support my studies. I especially enjoyed the engaging chemistry discussion we had in classes and seminars; and appreciate your time investment into my various academic endeavors.

To my mother Lily who showed me unconditional love and helped to raise me to this point of achievement in my life, thank you. And to George, my friend, I appreciate your support as well. Thank you, Xuan Nhan, my best friend, for your unwavering support and encouragement.

To my present and past group members Sang Gil Youm, Carlos Chavez, Sourav Chatterjee, Chien-Hung Chiang, Chun-Han Wang, Kefei Wang, Gerard Ducharme, Fatemeh Khamespanah, Andy Balgeman, Maxsim Anokhin, Joseph Mai, and Blake Mirman: Thank you for making our laboratory an enjoyable place to work every day.

I would also like to thank Joshua Lutz, Judith De Mel, Ashley Fulton, Nichole Kaufman, Christopher Sumner, Tia Vargas, Prof. Semin Lee and Prof. Isiah Warner for helping create the LSU GSSPC program. I can think of many endearing and memorable moments.

I would also like to acknowledge Louisiana State University for the helpful financial support through the Economic Development Assistantship as well as the U.S. Department of Energy for their generous support through Office of Science Graduate Student Research Program (SCGSR).

TABLE OF CONTENTS

LIST OF TABLES

LIST OF FIGURES

ABSTRACT

π-Conjugated polymer materials may have a significant economic impact on society by providing means for designing affordable, flexible, and portable organic electronic devices. Their successful commercialization will depend on major scientific advancements, which will challenge human society to seek out ever more detailed and fundamental processes to command. Controlled polymerization affords such a power; allowing for the design of meticulous and precisely defined systems granting detailed insight into structure-property relationships in the polymer materials and bettering understanding of novel physical phenomena.

This dissertation primarily focuses on development and preparation of well-defined hierarchically organized macromolecular systems. The novel chain-growth polymerization methodologies described herein depended on gaining new fundamental insights into transition metal catalyzed controlled polymerization reactions, including many intriguing aspects of their catalytic and self-assembly processes.

For example, a general approach towards deeper mechanistic understanding and improving the controlled polymerization reactions for preparing conjugated polymer is presented; subsequent applying this knowledge resulted in an approach for a general synthesis of various classes of π-conjugated polymers precisely incorporating specific structural units. Preparation of such materials led to the observation of novel and unusual photophysical phenomena that exclusively appear in these unique polymer systems.

In addition, the photophysical properties and energy transfer processes occurring in nano- and mesoscale conjugated polymer donor-acceptor materials were found to depend on the non-equilibrium conformations of supramolecular assemblies forming in kinetically controlled catalyst-transfer polymerization.

CHAPTER 1. CONTROLLED POLYMERIZATION FOR PREPARING π-CONJUGATED MATERIALS: AN INTRODUCTION

1.1. Synthesis of Conjugated Polymers by Controlled Polymerization

Conjugated polymers are an important subject of studies in macromolecular chemistry. Generally, they are characterized by a polymer backbone of sp^2-hybridized carbon (or hetero) atoms that each contain electrons in the π orbital.[1] The electrons are bound to a delocalized π-orbital system which allows them to move along the polymer chain.[2-4] In 1977, Heeger, MacDiarmid and Shirakawa demonstrated electrical conductivity in polyacetylene thin films.[5] It was a revolutionary discovery because it demonstrated unprecedented transport of energy in an organic polymer, which is a highly tunable medium.[6-7] Up until that time, the idea of conductive polymers had not existed, and this event rapidly evolved into rich field of conjugated polymer research today.[8-10]

Conjugated polymer research contains two dominating areas.[11] The first is synthetic methodology in which development of controlled polymerization techniques and the expansion of the monomer scope is a primary goal.[12-14] The second is applied functional systems, where the chemical,[15-17] electrical,[18,19] magnetic[20,21] and optical properties[22,23] of conjugated polymers are engineered into nanostructured materials with a specific purpose.[24-32] These areas are markedly separated by how their chemical model systems are prepared, either by chain-growth polymerization in the synthetic methodology community,[11,12,33-36] or step-growth polymerization used for preparing functional conjugated polymer materials.[37-41]

Controlled polymerization is a special type of chain-growth polymerization. It is notably advantageous because it produces polymers with a pre-determined and readily controlled molecular weight and allows for achieving narrow polydispersity.[42] Some controlled

polymerization reactions lack irreversible termination pathways and the polymer chain remains catalytically active after the monomers have been consumed. This property gives powerful control over the polymer chain end functionality.[43] Controlled polymerization grants access to sequence defined polymers such as block co-polymers[44], graft co-polymers[45-47], dendrimers[48] and hierarchical star polymers (Figure 1.1).[49,50]

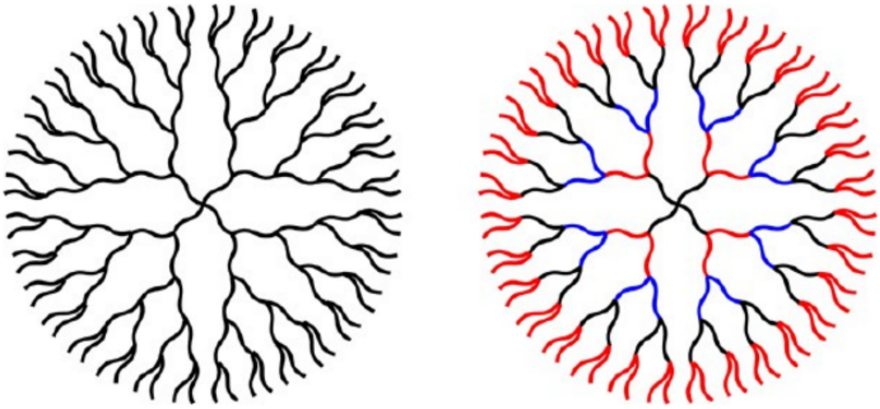

Figure 1.1. Simplified representation of a 5th generation dendrimer-like star polymer prepared by anionic living polymerization (left) and its block-terpolymer structure (right). Reproduced with permission from Ref. 43. Copyright © 2014 American Chemical Society.

For conjugated polymers, controlled polymerization can be achieved with the reaction Catalyst-Transfer-Polymerization (CTP). Developments in CTP techniques have led to precisely defined structural topologies which are often needed for studying important properties of π-conjugated polymer systems.[11-13,34] But unlike classical coupling reactions used in step-growth polymerization (Heck, Kumada, Murahashi, Negishi, Stille or Suzuki-Miyaura carbon-carbon coupling reactions), their chain-growth analogs using CTP require the catalyst to stay bound to the conjugated backbone through various π-associated complexes (Figure 1.2).[51] This additional mechanistic demand makes it difficult to find matching catalyst/ancillary ligand combinations that are also compatible for preparing various classes of conjugated polymers.[13]

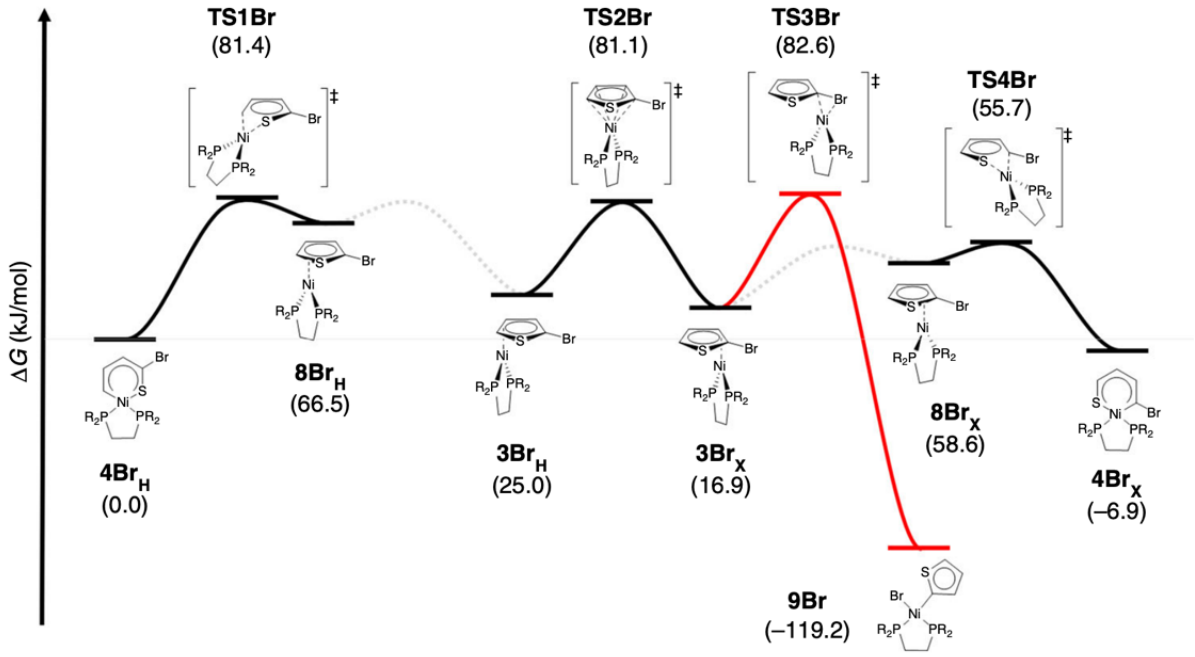

Figure 1.2. DFT calculated free energies of various Ni^0 π-complexes with 2-bromothiophene. The "ring-walking" process shown here allows the catalyst to migrate over the polymer backbone and it is a mechanistic requirement for Catalyst-Transfer Polymerization. R = methyl. Reproduced with permission from Ref. 51. Copyright © 2018 Springer Nature.

On the other hand, using step-growth for making of π-conjugated polymers is a more mature technique. It has a wider synthetic scope and is applied ubiquitously for preparing conjugated polymer materials that require an elaborate chemical structure of the repeating unit. Such designer materials are often needed for today's high performance organic electronic devices (Figure 1.3).[52] Both areas of research are constantly striving to fill this discrepancy in synthetic knowledge.[13] Conjugated polymer research on controlled polymerization reactions strive to achieve the monomer scope used in modern conjugated polymer materials[53] and applied conjugated polymer material ventures aspire for the control and narrow polydispersity afforded by controlled polymerization.[54] The polydispersity index (PDI) is important parameter for optimizing conjugated polymer devices.[55] It describes the distribution of polymer chain lengths within a material. Although they may be chemically similar, individual conjugated polymer chains of

various lengths are still distinct macromolecules; showing different conformational behavior,[56] solid state packing energies[57] and electronic structures.[58] These small differences in chain lengths become critically important when the molecule is electronically coupled into an overall supramolecular potential energy landscape.[59] An energy carrier may visit many individual chromophores in a conjugated polymer material during its excited-state lifetime.[60]

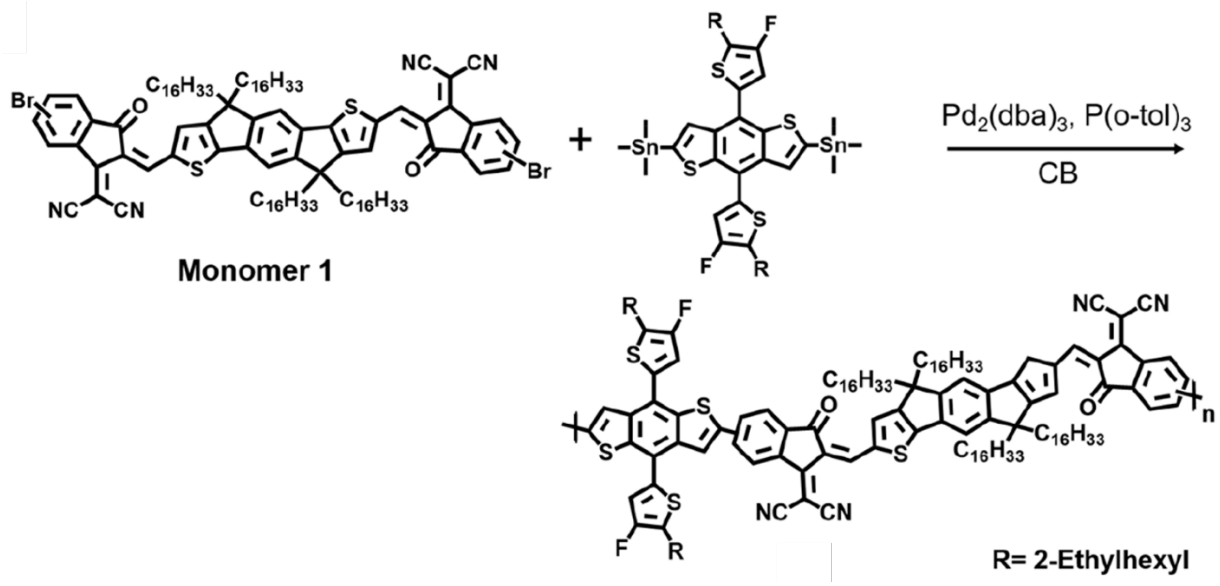

Figure 1.3. Polymer acceptor material in high performance all polymer solar cell with a power conversion efficiency of 8.3%. Prepared by step-growth Stille coupling. Reproduced with permission from Ref. 52. Copyright © 2019 American Chemical Society.

Introducing lower or higher energy molecular orbitals that are significantly different than the average electronic energy levels within the material can hinder energy migration even at long distances from the location of the primary excitation.[61] Therefore, the uniformity of the polymer material affects fundamental properties of conjugated polymer systems, and the development of robust controlled polymerization methods affording controlled polymer molecular weight and narrow polydispersity is an important technological challenge.

1.2. Recent Developments in Controlled Catalyst-Transfer Polymerization

1.2.1. The Initial Discovery and Mechanism of Kumada Catalyst-Transfer Polymerization

The development of controlled polymerization via CTP is dominated by the preparation of poly(3-alkylthiophene) (P3AT), poly(9,9-dialkylfluorenes) (PF) and poly(*p*-2,5-dialkylphenylene) or poly(*p*-2,5-dialkyloxyphenylene) (PPP) and their block co-polymers.[11,14] P3AT's are the most prevalent class of conjugated polymers prepared by CTP. Their electron rich π-system can form effective associative complexes with phosphine and diimine-based Ni^0 and Pd^0 catalysts and facilitating the intramolecular catalyst-transfer process.[62] In 2004, McCullough[63] and Yokozawa[64] independently discovered the chain-growth nature of Ni-catalyzed polymerization of 2-bromo-5-chloromagnesio-3-hexylthiophene supported by 1,3-(diphenylphosphino)propane (dppp) ligation. The Kumada type reaction set the first example of preparing conjugated polymers by CTP. The mechanism of Kumada Catalyst-Transfer Polymerization (KCTP) follows a typical transition metal mediated carbon-carbon coupling catalytic cycle (Figure 1.4).

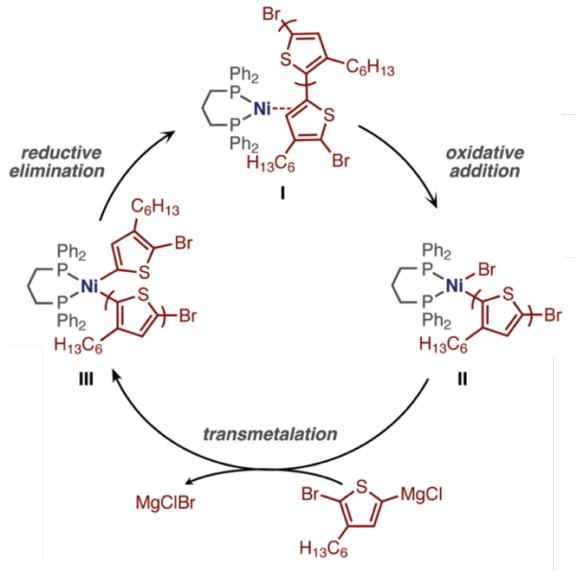

Figure 1.4. Kumada Catalyst-Transfer Polymerization catalytic cycle showing oxidative addition, transmetalation and reductive elimination steps. In structure I, a simplified Ni^0(dppp) π-associative complex is shown. Reproduced with permission from Ref. 53. Copyright © 2013 American Chemical Society.

First, the catalytically active $L_2ArNi^{II}Br$ species undergoes transmetalation with the organometallic Grignard monomer, and then reductive elimination increases the polymer chain length by one repeating unit. Afterwards, the catalyst must be able to migrate intramolecularly (by forming a series of π-associative complexes) to the carbon-halogen bond at the chain end. An efficient intramolecular catalyst-transfer is the vital step distinguishing chain-growth from the step-growth mechanism.[65] Subsequently, oxidative addition into the carbon-halogen bond regenerates the catalytically active $L_2Ar_{n+1}Ni^{II}Br$ species. The mechanism only permits chain-growth to occur on polymer species that are bound to the transition metal. This process allows for the polymer molecular weight to be controlled using the monomer to catalyst molar ratio defined at the beginning of the reaction (known as feed ratio). KCTP can be used to reliably prepare P3HT with controlled chain-growth up to approximately 120 repeating units, with narrow polydispersity (PDI < 1.2) and in excellent yields (>90%).[66]

Kumada type reactions formed the foundation of CTP research. But beyond the controlled polymerization of P3AT, very few ancillary ligand/catalyst combinations have shown reliable controlled chain-growth for other classes of conjugated polymers.[12,14,34,36,65-66]

1.2.2. State-of-the-Art: Suzuki-Miyaura Catalyst-Transfer Polymerization

Yokozawa was also the first to report Suzuki-Miyaura Catalyst-Transfer Polymerization (SCTP). Much less is known about the reaction in comparison to KCTP and the complete mechanism has not been elucidated. In his initial 2007 report, Yokozawa *et al.* prepared poly(9,9-dioctylfluorene) and poly(*p*-2,5-dibutyloxyphenylene) using aryl boronic acid and pinacol ester monomers, and using $PhPd(P^tBu_3)Br$ as an external initiator (Figure 1.5).[67]

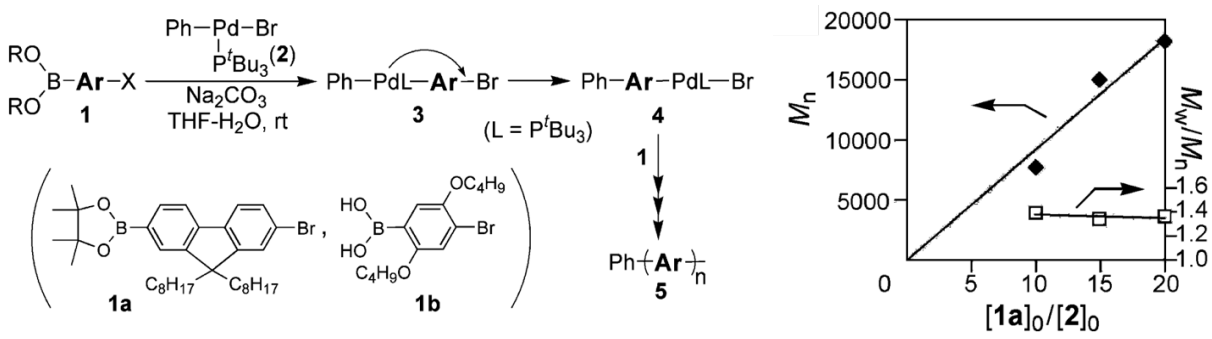

Figure 1.5. Reaction scheme of Suzuki-Miyaura Catalyst-Transfer Polymerization towards poly(9,9-dioctylfluorene) and poly(*p*-2,5-dibutyloxyphenylene) using PhPd(P^{t}Bu$_3$)Br as an external initiator (left). M_n vs feed ratio showing controlled chain-growth behavior of the polymerization process (right). Reproduced with permission from Ref. 67. Copyright © 2007 American Chemical Society.

The resulting PF showed molecular weight up to 19 kDa and produced a modest PDI = 1.33. Likewise, preparation of PPP by this method gave modest results of M_n = 11 kDa and PDI = 1.53.

Later in 2010, Yokozawa *et al.* conducted a more detailed optimization study on the controlled preparation of PPP using 4-iodo-2,5-dihexyloxyphenylboronic acid (Figure 1.6).

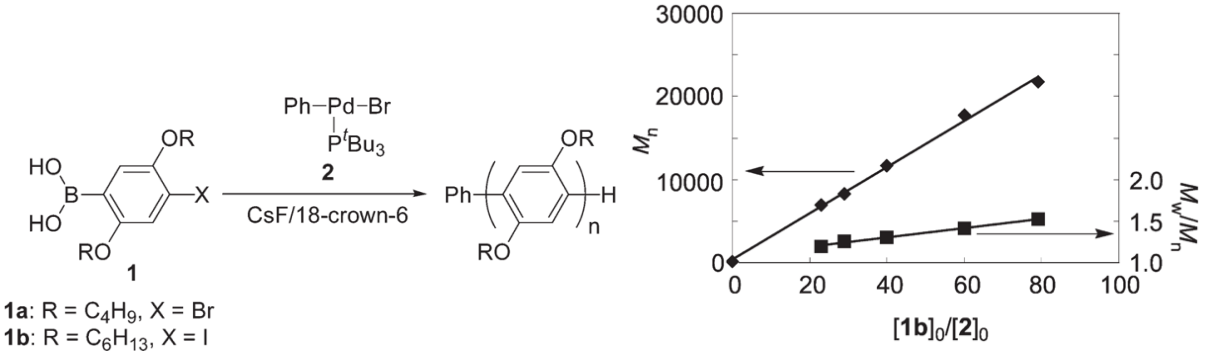

Figure 1.6. Scheme of Suzuki-Miyaura Catalyst-Transfer Polymerization of 4-halo-2,5-dihexyloxyphenylboronic acid using PhPd(P^{t}Bu$_3$)Br as the external initiator (left). M_n/M_w versus feed ratio showing controlled chain-growth polymerization of 4-iodo-2,5-dihexyloxy-phenylboronic acid (right). Reproduced with permission from Ref. 68. Copyright © 2010 American Chemical Society.

In the optimized conditions, he and co-workers were able to achieve a M_n up to 21 kDa and PDI = 1.44-1.89 for PPP with greater than 60 repeating units. In that work, they adopted several strategies

to improve the polymerization reaction. First, the reaction temperature was lowered to -20°C in order to control the temperature-dependent intermolecular chain-transfer process (involving dissociation of the π-associative complex). Second, they switched from aqueous Na_2CO_3 to CsF as a soluble in organic solvents base. Third, they increased the THF/H_2O ratio from 10:1 to 17:1 (v/v) based on the claim that excess amount of water was detrimental to the final M_n and solubility of PPP. Lastly, they switched from bromoarene monomers to iodoarene boronic acid monomers. Polymerization reaction yields were not reported in that work.

Following Yokozawa's reports, Hu *et al.* were able to improve SCTP preparation of PF using in-situ generated PhPd(^{t}Bu$_3$)I as the external initiator and aqueous K_3PO_4 as base. In optimized conditions, they reported the preparation of PF with M_n up to 31 kDa (however this significantly exceeded a theoretical M_n of only 8.3 kDa), consistently low PDI 1.13-1.35 and good yields (>70%).[69] Obtaining polymers via SCTP with higher M_n than the theoretical M_n is generally considered an indication of poor initiator efficiency. Where only a fraction of the initiator can undergo polymerization with the monomers, the effective $[M]_0/[I]_0$ ratio is increased proportionally and leading to higher molecular weight polymers.

Wang demonstrated the use of a non-phosphine containing ligand for SCTP and utilized Pd(IPr)$(OAc)_2$ as the precatalyst for controlled preparation of PF and P3HT.[70] Pd CTP catalysts with NHC ligands (Figure 1.7) have longer catalyst lifetimes than their phosphine containing analogs.

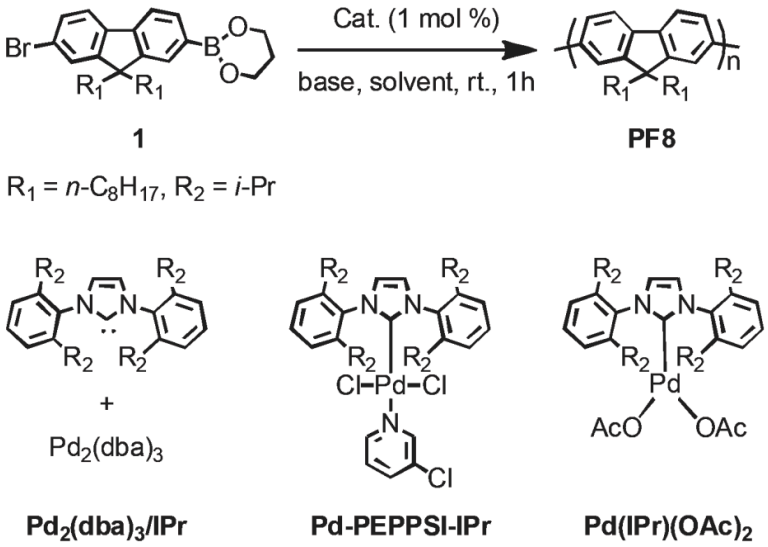

Figure 1.7. Pd/NHC complexes used in SCTP reaction for preparing poly(9,9-dialkylfluorenes).

Also, such catalysts are suggested to facilitate the intramolecular catalyst-transfer process due to lower activation energies for the ring walking process. Nevertheless, the resulting polymers showed uncontrolled molecular weight and broad polydispersity. As such, Wang obtained PF with M_n 69 kDa (PDI 1.56-1.78), ~70% yield and P3HT with M_n 64 kDa (PDI 1.40-1.81) and >95% yields.

In typical Suzuki-Miyaura conditions, aryl boronic acids readily undergo hydrodeboronation; such monomer degradation results in significant loss of polymerization control.[71] Carrillo *et al.* attempted to address this issue by utilizing *N*-methyliminodiacetic acid (MIDA) protected aryl boronic acid monomers.[72] MIDA hydrolysis rate depends on the pH, temperature and water concentration; releasing cross-coupling active aryl boronic acid monomers at small steady concentrations over an extended time.[72] The slow hydrolysis of MIDA boronates limits the transient concentration of $ArB(OH)_2$ and therefore decreases the rate of side reactions (Figure 1.8).

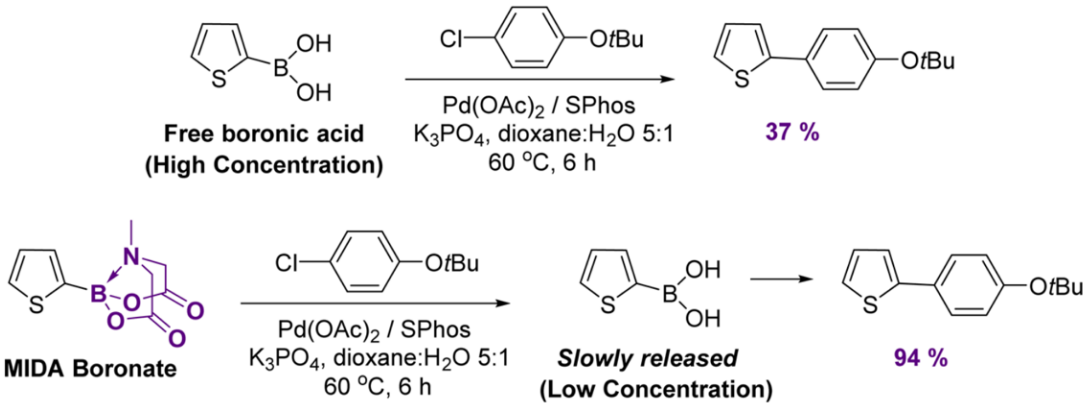

Figure 1.8. Synthesis of thiophene cross-coupled products using boronic acid (top) versus *N*-methyliminodiacetic acid (MIDA) protected boronate esters (bottom). Slow hydrolysis of MIDA boronates into their corresponding aryl boronic acids reduces protodeboronation and increases reaction yields. Reproduced with permission from Ref. 72. Copyright © 2014 American Chemical Society.

Carrillo *et al.* chose SPhos/$Pd(OAc)_2$ as the pre-catalyst for the preparation of P3HT. They conducted the polymerization reaction at a high temperature of 55-60°C, resulting in P3HT with broad polydispersity (PDI 2.7 – 3.1) in optimized conditions. Carrillo's main focus was on improving the regioregularity of P3HT in Suzuki-Miyaura chain-growth polymerization via novel preparation of 5-bromo-4-hexylthiophene boronic acid MIDA ester using direct electrophilic borylation. Along this route, they were able to achieve a P3HT regioregularity of >97%. These authors also investigated the effect of various H_2O : monomer molar ratios on the SPhos/Pd catalyzed polymerization of 5-bromo-4-hexylthiophene boronic acid MIDA ester. They implied that the polymerization rate was accelerated using increasing amounts of H_2O (80 vs 40 equiv H_2O : monomer); an effect that is not discussed in detail in SCTP literature. However, this reaction caused severe hydrodeboronation and broadening of the PDI relative to reactions using 40 equiv H_2O : monomer. Carrillo was also one of the first to imply on the nature of the Pd catalytic cycle involved in the polymerization. They presumed that Suzuki-Miyaura polymerization of 5-bromo-

4-hexylthiophene boronic acid MIDA ester using SPhos/Pd system occurred via the boronate pathway of the Suzuki-Miyaura reaction.

Shortly after Carrillo *et al.*'s reported finding of the water effect on the course of SCTP, Yokozawa further commented on the role of H_2O in Pd SCTP of triolborate thiophene monomers in anhydrous conditions.[73] Similar to Carrillo, he also assumed that controlled SCTP proceeded via the boronate pathway of Suzuki-Miyaura reaction and that water was unnecessary for the reaction. But instead, Yokozawa found that water was essential for producing P3HT with narrow polydispersity. In anhydrous conditions, undesired intermolecular catalyst-transfer process dominated resulting in low quality P3HT (M_n = 3.6 kDa, PDI = 1.78 – 2.15). Yokozawa convincingly demonstrated that water, when present in the reaction mixture, facilitates intramolecular catalyst-transfer at room temperature, but he admitted that he could not conclude on the reason for its remarkable effects on the SCTP process.

In 2015, Hong reported similar results as Hu in the preparation of PF using *p*-TsOArX (X = I, Br) as the external catalytic initiator precursor.[74] Both research groups were able to achieve low polydispersity, high yield, and yet the final molecular weight of the produced polymers was much higher than the theoretical M_n. Hong's data demonstrated that in-situ initiation using aryl iodides were more efficient than by aryl bromides, and this was likely related to a finding in Yokozawa's report showing that aryl iodide monomers were superior to aryl bromides in the SCTP reaction for preparing PPP. Hong *et al.* did not discuss the halogen's role in external initiator efficiency or how it related to average molecular weight of the polymers. Also, neither of Yokozawa's systems were ideal (exhibiting uncontrolled molecular weight and broad polydispersity of the resulting polymers), so it would be difficult to explicitly elucidate the effect of varying halogens in the monomer or initiator. Hong *et al*. carried out multiple experiments using aryl iodide precursors

that resulted in better initiation than using aryl bromides (as indirectly indicated by the observed M_n vs theoretical M_n). They obtained exceptionally clean MALDI-TOF spectra (Figure 1.9) of the PF polymers exhibiting only a single set of polymer chain distributions containing the external initiator. This clearly demonstrated that undesired chain-transfer process was essentially non-occurring in these polymerization conditions.

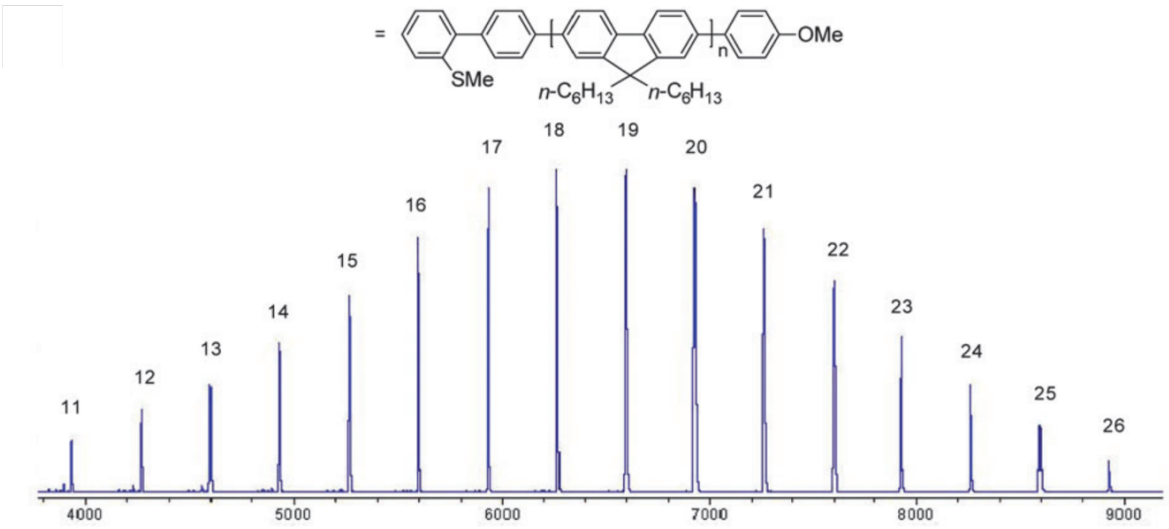

Figure 1.9. MALDI-TOF spectrum of poly(9,9-dihexylfluorene) prepared by Suzuki-Miyaura Catalyst-Transfer Polymerization. MALDI-TOF spectrum demonstrates a single set of polymer chains therefore indicating insignificant presence of chain-transfer products when polymerization is carried out using $Pd_2(dba)_3$/*t*-Bu_3P as the catalyst. Reproduced with permission from Ref. 74.

Despite these findings, they chose to continue their study using aryl bromide (rather than aryl iodide) precursors combined with $Pd_2(dba)_3$/*t*-Bu_3P as the in-situ initiating species due to better control over the polymer chain ends. The combination of poor initiator efficiency and narrow polydispersity generally indicates the existence of a chemoselective polymerization process. Hypothetically speaking, either a fraction of the Pd species are deactivated at the beginning of the reaction (e.g. through Pd black nanoparticles formation or phosphine ligand oxidation), or the Pd species that are not initiated in the beginning of the reaction are forbidden from entering the

catalytic cycle throughout the reaction progress. However, catalyst degradation is a less likely hypothesis, considering that multiple independent groups reported this effect, and the chemical pathways for ligand dissociation are reversible. From a synthetic standpoint, Hu and Hong's results were interesting because they showed two unexplored phenomena related to SCTP reactions: halogens in then initiator affecting the polymerization efficiency, and possible monomer deactivation in SCTP which results in narrow polydispersity. Many reports on CTP have demonstrated these effects, but the underlying process causing them has not been elucidated.

More recently, Hong also reported an interesting SCTP resulting in *"ortho"*-connected poly(5-alkyl-2,3-thiophene) (P5AT) which self-assembles into a helical structure (Figure 1.10).[75] The highly twisted morphology of P5AT caused a large blue-shift in the fluorescence emission relative to P3HT and the nanostructure's rigidity is apparent by narrow emission bands with sharp vibronic structures. The blue shifted emission is a result of a shorter average conjugation path length caused by kinking and twisting in the unusually connected polymer chain.

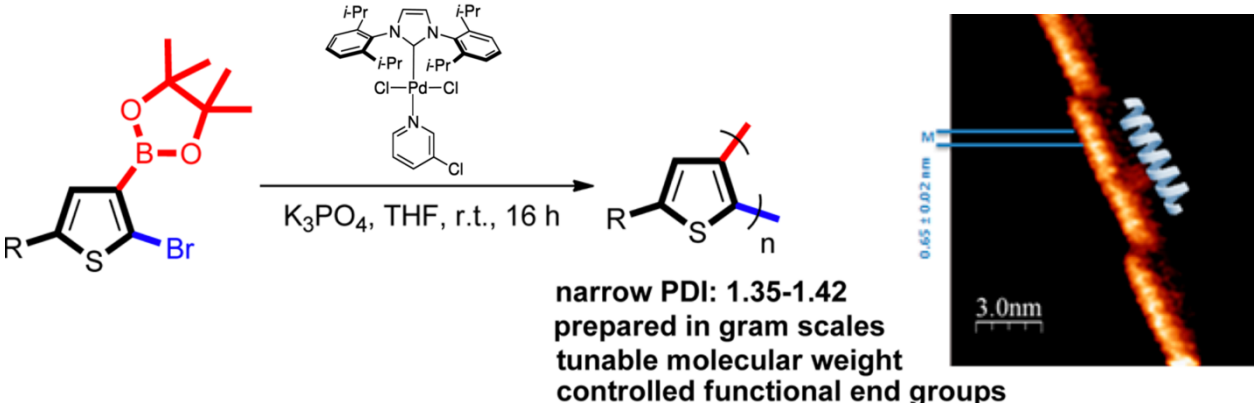

Figure 1.10. Helical poly(5-alkyl-2,3-thiophene) prepared by Suzuki-Miyaura Catalyst-Transfer Polymerization using Pd/NHC catalyst and K_3PO_4 as base at room temperature. Reproduced with permission from Ref. 75. Copyright © 2016 American Chemical Society.

In 2017, reports of SCTP using Buchwald ligands/pre-catalysts began to surface in literature. Exploring a large set of Buchwald ligands, Yokozawa identified Pd/AmPhos as a modestly suitable

system for preparing P3HT (M_n = 16.6 kDa, PDI = 1.35, however theoretical M_n = 3.3 kDa).[76] As in previous cases, the polymers showed uncontrolled molecular weight likely due to an inefficient initiation process similar to the situation described in Hong and Hu's reports. To mitigate this problem, Yokozawa tried utilizing an isolated ArPd(AmPhos)Br catalyst to achieve uniform initiation but found that it resulted in an even broader polydispersity relative to the case of the initiators he generated in-situ (where the catalyst was incubated with aqueous base prior to polymerization). The data implied that ArPd(AmPhos)Br was actually the pre-catalytic species; a potentially valuable finding. Yokozawa mentioned that the odd observation might have been due to the slow formation of palladium hydroxo complex (a key intermediate in the oxo-palladium pathway of the Suzuki-Miyaura reaction) and all but conducted the necessary experiments proving this. He supported his statement by showing that the in-situ generated catalysts provided a more uniform initiation, yielding a narrower polydispersity versus the isolated Pd halide complex.

Seo *et al*. authored the second report utilizing MIDA boronates to control hydrodeboronation in SCTP reactions.[77] They found that SPhos and RuPhos supported Pd SCTP produced P3HT and P3EHT polymers with controllable molecular weight, consistently low polydispersity and excellent yields (M_n up to 17.6 kDa, PDI >1.08, >90% yield). This report is remarkable because it represented the first robust and completely controlled chain-growth polymerization for the preparation of a conjugated polymer by SCTP. They also showed that the initiation time could be reduced by using electron deficient initiator precursors, and they controlled the initiator efficiency by utilizing commercially available 3rd generation Buchwald pre-catalysts and aryl iodide precursors. Using this strategy, they successfully prepared all-conjugated P3HT-*block*-P3EHT with molecular weight up to 9.2 kDa and polydispersity index of 1.18.

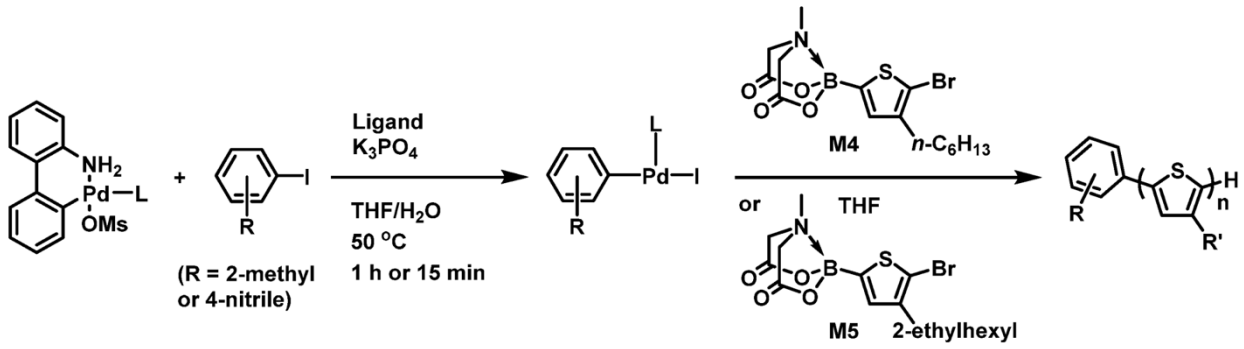

Figure 1.11. Suzuki-Miyaura Catalyst-Transfer Polymerization of 2-bromo-3-hexylthiophene boronic acid MIDA ester and 2-bromo-3-ethylhexylthiophene boronic acid MIDA ester using RuPhos supported external initiator. Reproduced with permission from Ref. 77. Copyright © 2017 American Chemical Society

Recently, Yokozawa reported studies of the intramolecular catalyst-transfer of $^{t}Bu_3P$/Pd catalysts over various functional groups using 2nd generation Buchwald pre-catalysts. Poly(*p*-phenylenevinylene)s (PPVs) are an important class of conjugated polymers used in organic electronic devices which have historically been difficult to synthesize using KCTP because of irreversible binding of Ni based catalysts onto the carbon-carbon double bonds. Using Pd($^{t}Bu_3$) based 2nd generation Buchwald precatalyst, Yokozawa demonstrated that these can efficiently undergo intramolecular catalyst transfer through stilbene when the phenylene moiety is functionalized with alkyloxy substituents in the *ortho* position.[78] He used CsF/18-crown-6 as a base in 18:1 (v/v) THF/H_2O. Using the same catalytic system, he also demonstrated intramolecular catalyst-transfer over carbon-carbon triple bond, and nitrogen-nitrogen double bonds.[79] Most interestingly, Yokozawa *et al*. reported the intramolecular catalyst-transfer over methylene, carbonyl, tertiary nitrogen, oxygen and sulfoxide units.[80] Intramolecular transfer over methylene unit was particularly odd because it is a non-conjugated functional group lacking the ability to form π-associative complexes.

KCTP and SCTP are the main and most promising synthetic methods for preparation of conjugated polymers using controlled chain-growth polymerization. The reports discussed above comprise the most recent and impactful developments in SCTP research. From analysis of these reports (and corresponding discussion) it is apparent that many important questions are still left unanswered. What is the unequivocal role of water in SCTP and how does it enhance the polymerization rate and polydispersity as noticed in Carrillo and Yokozawa's reports? Does SCTP proceed via the oxo-palladium or boronate pathway of the Suzuki-Miyaura cross-coupling reaction? What are the processes enabling halogens to play such a critical role in the initiating catalytic cycle of Pd SCTP as reported in Hu and Hong's report? And is monomer deactivation responsible for the narrow polydispersity in reactions that have inefficient initiation? Chapter 2 of this dissertation will include a detailed discussion of the research project we undertook to address the underlying process at the center of these phenomena.

1.2.3. Other Notable Developments in CTP Controlled Chain-Growth Polymerization

Besides these and other avenues of research that are reviewed above, some unconventional techniques have been recently developed for expanding the possible monomer scope and π-conjugated material properties achieved by CTP. There were also some reports revealing neat mechanistic insights of the transmetalation step in SCTP reactions (still remaining a controversial topic).

The dihedral angle between repeating units is an uncommon but effective element for controlling the electronic structure of π-conjugated polymer systems. Sugiyasu provided[81] proof-of-concept of a cyclopolymerization towards P3HT using KCTP to control the twisting of the conjugated polymer backbone. Controlling the dihedral angle between chromophores allows for

tuning excited state electronic energy levels and is valuable for the field of thermally activated delayed fluorescence.[82]

Koeckelberghs' group has been spearheading the alternative preferential oxidative addition mechanism for the controlled chain-growth of conjugated polymers without an associative complex and demonstrated a broader monomer scope than traditional CTP.[83-85] Jagadesan *et al.* reported on preparation of poly(*p*-phenyleneethynylene) (PPE) by Sonagashira chain-growth polymerization using ArPd(^{t}Bu$_3$)Br as an external initiator with efficient initiation, resulting in excellent yields (>85%) and narrow polydispersity (PDI = 1.13-1.21).[86] Grisorio and Suranna developed Buchwald-Hartwig CTP of aryl amines yielding polymers with good polydispersity (PDI = 1.11.1-79) and excellent yields (>80%).[87]

On the mechanistic side, Li *et al.* demonstrated base-free Suzuki-Miyaura coupling of aryl bromides with aryl boronic acids in water. They found that the irreversible catalytic cycle drives the reaction towards gradually increasingly acidity of the reaction medium in the absence of base. Using JohnPhos supported Pd(OAc)$_2$ as their catalytic system, they conducted Suzuki-Miyaura coupling with near quantitative yields and measured the changing pH as the reaction progressed. They found that Suzuki-Miyaura coupling occurred down to pH 3.0 (the acidity they found at the completion of the reaction in their conditions, but might possibly operate at lower pH), with yields above 90%. But below pH = 6.0, the phosphine ligand became protonated and dissociated from the catalyst. This is particularly interesting because it implies the existence of an unconventional palladium catalytic pathway that proceeds without base. This essentially rules out both the traditional oxo-palladium and boronate pathways. Li *et al.* proposed an unconventional oxo-palladium pathway, generating the palladium hydroxo intermediate through intramolecular deprotonation of a Pd aqua complex by lone pairs existing on a 2-heteroarylene reactive ligand.[88,89]

In our own lab, we tried the SCTP of 2-bromo-3-hexylthiophene boronic acid MIDA ester (with RuPhos Pd G3 as precatalyst) using THF/acetate buffer (pH = 4.75) and found obtained a moderate polydispersity polymer (PDI = 1.32) with M_n = 4.2 kDa (theoretical M_n = 6.1 kDa) and yield = 49%. Acidity control in mediation of SCTP has never been demonstrated. It is possible that utilizing acidic conditions may be an alternative method for deterring hydrodeboronation due to the pH dependent Kuivila process. Obliterating the slow MIDA hydrolysis rate while reducing monomer degradation could allow to control the speed of polymerization reactions to a tremendous degree (Buchwald has shown that quantitative conversion between $L_2ArPdOH$ and $ArB(OH)_2$ can occur in under two minutes in similar conditions as used in SCTP reactions). A fast polymerization rate for making conjugated polymer materials is useful for generating kinetically driven nanostructures, a topic which is discussed in Chapter 3.

1.3. Energy Transfer in Conjugated Polymer Materials

1.3.1. Conformational Subunits Within Conjugated Polymer Chains

For a planar and infinitely long conjugated polymer chain isolated in vacuum, the electronic structure of the macromolecule may be relatively homogenous. But in real-life disordered conjugated polymer materials (such as in solution, thin-films and nanoparticles), the dynamic nature of structural conformations produces segmented chromophores within the polymer chain.[58] These chromophores having different electronic structures (referred to as conformational subunits) combine into a statistical distribution of energy levels within the material which govern the thermodynamics of energy migration.[90]

1.3.2. Excitons Quasiparticles

Photoexcitation spatially separates the electron from its nuclei and produces an electric field polarization around the local atomic lattice. Concomitant, the altered electron density in the excited

state molecular orbitals causes nearby structural changes to occur (such as altered bond lengths).[58] These perturbations and the associated electron/nuclei pair are together referred to as an exciton. Singlet intrachain excitons have strongly bound excited states and quickly recombine to emit a photon. This species is mainly responsible for the fluorescence observed in conjugated polymer materials.[91] There are also non-emissive excitons where the electron/nuclei polarons (simply termed "electron" and "hole") are deterred from recombination by existing on different polymer chains.[92] Excitons dissipate energy as they migrate from higher energy chromophores in the conjugated polymer system to lower energy chromophores, eventually being trapped in the low energy states where they can fluoresce as a singlet intrachain exciton, exist as non-emissive excited states, or relax non-radiatively.[93]

1.3.3. Energy Transfer Pathways in π-Conjugated Materials

The energy transfer of photoinduced excited states through π-conjugated materials occur through two main processes. In systems where the energy donor and acceptor have an efficient molecular orbital overlap, an excited state electron can physically transfer from the higher energy chromophore to the lower energy one (exchange, or Dexter mechanism). This process is often associated with intrachain energy migration through covalent bonds.[94] Energy can also be transferred through dipole – induced dipole interactions that do not require direct molecular orbital overlap and thus can occur through space (Förster mechanism).[95]

Dexter and Förster pathways are often intertwined in energy transfer processes.[96] Their individual contributions can only be deciphered in exceptionally ordered or specially designed conjugated polymer systems. Swager has demonstrated the relative dynamics of the Dexter and Förster energy migration in a rigid poly(*p*-phenyleneethynylene) containing a low energy gap acridine orange (AO) chromophore.[97] The linear framework of *p*-phenyleneethynylene (PPE)

conjugated backbone limits some intrachain Förster energy pathways (as the rigid rod-like structure of PPE would prevent them from folding and therefore bringing intrachain chromophores in close proximity). Swager *et al.* synthesized highly aligned PPE Langmuir-Blodgett films with low energy AO traps within the film with well-defined number of layers. The meticulously controlled anisotropic energy transfer from the multiple PPE layers showed that photogenerated excitons undergo very efficient interchain energy transfer perpendicular to the molecular axis. The energy migration kinetics were modeled mathematically to show efficient Förster mechanism taking place.

Energy migration by the Dexter mechanism is generally considered slower and less efficient due to poor electronic coupling between intrachain chromophores and the presence of defects. Schwartz *et al.* showed that intrachain energy transfer within PPV chains isolated in mesoporous silica composites was orders of magnitudes slower than the interchain process.[98] In some of the early reports of theoretical treatment of the energy migration process, Dexter energy transfer was completely neglected due to its perceived slower energy transfer rate relative to Förster energy transfer. However, there were also some reports showing essential role of the through-bond energy transfer in conjugated polymer systems,[99] and it is still a critical element to consider in designing conjugated polymer systems with certain optical and optoelectronic properties.

1.3.4. Other Excited State Species Affecting Energy Migration

Photoexcitation energy can be diverted into other species that interact strongly with the initially photogenerated excited state and can also affect energy migration processes. For example, singlet excitons in polythiophenes (PTs) can undergo a fast intersystem crossing (ISC) to form relatively stable triplet states due to the large energy difference between the T_1 and S_1 energy levels.[93] This stabilization effect may lower the intrinsic photoluminescence of PT, but also can be utilized to

facilitate charge transport in electronic devices. Alternatively, an excited state can be stabilized by interacting with a proximate chromophore in its ground state. The resulting excited state complex (exciplex) and the stabilizing effect manifest themselves as a bathochromic shift in the emission band (relative to the emission band of an isolated excited state) in the fluorescence spectra. Charge-transfer complexes are also common in donor-acceptor systems and also produce low lying energy levels, which can trap and non-radiatively deactivate excited states often lowering quantum yields.

The difficulty of controlling energy migration is further complicated by the fact that the formation of conjugated polymer nanostructures is strongly influenced by synthetic methodology. Schwartz has demonstrated that MEH-PPV chains can aggregate showing both a concentration and solvent dependency. In relatively poor solvents for MEH-PPV, aggregates are pre-formed in solution and translate their low energy electronic states into the thin-film, making up a significant fraction of the total excited states and reducing the photoluminescence quantum yield.[100]

1.3.5. Regioregularity in P3HT by KCTP and Its Impact On Energy Migration

Structural abnormalities affecting the electronic levels of conjugated polymer materials can also come from chemical defects on the polymer chain.[101] In the case of P3HT prepared by KCTP, the organometallic Grignard monomer is generated in-situ via magnesium-halogen exchange (metathesis) reaction which can produce one of two possible regioisomers of 2,5-dibromo-3-hexylthiophene precursors. Although the "wrong" isomer of the Grignard monomer has been shown to be less reactive and not actively participating in polymerization process, it still has the ability to incorporate in the resulting conjugated polymer chain. In a case of such incorporation, asymmetric segments of 3-hexylthiophene repeating units with alkyl side chains would be facing each other (tail-to-tail) experiencing increased steric bulkiness between repeating units and causing torsion strain along the backbone.[102] The kinking due to these torsional defects in P3HT chains

can cause changes in electronic energy levels and reduce the conjugation pathlength and exciton diffusion length, thus inhibiting charge and energy transfer in the π-conjugated system.[103]

1.4. Practical Significance of Conjugated Polymer Systems – Recent Examples

Conjugated polymers possess a number of unique fundamental properties that make this class of materials capable to be used for addressing some modern economic and technological problems. The previous sections discussed the controlled chain-growth polymerization for the preparation of conjugated polymers and how their careful preparation affects energy migration processes. With meticulous care, these fundamental properties can be harnessed to do useful work. This section of the dissertation will highlight more recent technologically and economically relevant advances in conjugated polymer devices based on their unique properties. Conjugated polymers are traditionally integrated into organic photovoltaic cells, organic light emitting diodes and organic field effect transistors. These traditional applications have been reviewed comprehensively elsewhere.[9,30,31,37,38,52] The focus of this section is to demonstrate broad utility and novel applications of modern conjugated polymer material systems.

1.4.1. Flexible Energy Harvesting Organic Electronic Devices

Organic solar cells incorporating thin-films of conjugated polymers experience a tremendous rate of development. The physical performance including power conversion efficiencies being reported are increasing exponentially with time (Figure 1.12).[37] All-polymer solar cells (all-PSCs) have a particular niche for wearable electronics. Yan *et al.* recently reported a flexible ternary heterojunction solar cells reaching an incredible 14.06% power conversion efficiency (PCE), a record increase from 12.5% reported just earlier in 2019.[103] They utilized conjugated polymers as both donor and acceptor materials and also incorporated $PC_{71}BM$ as additive to facilitate exciton dissociation and charge carrier generation at the donor-acceptor interface. Ternary devices rely on

recently developed charge transfer models[104] to affect the open-circuit voltage using an energy cascade mechanism.

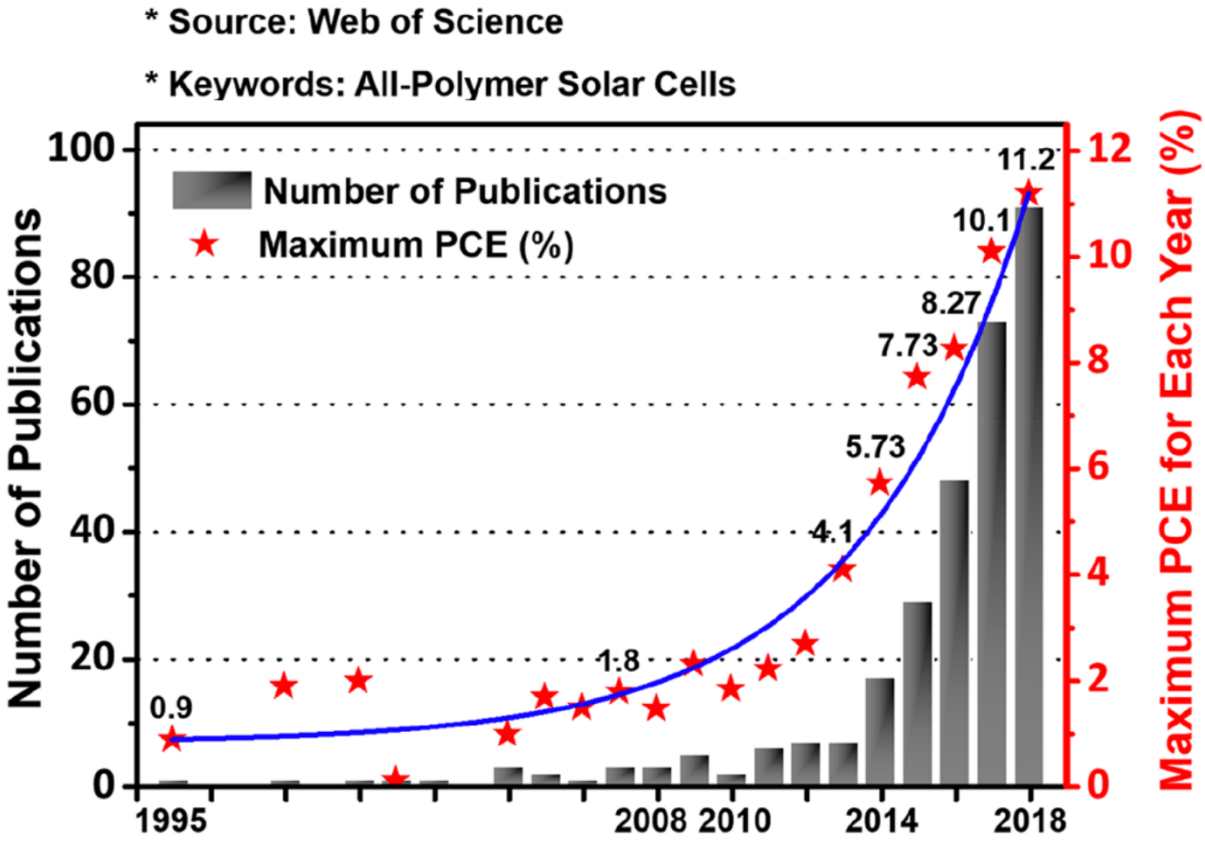

Figure 1.12. A plot of the maximum power conversion efficiency and number of publications reported each year for research into all-polymer solar cells showing an exponential increase up to 2018. Reproduced with permission from Ref. 37. Copyright © 2019 American Chemical Society.

In an interesting development, Allison and Andrew created a wearable thermoelectric generator on cotton substrate by vapor deposition of poly(3,4-ethylenedioxythiophene).[105] When wore on the hand, it generates 20 mV. The unique material has a Seebeck coefficient of 16 μV K^{-1} and thermopower factor of 0.48 μ$Wm^{-1}K^{-2}$. Important research is directed towards decreasing overall cost of conjugated polymer devices. For example, Sun *et al.* reported a low-cost polymer solar cell with 12.70% PCE using an efficient two step synthesis (overall yield 87%) involving step growth polymerization based on Stille coupling reaction.

1.4.2. Electroluminescent Devices

Lin *et al.* prepared a deep-blue OLED device based on poly(9,9-diphenylfluorene) which self-assembles into a linear rod structure.[106] The solubilizing groups prevent interchain exciton transfer and also serve as self-encapsulating layer, preventing water and oxygen from degrading the electroluminescent material. The flexible thin-film devices demonstrated a power efficiency of 1.73 cd A^{-1} and a turn on voltage of 4.55 V (Figure 1.13).

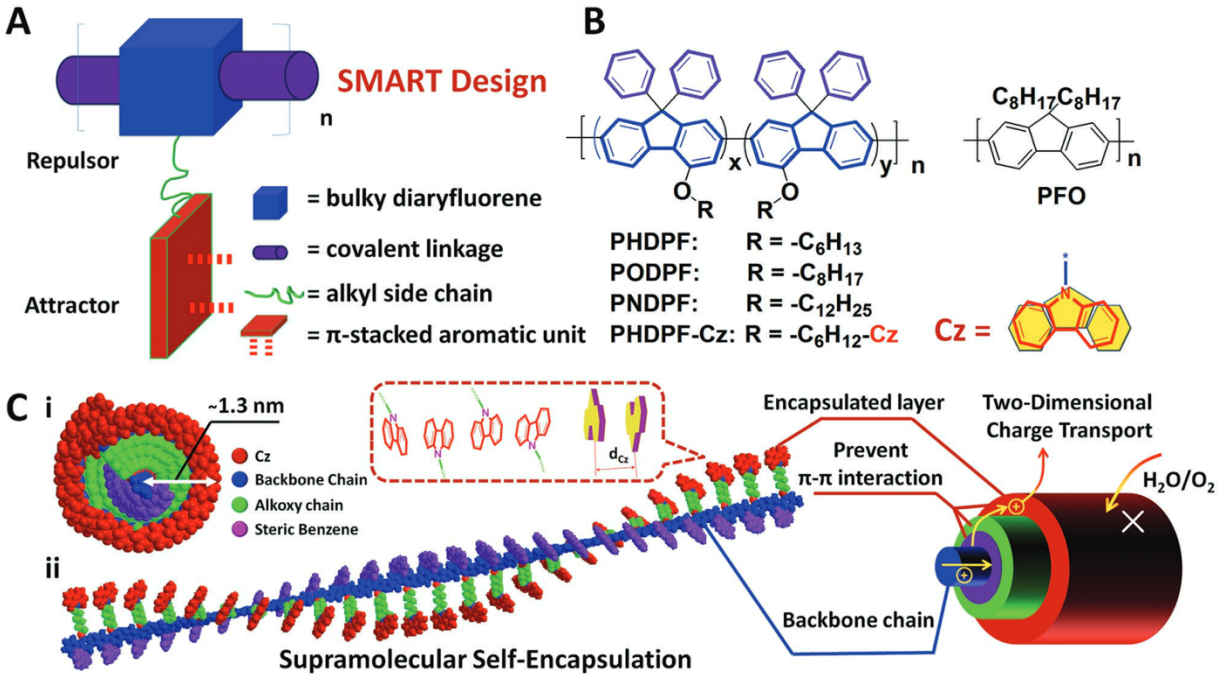

Figure 1.13. A self-encapsulating polyfluorene-based polymer light-emitting diode. PF was prepared by Yamamoto coupling polycondensation.

Conjugated polymers possess inherently high large extinction coefficients and low cytotoxicity which are beneficial attributes for biological analysis applications. Recently, Tang *et al*. developed an optofluidic laser using PPV as gain medium which showed a 70% quantum yield in THF solution.[107]

1.4.3. Electro-Mechanical Devices: Conjugated Polymer Actuators

Polypyrroles (PPy) have excellent mechanical and electrical properties that make them suitable for generating physical force while maintaining robust stability in various media. Almost two decades ago, Jager developed micro-robotic arm using PPy thin films to move objects over a small distance.[108] The mechanical action was driven by mass transport of anions in and out of the polymer network in aqueous media. Oxidation and reduction of PPy causes anions to flood into the polymer network in order to achieve a neutral charge density and thus creates swelling and shrinking that affects the length of the film parallel to the plane of the material. Recently, 3D printing techniques have allowed for creating PPy materials with complex geometries, enabling multidirectional force to be applied at precise positions and amplifying the anisotropic swelling or shrinking mechanism.[109]

1.4.4. Other Notable Developments: Energy Storage and Spintronics Materials

Recently, London *et al*. reported a donor-acceptor conjugated polymer material utilizing cyclopentadithiophene as a donor and thiadiazoloquinoxaline as acceptor and having an optical bandgap of 0.30 eV. It possesses a narrow transition between the S_1 and T_1 states with a difference of 0.0093 kcal/mol and causes the polymer to exist in high-spin ground state. The polymer can be dissolved in organic solvents and the spin-state is preserved upon forming amorphous thin-films.[110] High-spin polymers have enormous potential as energy storage, quantum computing, and magnetic materials to be used in various fields. A supercapacitor retaining high capacitance and coulombic efficiencies over 6000 cycles was developed by Liao *et al*. based on 3D aminoanthraquinone oligomeric networks. This represents an exceptional system for π-conjugated materials for energy storage.[111] Lately, conjugated polymer materials have also made considerable advances as electrode materials for rechargeable batteries.[112,113]

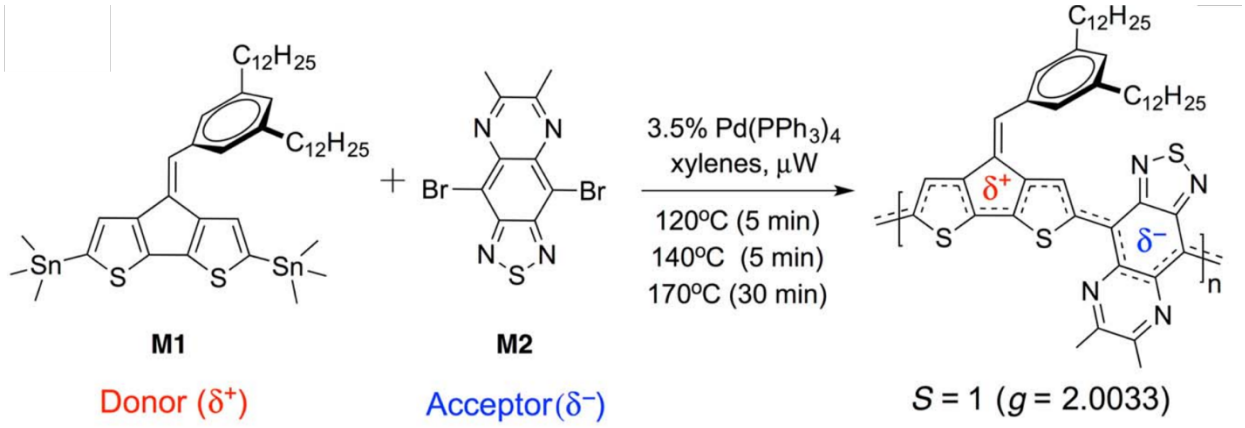

Figure 1.14. High spin conjugated polymer synthesized by step-growth Stille coupling. ref. 108. Reprinted with permission from AAAS.

1.5. Research Focus

The main focus of this dissertation is the development of precisely controlled conjugated polymer structures and nano- and mesoscale architectures through transition metal catalyzed controlled polymerizations. A review of recent developments in controlled chain-growth polymerization mechanisms for making conjugated polymers and the energy migration processes in π-conjugated materials underlines their importance in modern organic electronic devices.

In Chapter 2, rational, mechanism-based development of a universal system for externally initiated Suzuki-Miyaura Catalyst-Transfer controlled polymerization suitable for preparing poly(2,5-dialkylphenylenes), poly(9,9-dialkylfluorenes) and poly(3-alkylthiophenes) is described. An extensive discussion on the oxo-palladium and boronate pathways, as well as other mechanistic aspects of the polymerization catalytic cycle is supported by experimental evidence. Mechanism-based optimization studies on the polymerization reaction leading to PPP yielded discovery of the underlying role of the halide anion in the kinetics of the polymerization reaction. Using this mechanistic knowledge, the polymerization rate, M_n, yield and polydispersity of the resulting conjugated polymers were substantially improved through the use of Ag(I) salts. Ag^+ cations react

with Br^- to form AgBr during the polymerization and eliminate the anion's antagonistic influence on the polymerization outcomes. The described method represents a novel and universally applicable approach to refining CTP reaction conditions and optimizing polymerization outcomes. By this way, CTP polymerization reaction can be rationally optimized synergistically or independently from any catalyst /ancillary ligand combination. In this work, Ag(I) mediated SCTP resulted in P3HT, PPP and PF with controlled molecular weight and consistently narrow polydispersity and excellent yields.

Chapter 3 describes the preparation of NIR fluorescent conjugated polymer nano- and mesoscale structures by kinetically driven self-assembly process using Kumada Catalyst-Transfer Polymerization. Perylenecarboxybisimide based external initiator was utilized to incorporate low energy chromophores into the structures, and the structurally dependent photophysical properties of these kinetically self-assembled systems were controlled by adjusting the reaction temperature and other reaction parameters. The photophysical properties of these kinetically stabilized nanostructures displayed a strong dependence on these parameters and their fluorescent emission could be tuned between 450-950 nm. Adjusting the reaction conditions also led to conjugated polymer nanostructures with varying conjugation path length, which allowed to attenuate the energy transfer related characteristics of the resulting materials. We also demonstrated that upon heating above the glass transition temperature, the metastable nano- and mesoscale structures rearranged into a common structural state as was observed from UV/vis absorbance and fluorescence spectroscopy. Detailed structural characterization using X-ray and neutron scattering experiments revealed a complex hierarchical structure of the systems.

1.6. References

(1) Kertesz, M.; Choi, C. H.; Yang, S. Conjugated Polymers and Aromaticity. *Chem. Rev.* **2009**, 105, 3448-3481.

(2) Heeger, A. J. Nobel Lecture: Semiconducting and Metallic Polymers: The Fourth Generation of Polymeric Materials. *Rev. Mod. Phys.* **2001**, 73, 681.

(3) MacDiarmid, A. G. Nobel Lecture: "Synthetic Metals": A Novel Role for Organic Polymers. *Rev. Mod. Phys.* **2001**, 73, 701.

(4) Shirakawa, H. Nobel Lecture: The Discovery of Polyacetylene Film-The Dawning of an Era of Conducting Polymers. *Rev. Mod. Phys.* **2001**, 73, 713.

(5) Shirakawa, H.; Louis, E. J.; MacDiarmid, A. G.; Chiang, C. K.; Heeger, A. J. Synthesis of Electrically Conducting Organic Polymers: Halogen Derivatives of Polyacetylene, $(CH)_x$. *J. Chem. Soc., Chem. Commun.* **1977**, 578-580.

(6) Butcher, J. A.; Chambers, J. Q.; Pagni, R. M. Synthesis of Highly Conducting Films of Derivatives of Polyacetylene, $(CH)_x$. *J. Am. Chem. Soc.* **1978**, 100, 1013-1015.

(7) Shirakawa, H.; Louis, E. J.; Park, Y. W.; Heeger, A. J. Electrical Conductivity in Doped Polyacetylene. *Phys. Rev. Lett.* **1978**, 40, 1472.

(8) Patil, A. O.; Wudl, I. F.; Heeger, A. J. Water-Soluble Conducting Polymers. *J. Am. Chem. Soc.* **1987**, 109, 1858-1859.

(9) Burroughes, J. H.; Bradley, D. D. C.; Brown, A. R.; Marks, R. N; Mackay, K; Friend, R. H.; Burns, P. L.; Holmes, A. B. Light-Emitting Diodes Based on Conjugated Polymers. *Nature* **1990**, 347, 539-541.

(10) Friend, R. H.; Gymer, R. W.; Holmes, A. B.; Burroughes J. H.; Marks, R. N.; Taliani, C.; Bradley, D. D. C.; Dos Santos, D. A.; Brédas, J. L.; Lögdlund, M.; Salaneck, W. R. Electroluminescence in conjugated polymers. *Nature* **1999**, 397, 121-128.

(11) Leone, A. K.; Mueller, E. A.; McNeil, A. J. The History of Palladium-Catalyzed Cross-Coupling Should Inspire the Future of Catalyst-Transfer Polymerization. *J. Am. Chem. Soc.* **2018**, 140, 15126-15139.

(12) Aplan, M. P.; Gomez, E. D. Recent Developments in Chain-Growth Polymerizations of Conjugated Polymers. *Ind. Eng. Chem. Res.* **2017**, 56, 7888-7901.

(13) Leone, A. K.; McNeil, A. J. Matchmaking in Catalyst-Transfer Polycondensation: Optimizing Catalysts based on Mechanistic Insight. *Acc. Chem. Res.* **2016**, 49, 2822-2831.

(14) Verheyen, L.; Leysen, P.; Eede, M.-P. V. D.; Ceunen, W.; Hardeman, T.; Koeckelberghs, G. Advances in the Controlled Polymerization of Conjugated Polymers. *Polymer* **2017**, 108, 521-546.

(15) McQuade, D. T.; Pullen, A. E.; Swager, T. M. Conjugated Polymer-Based Chemical Sensors. *Chem. Rev.* **2000**, 100, 2537-2574.

(16) Fukumoto, H.; Nakajima, H.; Kojima, T.; Yamamoto, T. Preparation and Chemical Properties of π-Conjugated Polymers Containing Indigo Unit in the Main Chain. *Materials* **2014**, 7, 2030-2043.

(17) Rana, S.; Elci, S. G.; Mout, R.; Singla, A. K.; Yazdani, M.; Bender, M.; Bajaj, A.; Saha, K.; Bunz, U. H. F.; Jirik, F. R.; Rotello, V. M. Ratiometric Array of Conjugated Polymers-Fluorescent Protein Provides a Robust Mammalian Cell Sensor. *J. Am. Chem. Soc.* **2016**, 138, 4522-4529.

(18) Liang, Z.; Zhang, Y.; Souri, M.; Luo, X.; Boehm, A. M.; Li, R.; Zhang, Y.; Wang, R.; Kim, D.-Y.; Mei, J.; Marder, S. R.; Graham, K. R. Influence of Dopant Size and Electron Affinity on the Electrical Conductivity and Thermoelectric Properties of a Series of Conjugated Polymers. *J. Mater. Chem. A.* **2018**, 6, 16495-16505.

(19) Swager, T. M. 50th Anniversary Perspective: Conducting/Semiconducting Conjugated Polymers. A Personal Perspective on the Past and the Future. *Macromolecules* **2017**, 50, 4867-4886.

(20) Zotti, G.; Schiavon, G.; Zecchin, S.; Morin, J.-F.; Leclerc, M. Electrochemical, Conductive, and Magnetic Properties of 2,7-Carbazole-Based Conjugated Polymers. *Macromolecules* **2002**, 35, 2122-2128.

(21) London, A. E.; Chen, H.; Sabuj, M. A.; Tropp, J.; Saghayezhian, M.; Eedugurala, N.; Zhang, B. A.; Liu, Y.; Gu, X.; Wong, B. M.; Rai, N.; Bowman, M. K.; Azoulay, J. D. A High-Spin Ground-State Donor-Acceptor Conjugated Polymer. *Sci. Adv.* **2019**, 5, eaav2336.

(22) Sun, B.; Sun, M.-J.; Gu, Z.; Shen, Q.-D.; Jiang, S.-J.; Xu, Y.; Wang, Y. Conjugated Polymer Fluorescence Probe for Intracellular Imaging of Magnetic Nanoparticles. *Macromolecules* **2010**, 43, 10348-10354.

(23) Bouffard, Swager, T. M. Fluorescent Conjugated Polymers That Incorporate Substituted 2,1,3-Benzooxadiazole and 2,1,3-Benzothiadiazole Units. *Macromolecules* **2008**, 41, 5559-5562.

(24) Howes, P.; Green, M.; Bowers, A.; Parker, D.; Varma, G.; Kallumadil, M.; Hughes, M.; Warley, A.; Brain, A.; Botnar, R. Magnetic Conjugated Polymer Nanoparticles as Bimodal Imaging Agents. *J. Am. Chem. Soc.* **2010**, 132, 9833-9842.

(25) Wang, C.-H.; Nesterov, E. E. Amplifying Fluorescent Conjugated Polymer Sensor for Singlet Oxygen Detection. *Chem. Commun.* **2019**, 55, 8955-8958.

(26) Wu, C.; Szymanski, C.; McNeill, J. Preparation and Encapsulation of Highly Fluorescent Conjugated Polymer Nanoparticles. *Langmuir* **2006**, 22, 2956-2960.

(27) Beaupré, S.; Boudreault, P. T.; Leclerc, M. Solar-Energy Production and Energy-Efficient Lighting: Photovoltaic Devices and White-Light-Emitting Diodes Using Poly(2,7-fluorene), Poly(2,7-carbazole), and poly(2,7-dibenzosilole) Derivatives. *Adv. Mater*. **2010**, 22, E6-E27.

(28) Scherf. U.; List, E. J. Semiconducting Polyfluorenes – Towards Reliable Structure-Property Relationships. *Adv. Mater.* **2002**, 14, 477-487.

(29) Coakley, K. M.; McGehee, M. D. Conjugated Polymer Photovoltaic Cells. *Chem. Mater.* **2004**, 16, 4533-542.

(30) Yumusak, C.; Sariciftci, N. S. Organic Electrochemical Light-Emitting Field Effect Transistors. *Appl. Phys. Lett.* **2010**, 97, 033302.

(31) Kim, N.-K.; Jang, S.-Y.; Pace, G.; Caironi, M.; Park, W.-T.; Khim, D.; Kim, J.; Kim, D.-Y.; Noh, Y.-Y. High-Performance Organic Field-Effect Transistors with Directionally Aligned Conjugated Polymer Film Deposited from Pre-Aggregated Solution. *Chem. Mater.* **2015**, 27, 8345-8353.

(32) Chen, Z.; Yan, L.; Rech, J. J.; Hu, J.; Zhang, Q.; You, W. Green-Solvent-Processed Conjugated Polymers for Organic Solar Cells: The Impact of Oligoethylene Glycol Side Chains. *ACS Appl. Polym. Mater.* **2019**, 1, 804-814.

(33) Baker, M. A.; Ayuso-Carrillo, J.; Koos, M. R. M.; Macmillan, S. N.; varni, A. J.; Gil, R. R.; Noonan, K. J. T. A Robust Nickel Catalyst with an Unsymmetrical Propyl-Bridged Diphosphine Ligand for Catalyst-Transfer Polymerization. *Polym. J.* **2019**,

(34) Grisorio, R.; Suranna, G. P. Intramolecular Catalyst-Transfer Polymerization of Conjugated Monomers: From Lessons Learned to Future Challenges. *Polym. Chem.* **2015**, 6, 7781-7795.

(35) Wilot, P.; Govaerts, S.; Koeckelberghs, G. The Controlled Polymerization of Poly(cyclopentadithiophenes)s and Their All-Conjugated Block Copolymers *Macromolecules* **2013**, 46, 8888-8895.

(36) Yokozawa, T.; Ohta, Y. Scope of Controlled Synthesis via Chain-Growth Condensation Polymerization: From Aromatic Polyamides to π-Conjugated Polymers. *Chem. Commun.* **2013**, 49, 8281-8310.

(37) Holliday, S.; Li, Y.; Luscombe, C. K.; Recent Advances in High Performance Donor-Acceptor Polymers for Organic Photovoltaics. *Prog. Polym. Sci.* **2017**, 70, 34-51.

(38) Lu, L.; Zheng, T.; Wu, Q.; Schneider, A. M.; Zhao, D.; Yu, L. Recent Advances in Bulk Heterojunction Polymer Solar Cells. *Chem*. *Rev.* **2015**, 115-12666-12731.

(39) Schon, T. B.; McAllister, B. T.; Li, P.-F.; Seferos, D. S.; The Rise of Organic Electrode Materials for Energy Storage. *Chem. Soc. Rev.* **2016**, 45, 6345-6404.

(40) Li, S.; Ye, L.; Zhao, W.; Yan, H.; Yang, B.; Liu, D.; Li, W.; Ade, H.; Hou, J. A Wide Band Gap Polymer with a Deep Highest Occupied Molecular Orbital Level Enables 14.2% Efficiency in Polymer Solar Cells. *J. Am. Chem. Soc.* **2018**, 140, 7159-7167.

(41) Liang, Y.; Xu, Z.; Xia, J.; Tsai, S.-T.; Wu, Y.; Li, G.; Ray, C.; Yu, L. For the Bright Future-Bulk Heterojunction Polymer Solar Cells with Power Conversion Efficiency of 7.4%. *Adv. Mater.* **2010**, 22, E135-E138.

(42) Yokozawa, T.; Yokoyama, A. Chain-Growth Condensation Polymerization for the synthesis of Well-Defined Condensation Polymers and π-Conjugated Polymers. *Chem. Rev.* **2009**, 109, 5595-5619.

(42) Grubbs, R. B.; Grubbs, R. H. 50th Anniversary Perspective: Living Polymerization-Emphasizing the Molecule in Macromolecules. *Macromolecules* **2017**, 6979-6997.

(43) Hirao, A.; Goseki, R.; Ishizone, T. Advances in Living Anionic Polymerization: From Functional Monomers, Polymerization Systems, to Macromolecular Architectures. *Macromolecules* **2014**, 47, 1883-1905.

(44) Hadjichristidis, N; Pitskalis, M; Pispas, S.; Iatrou, H. Polymers with Complex Architecture by Living Anionic Polymerization. *Chem. Rev.* **2001**, 101, 3747-3792.

(45) Steverlynck, J.; De Cattelle, A.; De Winter, J.; Gerbaux, P.; Koeckelberghs, G. Energy Transfer in Poly(3-hexylthiophene)-*g*-Polyfluorene graft copolymers. *J. Polym. Sci. Part A Polym. Chem.* **2016**, 54, 1252-1258.

(46) Beers, K. L.; Gaynor, S. G.; Matyjaszewski, K.; Sheiko, S. S.; Möller, M. The Synthesis of Densely Grafted Copolymers by Atom Transfer Radical Polymerization. *Macromolecules* **1998**, 31, 9413-9415.

(47) Feng, C.; Li, Y.; Yang, D.; Hu, J.; Zhang, X.; Huang, X. Well-Defined Graft Copolymers: From Controlled Synthesis to Multipurpose Applications. *Chem. Soc. Rev.* **2011**, 40, 1282-1295.

(48) Konkolewicz, D.; Monteriro, M. J.; Perrier, S. Dendritic and Hyperbranched Polymers from Macromolecular Units: Elegant Approaches to the Synthesis of Functional Polymers. *Macromolecules* **2011**, 44, 7067-7087.

(49) Vazaios, A.; Lohse, D. J.; Hadjichristidis, N. Linear and Star Block Copolymers of Styrenic Macromonomers by Anionic Polymerization. *Macromolecules* **2005**, 38, 5468-5474.

(50) Junnila, S.; Houbenov, N.; Karatzas, A.; Hadjichristidis, N.; Hirao, A.; Iatrou, H.; Ikkala O. Side-Chain-Controlled Self-Assembly of Polystyrene-Polypeptide Miktoarm Star Copolymers. *Macromolecules* **2012**, 45, 2850-2856.

(51) He, W.; Patrick, B. O.; Kennepohl, P. Identifying the Missing Link in Catalyst-Transfer Polymerization. *Nat. Commun.* **2018**, 9, 3866.

(52) Lee, C.; Lee, S.; Kim, G.-U.; Lee, W.; Kim, B. Recent Advances, Design Guidelines, and Prospects of All-Polymer Solar Cells. *Chem. Rev.* **2019**, 119, 8028-8086.

(53) Bryan, Z.; McNeil, A. J. Conjugated Polymer Synthesis via Catalyst-Transfer Polycondensation (CTP): Mechanism, Scope, and Applications. *Macromolecules* **2013**, 8395-8405.

(54) Lee, S. M.; Park, K. H.; Jung. S.; Park. H.; Yang, C. Stepwise heating in Stille Polycondensation Toward No Batch-To-Batch Variations in Polymer Solar Cell Performance. *Nat. Commun*. **2018**, 9, 1867.

(55) Menon, A.; Dong, H.; Niazimbetova, Z. I.; Rothberg, L. J.; Galvin, M. E. Polydispersity Effects on Conjugated Polymer Light-Emitting Diodes. *Chem. Mater.* **2002**, 14, 3668-3675.

(56) Cherniawski, B. P.; Lopez, S. A.; Burnett, E. K.; Yavuz, I.; Zhang, I.; Parkin, S. R.; Houk, K. N.; Briseno, A. L. The Effect of Hexyl Side Chains on Molecular Conformations, Crystal Packing, and Charge Transport of Oligothiophenes. *J. Mater. Chem. C.* **2017**, 5, 582-588.

(57) Burnett, E. K.; Ai, Q.; Cherniawski, B. P.; Parkin, S. R.; Risko, C.; Briseno, A. L. Even-Odd Alkyl Chain-Length Alternation Regulates Oligothiophene Crystal Structure. *Chem. Mater.* **2019**, 31, 6900-6907.

(58) Bässler, H. Charge Transport in Disordered Organic Photoconductors. *Phys. Stat. Sol.* **1993**, 175, 15-36.

(59) Thienpoint, H.; Rikken, G. L. J. A.; Meijer, E. W. Saturation of the Hyperpolarizability of Oligothiophenes *Phys. Rev. Lett.* **1990**, 65, 2141-2144.

(60) Levitsky, I. A.; Kim, J.; Swager, T. M. Energy Migration in a Poly(phenylene ethnylene): Determination of Interpolymer Transport in Anisotropic Langumuir-Blodgett Films. *J. Am. Chem. Soc.* **1999**, 121, 1466-1472.

(61) Yan, M. Y.; Rothberg, L. J.; Papadimitrakopoulos, F.; Galvin, M. E.; Miller, T. M. Defect Quenching of Conjugated Polymer Luminescence. *Phys. Rev. Lett.* **1994**, 73, 744-747.

(62) Leone, A. K.; Souther, K. D.; Vitek, A. K.; LaPointe, A. M.; Coates, G. W.; Zimmerman, P. M.; McNeil, A. J. Mechanistic Insight into Thiophene Catalyst-Transfer Polymerization Mediated by Nickel Diimine Catalsyt. *Macromolecules* **2017**, 9121-9127.

(63) Sheina, E. E.; Liu, J. S.; Iovu, M. C.; Laird, D. W.; McCullough, R. D. Chain-Growth Mechanism for Regioregular Nickel-Initiated Cross-Coupling Polymerizations. *Macromolecules* **2004**, 37, 3526-3528.

(64) Yokoyama, A.; Miyakoshi, R.; Yokozawa, T. Chain-Growth Polymerization for Poly(3-hexylthiophene) with a Defined Molecular Weight and a Low Polydispersity. *Macromolecules* **2004**, 37, 1169-1171.

(65) Kiriy, A.; Senkovskyy, V.; Sommer, M. Kumada Catalyst-Transfer Polycondensation: Mechanism, Opportunities, and Challenges. *Macromol. Rapid Commun.* **2011**,32, 1503-1517.

(66) Lutz, J. P.; Hannigan, M. D.; McNeil, A. J. Polymers Synthesized via Catalyst-Transfer Polymerization and Their Applications. *Coord. Chem. Rev.* **2018**, 376, 225-247.

(67) Yokoyama, A.; Suzuki, H.; Kubota, Y.; Ohuchi, K.; Higashimura, H.; Yokozawa. Chain-Growth Polymerization for the Synthesis of Polyfluorene via Suzuki-Miyaura Coupling Reaction from an Externally Added Initiator Unit. *J. Am. Chem. Soc.* **2007**, 129, 7236-7237.

(68) Yokozawa, T.; Kohno, H.; Ohta, Y.; Yokoyama, A. Catalyst-Transfer Suzuki-Miyaura Coupling Polymerization for Precision Synthesis of Poly(*p*-phenylene). *Macromolecules* **2010**, 43, 7095-7100.

(69) Zhang, H.-H.; Xing, C.-H.; Hu, Q.-S. Controlled Pd(0)/*t*-Bu_3P-Catalyzed Suzuki Cross-Coupling Polymerization of AB-Type Monomers with PhPd(*t*-Bu_3P)I or $Pd_2(dba)_3$/*t*-Bu_3P/ArI as the Initiator. *J. Am. Chem. Soc.* **2012**, 134, 13156-13159.

(70) Sui, A.; Shi, X.; Tian, H.; Gend, Y.; Wang. Suzuki-Miyaura Catalyst-Transfer Polycondensation with Pd(IPr)$(OAc)_2$ as the catalyst for the controlled synthesis of polyfluorenes and polythiophenes. *Polym. Chem.* **2014**, 5, 7072-7080.

(71) Cox, P. A.; Reid, M.; Leach, A. G.; Campbell, A. D.; King, E. J. Lloyd-Jones, G. C. Base-Catalyzed Aryl-B$(OH)_2$ Protodeboronation Revisited: From Concerted Proton Transfer to Liberation of a Transient Aryl Anion. *J. Am. Chem. Soc.* **2017**, 13156-13165.

(72) Carrillo, J. A.; Ingleson, M. J.; Turner, M. L. Thienyl MIDA Boronate Esters as Highly Effective Monomers for Suzuki-Miyaura Polymerization Reactions. *Macromolecules* **2015**, 48, 979-986.

(73) Kosaka, K.; Ohta, Y.; Yokozawa, T. Influence of the Boron Moiety and Water on Suzuki-Miyaura Catalyst-Transfer Condensation Polymerization. *Macromol. Rapid Commun.* **2015**, 36, 373-377.

(74) Zhang, H.-H.; Hu, Q.-S.; Hong, K. Accessing Conjugated Polymers with Precisely Controlled Heterobisfunctional Chain Ends via Post-Polymerization Modification of the OTf Group and Controlled Pd(0)/*t*-Bu_3P-Catalyzed Suzuki-Cross-Coupling Polymerization. *Chem. Commun.* **2015**, 51, 14869-14872.

(75) Zhang, H.-H.; Ma, C.; Bonnesen, P. V.; Zhu, J.; Sumpter, B. G.; Carrillo, J.-M. Y.; Yin, P.; Wang, Y.; Li, A.-P.; Hong, K. Helical Poly(5-alkyl-2,3-thiophenes)s: Controlled Synthesis and Structure Characterization *Macromolecules* **2016**, 49, 4691-4698.

(76) Kosaka, K.; Uchida, T.; Mikami, K.; Ohta, Y.; Yokozawa, T. AmPhos Pd-Catalyzed Suzuki-Miyaura Catalyst-Transfer Condensation Polymerization: Narrower Dispersity by Mixing the Catalyst and Base Prior to Polymerization. *Macromolecules* **2018**, 51, 364-369.

(77) Seo, K.-B.; Lee, I.-H.; Lee, J.; Choi, I.; Choi, T.L. A Rational Design of Highly Controlled Suzuki-Miyaura Catalyst Transfer Polycondensation for Precision Synthesis of Polythiophenes and Their Block Copolymers: Marriage of Pallacycle Precatalysts with MIDA-Boronates. *J. Am. Chem. Soc.* **2017**, 140, 4335-4343.

(78) Nojima, M.; Kamigawara, T.; Ohta, Y.; Yokozawa, T. Catalyst-Trasnfer Suzuki-Miyaura Condensation Polymerization of Stilebene Monomer: Different Polymerization Behavior Depending on Halide and Aryl Group of Aryl Group of ArPd(^{t}Bu_3P)X Initiator *J. Polym. Sci. A.* **2019**, 57, 297-304.

(79) Kamigawara, T.; Sugita, H.; Mikami, K.; Ohta, Y.; Yokozawa, T. Intramolecular Transfer of Pd Catalyst on Carbon-Carbon Triple Bond and Nitrogen-Nitrogen Double Bond in Suzuki-Miyaura Coupling Reaction *Catalysis* **2017**, 7, 195.

(80) Yokozawa, T.; Harada, N.; Sugita, H.; Ohta, Y. Intramolecular Catalyst Transfer on a Variety of Functional Groups Between Benzene Rings in a Suzuki-Miyaura Coupling Reaction. *Chem. Eur. J.* **2019**, 25, 10059-10062.

(81) Zhao, C.; Nagura, K.; Takeuchi, M; Sugiyasu, K. Twisting Poly(3-substituted thiophene)s: Cyclopolymerization of Gemini Thiophene Monomers Through Catalyst-Transfer Polycondensation. *Polym. J.* **2017**, 49, 133-139.

(82) Lee, J.-H.; Chen, C.-H.; Lee, P.-H.; Lin, H.-Y.; Leung, M.-K.; Chiu, T.-L.; Lin, C.-F. Blue Organic Light-Emitting Diodes: Current Status, Challenges, and Future Outlook. *J. Mater. Chem. C.* **2019**, 5874-5888.

(83) Verheyen, L.; Janssens, K.; Marinelli, M.; Salatelli, E.; Koeckelberghs, G. Rational Design of Poly(fluorene)-*b*-poly(thiophene) Block Copolymers to Obtain a Unique Aggregation Behavior. *Macromolecules* **2019**, 52, 6578-6584.

(84) Eede, M.-P. V. D.; Winter, J. D.; Gerbaux, P.; Koeckelberghs, G. Controlled Polymerization of a Cyclopentadithiophene-Phenylene Alternating Copolymer. *Macromolecules* **2018**, 51, 9043-9051.

(85) Eede, M.-P. V. D.; Winter, J. D.; Gerbaux, P.; Teyssandier, J.; Feyter, S. D.; Goethem, C. V.; Vankelecom, I. F. J.; Koeckelberghs, G. Controlled Synthesis and Supramolecular Organization of Conjugated Star-Shaped Polymers. *Macromolecules* **2018**, 51, 8689-8697.

(86) Jagadesan, P.; Schanze, K. S. Poly(phenylene ethynylene) Conjugated Polyelectrolytes Synthesized via Chain-Growth Polymerization. *Macromolecules* **2019**, 52, 3845-3851.

(87) Grisorio, R.; Suranna, G. P. Catalyst-Transfer Polymerization of Arylamines by the Buchwald-Hartwig Cross-Coupling. *Polym. Chem.* **2019**, 10, 1947-1955.

(88) Li, Z.; Gelbaum, C.; Fisk, J. S.; Holden, B.; Jaganathan, A.; Whiteker, G. T.; Pollet, P.; Liotta, C. L. Aqueous Suzuki Coupling Reactions of Basic Nitrogen-Containing Substrates in the Absence of Added Base and Ligand: Observation of High Yields under Acidic Conditions. *J. Org. Chem.* **2016**, 81, 8520-8529.

(89) Li, Z.; Gelbaum, C.; Campbell, Z. S.; Gould, P. C.; Fisk, J. S.; Holden, B.; Jaganathan, A.; Whiteker, G. T.; Pollet, P.; Liotta, C. L. Pd-Catalyzed Suzuki Coupling Reactions of Aryl Halides Containing Basic Nitrogen Centers with Aryl Boronic Acids in Water in the Absence of Added Base. *New J. Chem.* **2017**, 41, 15420-15432.

(90) Bässler, H.; Brandl, V.; Deussen, M.; Göbel, E. O.; Kersting, R.; Kurz, H.; Lemmer, U.; Mahrt, R. F.; Ochse, A. Excitation Dynamics in Conjugated Polymers. *Pure & Appl. Chem.* **1995**, 67, 377-385.

(91) Bässler, H.; Schweitzer, B. Site-Selective Fluorescence Spectroscopy of Conjugated Polymers and Oligomers. *Acc. Chem. Res.* **1999**, 32, 173-182.

(92) Yan, M.; Rothberg, L. J.; Kwock, E. W.; Miller, T. M. Interchain Excitations in Conjugated Polymers. *Phys. Rev. Lett.* **1995**, 75, 1992-1995.

(93) Theander, M.; Inganäs, O. Photophysics of Substituted Polythiophenes *J. Phys. Chem. B.* **1999**, 103, 7771-7780.

(94) Swager, T. M.; Gil, C. J.; Wrighton, M. S. Fluorescence Studies of Poly(*p*-phenyleneethynlene)s: The Effect of Anthracene Substitution. *J. Phys. Chem.* **1995**, 99, 4886-4893.

(95) Murphy, C. B.; Zhang, Y.; Troxler, T.; Ferry, V.; Martin, J. J.; Jones, W. E. Probing Förster and Dexter Energy-Transfer Mechanisms in Fluorescent Conjugated Polymer Chemosensors. *J. Phys. Chem. B* **2004**, 108, 1537-1543.

(96) Faure, S.; Stern, C.; Guilard, R.; Harvey, P. D. Role of the Spacer in the Singlet-Singlet Energy Transfer Mechanism (Föster vs Dexter) in Cofacial Bisporphyrins. *J. Am. Chem. Soc.* **2004**, 126, 1253-1261.

(97) Levitsky, I. A.; Kim, J.; Swager, T. M. Energy Migration in a Poly(phenylene ethynylene): Determination of Interpolymer Transport in Anisotropic Langmuir-Blodgett Films. *J. Am. Chem. Soc.* **1999**, 121, 1466-1472.

(98) Nguyen, T.-Q.; Wu, J.; Doan, V.; Schwartz, B. J.; Tolbert, S. H. Control of Energy Transfer in Oriented Conjugated Polymer-Mesoporous Silica Composites. *Science* **2000**, 288, 652-656.

(99) Tretiak, S.; Saxena, A.; Martin, R. L. Bishop, A. R. Interchain Electronic Excitations in Poly(phenylenevinylene) (PPV) Aggregates. *J. Phys. Chem. B* **2000**, 104, 7029-7037.

(100) Nguyen, T.-Q.; Doan, V.; Schwartz, B. J. Conjugated Polymer Aggregates in Solution: Control of Interchain Interactions. *J. Chem. Phys.* **1999**, 110, 4068-4078.

(101) Ansari, M. A.; Mohiuddin, S.; Kandemirli, F.; Malik, M. I. Synthesis Characterization of Poly(3-hexylthiophene): Improvement of Regioregularity and Energy Band Gap. *RSC Adv.* **2018**, 8, 8319-8328.

(102) Cornil, J.; Beljonne, D.; Calbert, J.-P.; Brèdas, J.-L. Interchain Interactions in Organic π-Conjugated Materials: Impact on Electronic Structure, Optical Response, and Charge Transport. *Adv. Mater.* **2001**, 13, 1053-1067.

(103) Yan, T.; Song, W.; Huang, J.; Peng, R.; Huang, L.; Ge, Z. 16.67% Rigid and 14.06% Flexible Organic Solar Cells Enabled by Ternary Heterojunction Strategy. *Adv. Mater.* **2019**, 1902210.

(104) Xiong, S.; Hu. L.; Hu. L.; Sun, L.; Qin, F.; Liu, X.; Fahlman, M.; Zhou, Y. 12.5% Flexible Nonfullerene Solar Cells by Passivating the Chemical Interaction Between the Active Layer and Polymer Interfacial Layer. *Adv. Mater.* **2019**, 31, 1806616.

(105) Allison, L. K.; Andrew, T. L. A Wearable All-Fabric Thermoelectric Generator. *Adv. Mater. Technol.* **2019**, 1800615.

(106) Lin, J.; Liu, B.; Yu, M.; Wang, X.; Lin, Z.; Zhang, X.; Sun, C.; Cabanillas-Gonzalez, J.; Xie, L.; Liu, F.; Ou, C.; Bai, L.; Han, Y.; Xu, M.; Zhu, W.; Smith, T. A.; Stavrinou, P. N.; Bradley D. D. C.; Huang, W. Ultrastable Supramolecular Self-Encapsulated Wide-Bandgap Conjugated Polymers for Large-Area and Flexible Electroluminescent Devices. *Adv. Mater.* **2019**, 1804811.

(107) Tang, S.-J.; Liu, Z.; Qian, Y.-J.; Shi, K.; Sun. Y.; Wu, C.; Gong, Q.; Xiao, Y.-F. A Tunable Optofluidic Microlaser in a Photostable Conjugated Polymer *Adv. Mater.* **2018**, 30, 1804556.

(108) Jager, E. W. H.; Inganäs, O.; Lundström, I. Microrobots for Micrometer-Size Objects in Aqueous Media: Potential Tools for Single-Cell Manipulation. *Science* **2000**, 288, 2335.

(109) Cullen, A. T.; Price, A. D. Digital Light Processing for the Fabrication of 3D Intrinsically Conductive Polymer Structure. *Synth. Met.* **2018**, 235, 34.

(110) London, A. E.; Chen, H.; Sabuj, M. A.; Tropp, J.; Saghayezhian, M.; Eedugurala, N.; Zhang, B. A.; Liu, Y.; Gu, X.; Wong, B. M.; Rai, N.; Bowman, M. K.; Azoulay, J. D. A High-Spin Ground-State Donor-Acceptor Conjugated Polymer. *Sci. Adv.* **2019**, 5:eaav2336.

(111) Liao, Y.; Wang, H.; Zhu, M.; Thomas, A. Efficient Supercapacitor Energy Storage Using Conjugated Microporous Polymer Networks Synthesized from Buchwald-Hartwig Coupling. *Adv. Mater.* **2018**, 30, 1705710.

(112) Xie, J.; Gu, P.; Zhang, Q. Nanostructured Conjugated Polymers: Toward High-Performance Organic Electrodes for Rechargeable Batteries. *ACS Energy Lett.* **2017**, 2, 1985-1996.

(113) Xu, S.; Wang, G.; Biswal, B. P.; Addicoat, M.; Paasch, S.; Sheng, W.; Zhuang, X.; Brunner, E.; Heine, T.; Berger, R.; Feng, X. A Nitrogen-Rich 2D sp^2-Carbon-Linked Conjugated Polymer Framework as a High-Performance Cathode for Lithium-Ion Batteries. *Angew. Chem. Int. Ed.* **2019**, 58, 849-853.

CHAPTER 2. SILVER(I) MEDIATED SUZUKI-MIYAURA CATALYST TRANSFER POLYMERIZATION: EVIDENCE OF THE OXO-PALLADIUM PATHWAY

2.1. Introduction

Precision synthesis of complex macromolecular structures represents one of the major synthetic challenges still to be addressed in the polymer field. The ability to prepare macromolecular systems with structural exactness typical of the small-molecule synthesis is stimulated by the advanced practically useful properties as well as unique fundamental characteristics that the precise polymer systems may possess. Although scientists cannot yet rival Nature in the ability to prepare structurally precise polymers, recent developments in various living chain-growth polymerization methods started bringing such a possibility within reach. The field of conjugated polymers has recently experienced an impressive upswing towards the development of efficient controlled catalyst-transfer polymerization (CTP) protocols for the preparation of various classes of conjugated polymers (as described in Chapter 1). Conjugated polymers are materials of choice for a breadth of potential practical applications in electronic, optoelectronic and sensing devices due to tunability of their optical and electronic properties through manipulations of the polymers' chemical structure. Whereas some classes of conjugated polymers (and block copolymers) can now be readily prepared via CTP methods, the real challenge remains in applying CTP for the preparation of more complex well-defined structures[1] (e.g. where a specific structural unit would be precisely incorporated in the conjugated polymer chain – something that Nature routinely does for the case of biopolymers). For example, incorporation of a single electron deficient highly fluorescent perylenedicarboximide (PDCI) unit in a conjugated polymer chain has been previously demonstrated to dramatically alter the polymer's optical properties, even when it was done in a non-precise, step-growth polymerization.[2-3] One can argue that using an advanced CTP approach

to incorporate PDCI unit/s in conjugated polymer in a structurally precise fashion could deliver materials with novel and yet not well understood properties.[4-5] Can such a process be implemented through a rational design of a conjugated polymer coupled with a precise synthesis? In this chapter, we focus on developing externally-initiated Pd-catalyzed Suzuki-Miyaura CTP as a functional group tolerant method of choice for precision polymerization to furnish various classes of conjugated polymers. Specifically, we describe how improving understanding of various mechanistic features related to the steps involved in Suzuki-Miyaura coupling can be used to enhance the efficiency of this CTP process and bring about the previously unavailable macromolecular synthetic capabilities, as well as conjugated polymer materials with novel properties that can be rationally fine-tuned through the precision polymer synthesis.

2.2. Results and Discussion

2.2.1. Design and Preparation of the Perylenedicarboximide External Initiator

Recently, Buchwald's pre-catalysts have been shown to result in better initiation versus Pd(^{t}Bu$_3$) based catalytic systems (which are the predominant Pd CTP catalytic system, making 40% of the reports from 2008-2018).[6-8] For example, Seo *et al.* demonstrated that 3rd generation SPhos and RuPhos Pd pre-catalysts are capable of controlled polymerization of 2-bromo-3-hexylthiophene boronic acid MIDA esters, leading to controlled molecular weight, excellent yields and consistently low polydispersity for poly(3-alkylthiophenes).[9] The SCTP reaction using MIDA boronates is a remarkably complex chemical process involving more than a dozen chemical species, and many of them exist in dynamic equilibrium with each other. This requires the catalyst to be highly chemoselective in the presence of a variety of functional groups and conditions. The extraordinary performance of RuPhosPd^0 in the SCTP reaction for preparing P3HT demonstrated that it is a robust system for all of these chemical environments. To efficiently obtain a chain-

growth polymerization method for preparing alternative conjugated polymers such as poly(*p*-phenylene) (PPP) and polyfluorene (PF), we chose to focus our efforts to optimize the well-established catalytic system of RuPhos supported Pd rather than to search for a new catalyst/ancillary ligand combination and having to optimize all the other parameters from scratch. Therefore, RuPhos supported Pd was chosen as the catalytic species installed on the external initiator. Also, utilizing PDCI as an initiator precursor allowed for incorporating an electron deficient chemical unit into the polymer backbone. Intramolecular catalyst-transfer over electron deficient monomers is still an obscure problem in CTP synthesis and this was a simple solution for overcoming this barrier.[10] This strategy allowed to control the relative quantity of the acceptor molecule within the polymer chain and would allow us to study the structure dependent donor-acceptor photophysical properties in a precise manner. We also expected that the initiation process can be refined by isolating the external initiator as a solid, allowing for chemical purification and gravimetric measurements. External initiator **1** was prepared in one step by mixing a di-iodo derivative of PDCI (Figure 2.1) and stoichiometric ratio of RuPhos Pd G3 precatalyst in typical Suzuki-Miyaura conditions. After 1h at 50°C, the THF phase was precipitated into 1:5 (v/v) THF:hexanes, and then further purified by another reprecipitation step in the same solvent. Unreacted RuPhosPd^0, carbazole (produced from the Buchwald pre-catalyst activation step) and the excess free RuPhos ligand are soluble in the reprecipitation solvent, whereas the external initiator is not. The resulting brown powder is stable in air-free environments, can be easily weighted and is soluble in THF. External initiator **1** displayed typical absorption and fluorescence spectra of PDCI with bithienyl functional groups attached to the 1,7 positions. The short wavelength absorption at λ_{max} = 338 nm derives from thiophene centered electronic transition.

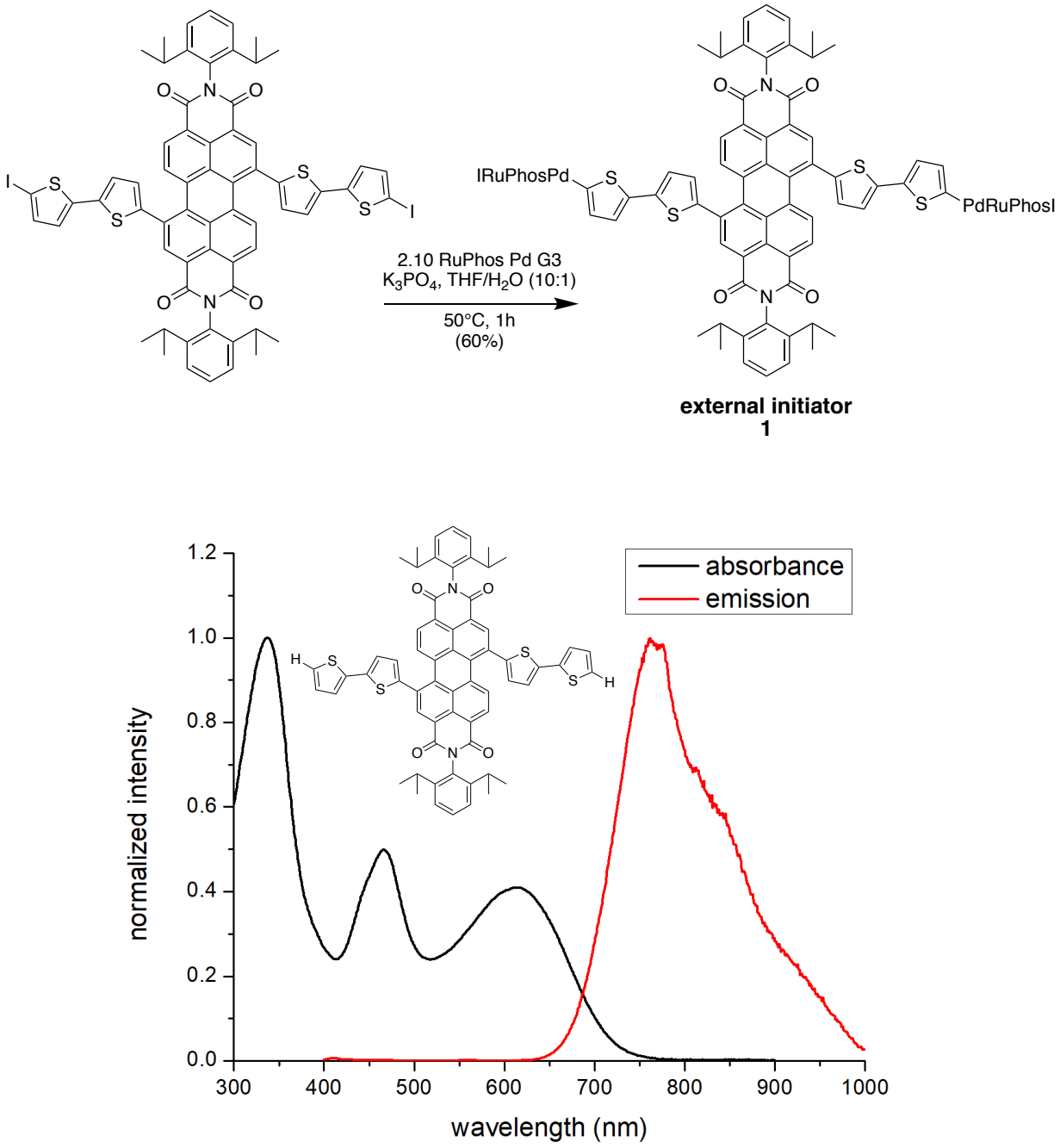

Figure 2.1. Reaction scheme for the synthesis of the external initiator **1** (top). UV-Vis absorbance (black) and emission spectra (red) of the electron deficient PDCI molecule (bottom).

The long wavelength absorption at λ_{max} = 613 nm is attributed to S_0 to S_1 transition and the absorption peak at λ_{max} = 460 nm comes from S_0 to S_2 transition taking place along the perylene long molecular axis.[11] Having bithiophene-substituted functionality in the 1,7 positions is

particularly advantageous for a functional Förster energy acceptor since both PF and PPP are expected to emit in the same UV-Vis region as the bithiophene absorbance band.[12,13]

A strong overlap of the donor molecule fluorescence bands with the absorbance bands of the energy acceptor is a critical requirement for Förster energy transfer.[14] Ideally, the design would allow for efficient long-range energy transfer from the excited state of PPP and PF to the low energy PDCI chromophore.

2.2.2. SCTP Monomer Screening Studies Using Suzuki-Miyaura Coupling Experiments

A robust intramolecular catalyst-transfer process is vital for CTP and its success is sensitive to the specific combination of the catalyst, ancillary ligand and monomer identity. As such, we explored the potential SCTP monomer scope of RuPhos Pd G3 by studying the Suzuki-Miyaura coupling of phenylboronic acid with 1,4-dibromo-2,5-dialkylbenzenes, 9,9-dialkyl-2,7-dibromofluorenes, 2,5-dibromo-3-alkylthiophenes and several related dihaloarenes.

Following the oxidative addition of $L_2Pd(0)$ onto the carbon-bromine bond and subsequent exchange of bromide ligand by hydroxide, $BrArL_2PdOH$ is expected to react with phenylboronic acid to produce a mono-substituted product **M1** (Figure 2.2). If intramolecular catalyst-transfer occurs after, the subsequent oxidative addition, transmetalation and reductive elimination cycle will produce a disubstituted arene **M2**. An absolute selectivity for **M2** indicates an ideal candidate for the controlled-polymerization studies. However, if L_2Pd^0 is not able to undergo intramolecular catalyst-transfer, only **M1** is expected. Because the intermolecular catalyst-transfer process (leading to chain-transfer and loss of controlled-chain growth character) is accelerated at higher reaction temperatures, the monomer screening reactions are conducted at room temperature and only dihaloarenes that can exclusively form **M2** under SCTP conditions are considered for further polymerization studies. Semi-quantitative analysis using liquid-chromatography/total ion count

mass spectrometry (LC-MS) allowed for fast screening of 13 dihaloarenes. Ten of them demonstrated exclusive conversion to **M2** with no **M1** detected by mass spectrometry (Figure 2.2).

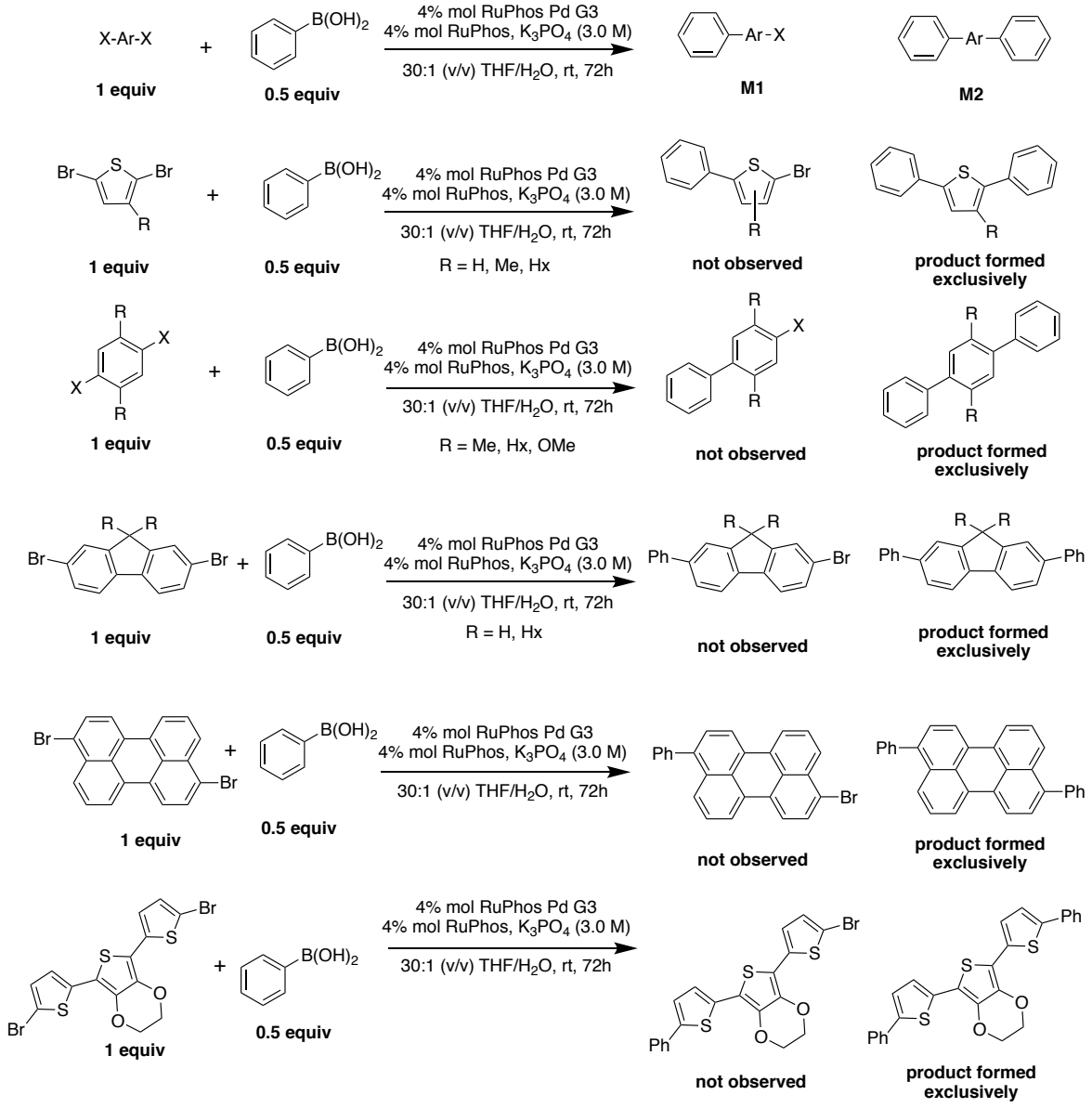

Figure 2.2.Summary of monomer screening studies showing dihaloarenes exclusively forming the intramolecular catalyst-transfer product **M2** in Suzuki-Miyaura Catalyst-Transfer Polymerization reaction conditions using RuPhos Pd G3 as the pre-catalyst.

Along with several 1,4-dibromo-2,5-dialkylbenzenes (Figures 2.6 and 2.7), 9,9-dialkyl-2,7-dibromofluorenes (Figures 2.3 and 2.4) and 2,5-dibromo-3-alkythiophenes (Figures 2.10, 2.11 and 2.12), 3,9-dibromoperylene (Figure 2.9), 2,5-di(5'-bromo-2-thienyl)-3,4-ethylenedioxythiophene

(Figure 2.13) and 4-iodo-1-bromobenzene (Figure 2.14) showed exclusive formation of **M2** and were identified to be promising candidates for Suzuki-Miyaura controlled-chain growth polymerization studies using RuPhos Pd G3 as the pre-catalyst. Expectedly, 2,5-divinyl-substituted 1,4-dibromobenzene (Figure 2.8) included in this experiment did not show strong intramolecular catalyst-transfer capabilities even at room temperature and thus was excluded from controlled chain-growth polymerization studies. Vinyl-substituents can form irreversible π-associative complexes with Ni and Pd based catalysts and inhibit controlled chain-growth. The exact mass of the **M1** product resulting from coupling between 3,9-dibromoperylene and phenylboronic acid coincided with the mass spectrometer noise ions but no **M1** products were detected above this background (Figure 2.9). 2,7-dibromo-9,9-di(6'-methoxyhexyl)fluorene produced both **M1** and **M2** products (Figure 2.5) and implies that either increased steric bulk of the solubilizing groups or the ether moiety interferes with the chain-walking process (relative to the excellent result of 2,7-dibromo-9,9-dialkylfluorene in Figure 2.4).

In Pd catalyzed SCTP reactions, oxidative addition onto aryl iodides are generally faster and more efficient than oxidative addition onto aryl bromides, and 2,5-methoxy-1,4-diiodobenzene was expected to undergo efficient intramolecular transfer with RuPhos supported Pd.[15] Although 2,5-dimethoxy-1,4-diiodobenzene showed good selectivity (implying an efficient intramolecular catalyst transfer process), the low ion intensities of the **M2** product relative to the starting material suggested an inefficient coupling reaction (Figure 2.15) in comparison to 2,5-dialkyl-1,4-dibromobenzene (Figure 2.7).

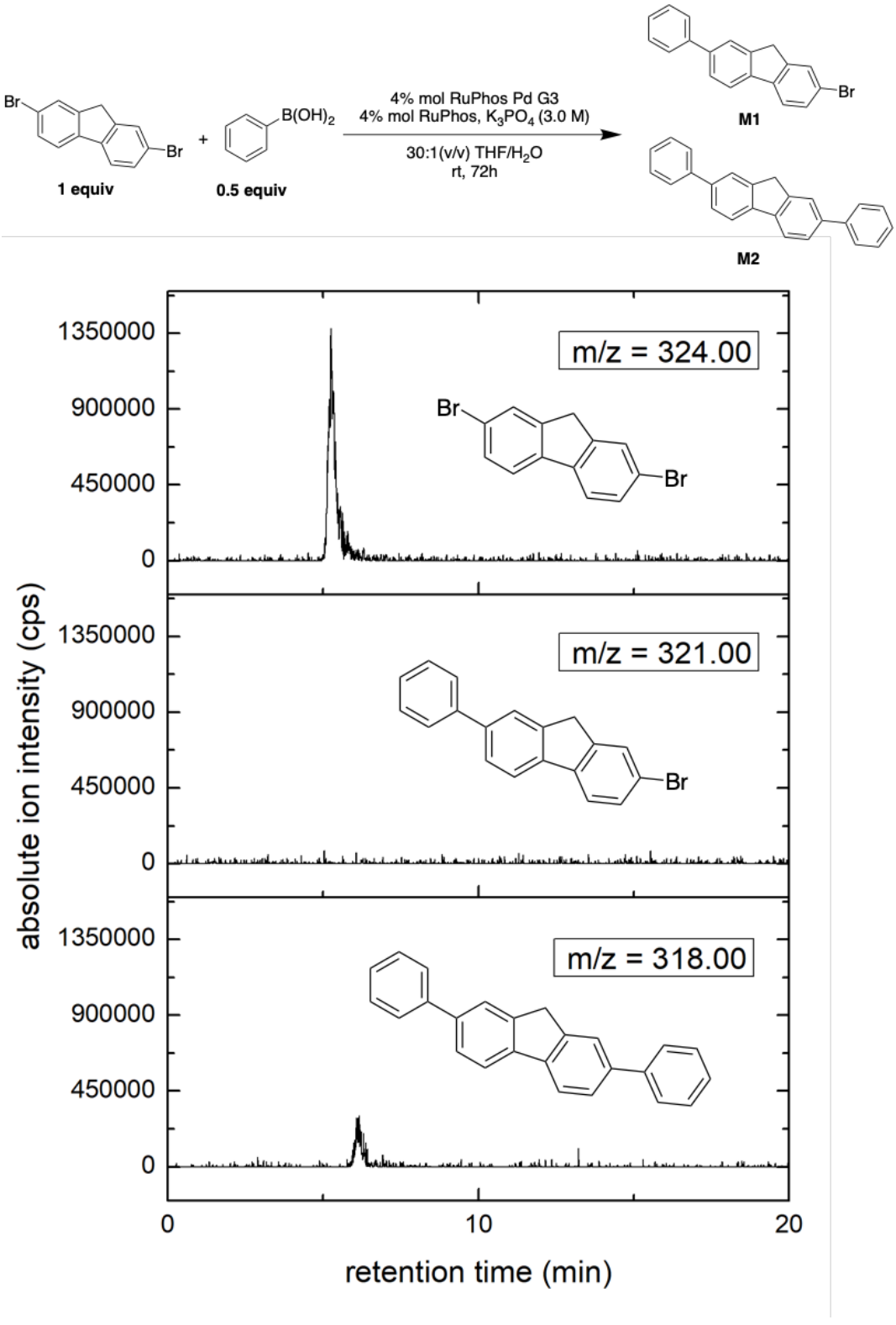

Figure 2.3.Reaction scheme of the Suzuki-Miyaura coupling between 2,7-dibromofluorene and phenylboronic acid using RuPhos Pd G3 as pre-catalyst (top). Extracted ion chromatogram of the reaction mixture after 72h at rt (bottom).

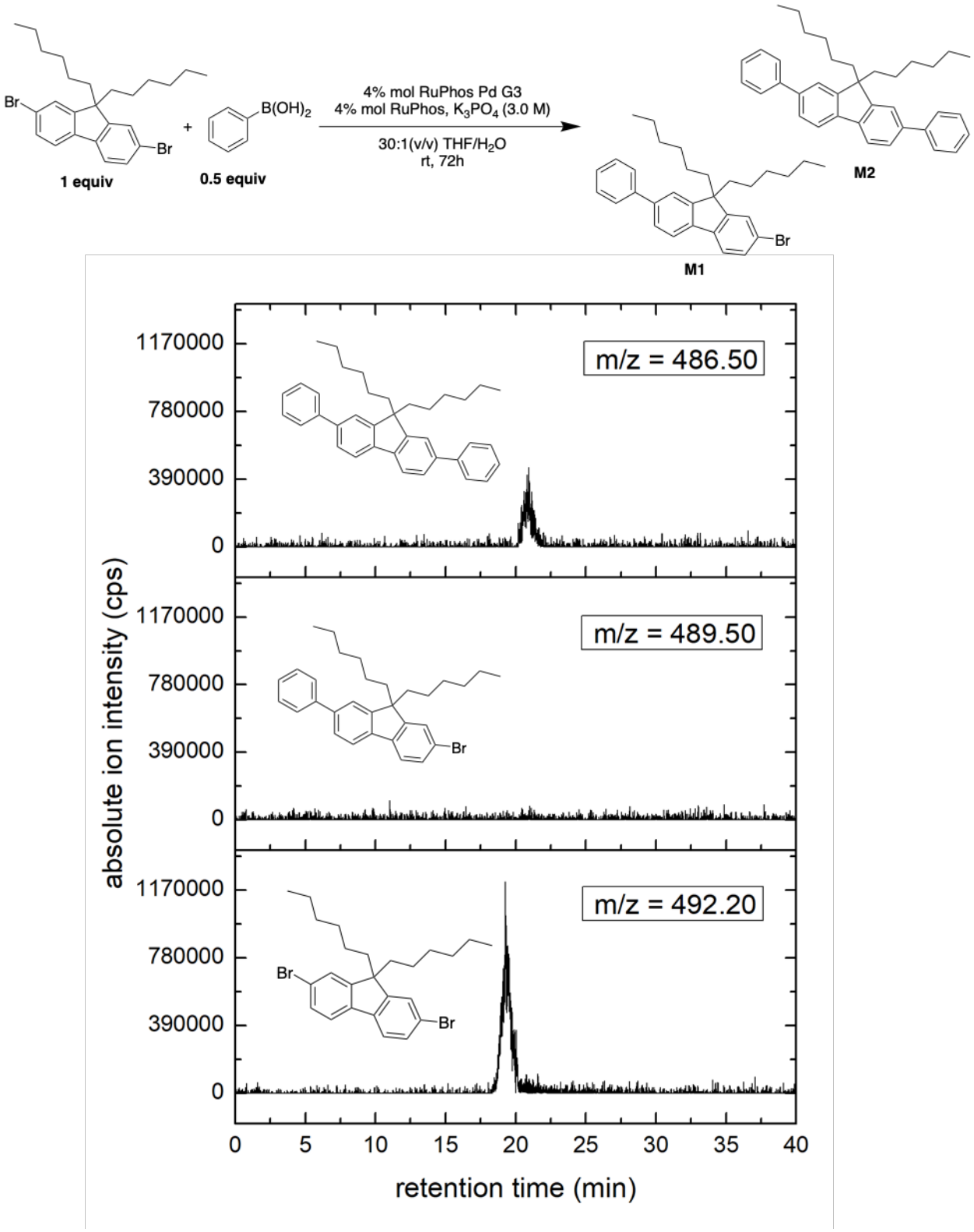

Figure 2.4. Reaction scheme of the Suzuki-Miyaura coupling between 9,9-dihexyl-2,7-dibromofluorene and phenylboronic acid using RuPhos Pd G3 as pre-catalyst (top). Extracted ion chromatogram of the reaction mixture after 72h at rt (bottom).

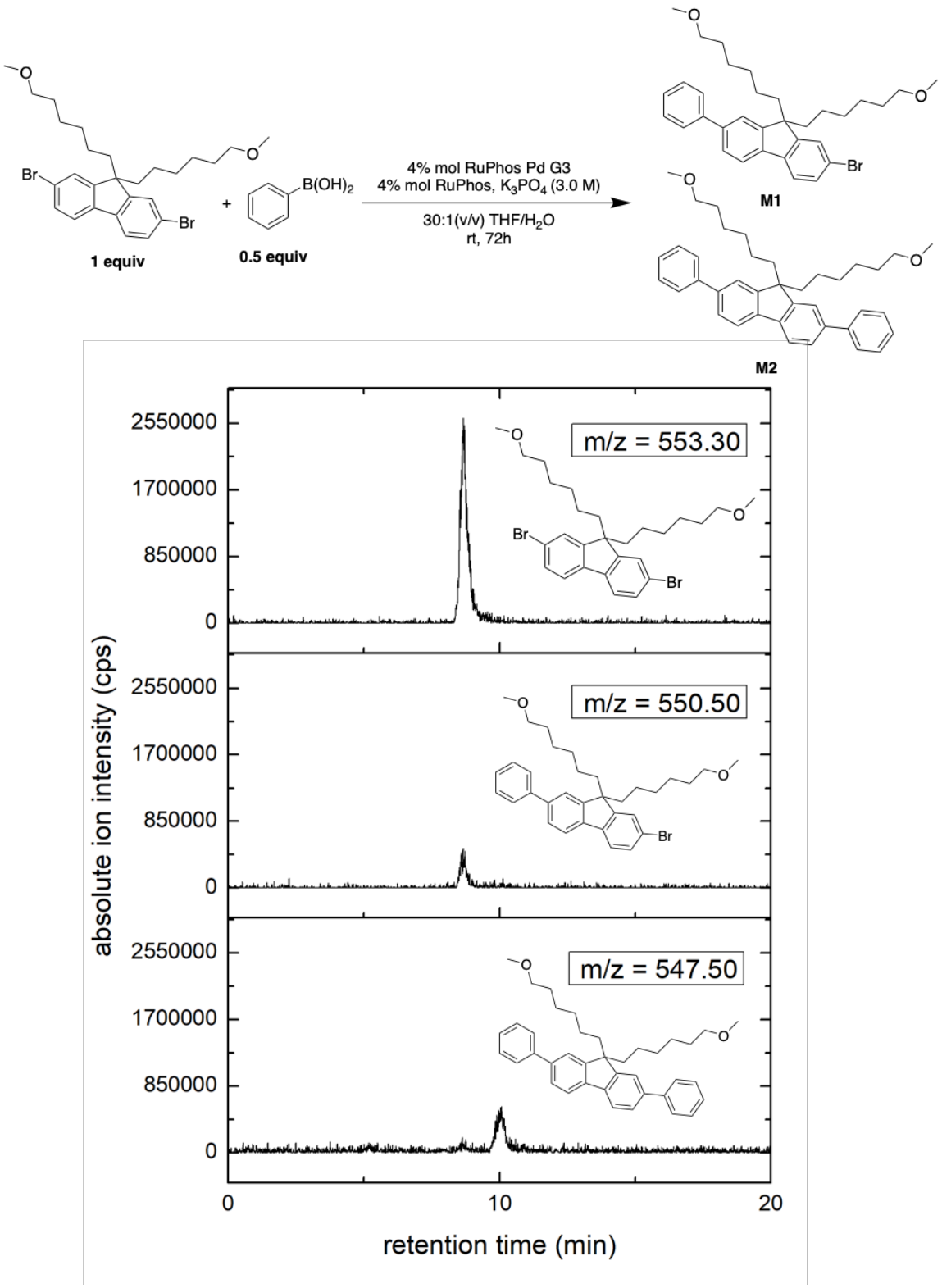

Figure 2.5. Reaction scheme of the Suzuki-Miyaura coupling between 9,9-di(6'-methoxyhexyl)-2,7-dibromofluorene and phenylboronic acid using RuPhos Pd G3 as pre-catalyst (top). Extracted ion chromatogram of the reaction mixture after 72h at rt (bottom).

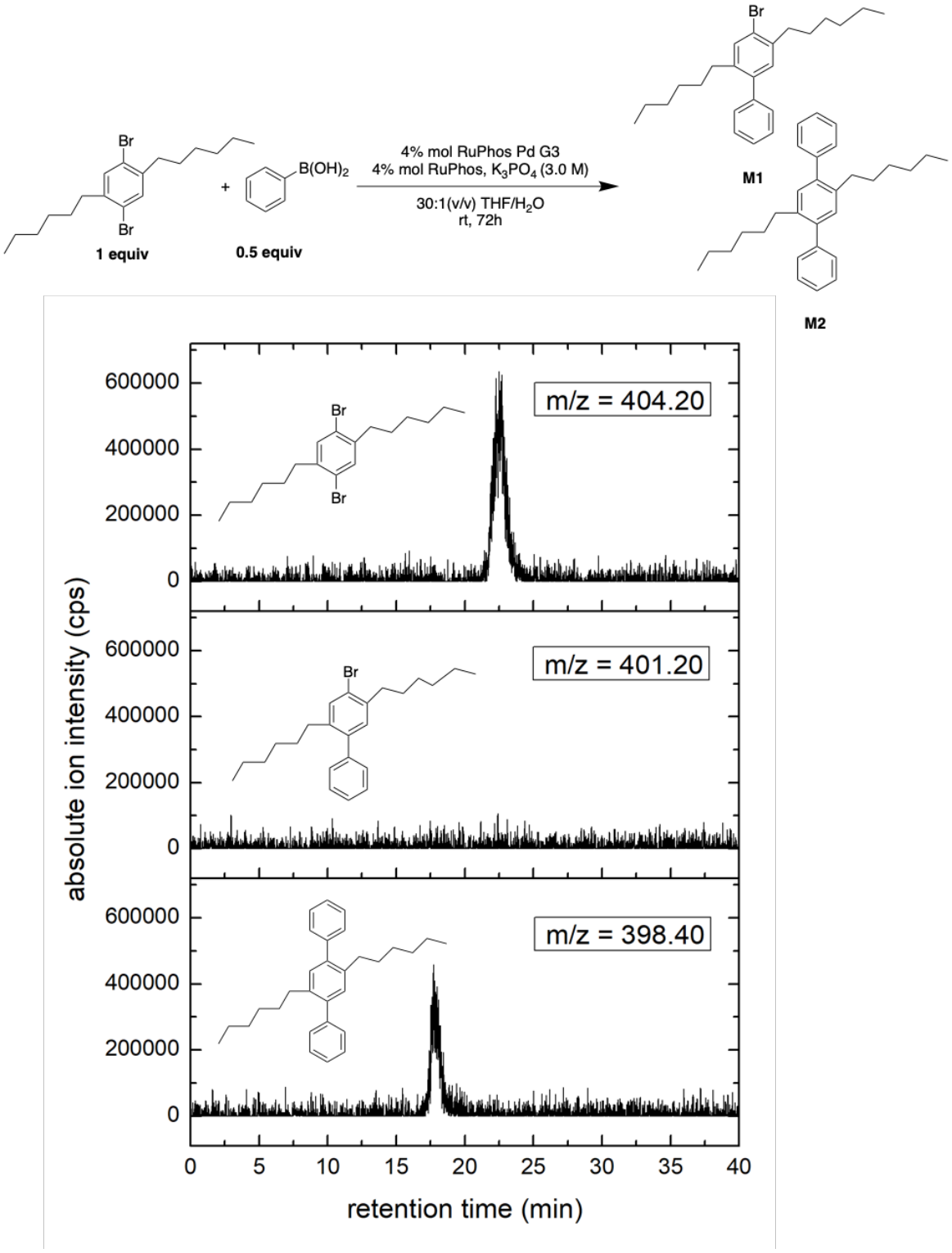

Figure 2.6.Reaction scheme of the Suzuki-Miyaura coupling between 2,5-dihexyl-1,4-dibromobenzene and phenylboronic acid using RuPhos Pd G3 as pre-catalyst (top). Extracted ion chromatogram of the reaction mixture after 72h at rt (bottom).

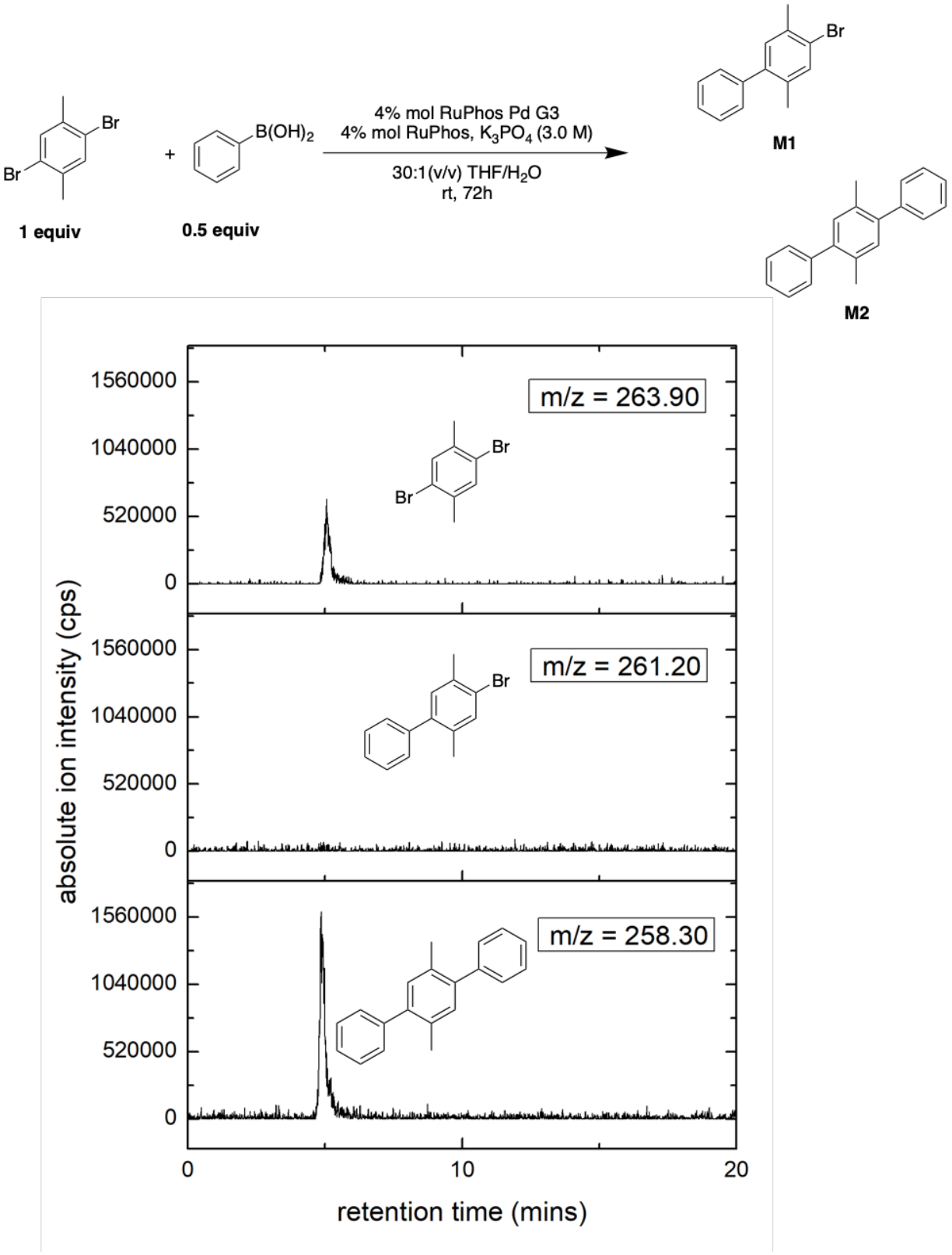

Figure 2.7. Reaction scheme of the Suzuki-Miyaura coupling between 2,5-dimethyl-1,4-dibromobenzene and phenylboronic acid using RuPhos Pd G3 as pre-catalyst (top). Extracted ion chromatogram of the reaction mixture after 72h at rt (bottom).

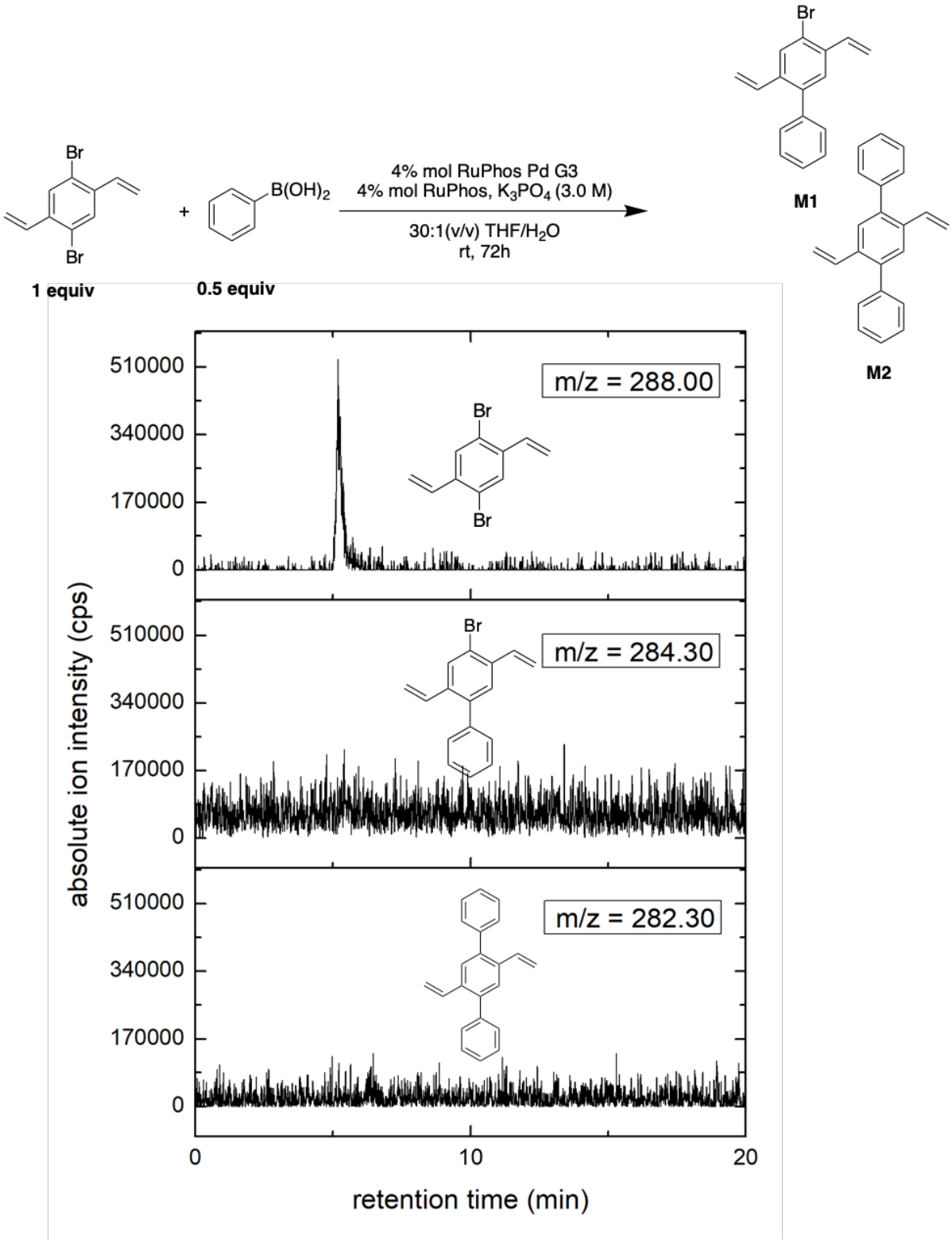

Figure 2.8. Reaction scheme of the Suzuki-Miyaura coupling between 2,5-divinyl-1,4-dibromobenzene and phenylboronic acid using RuPhos Pd G3 as pre-catalyst (top). Extracted ion chromatogram of the reaction mixture after 72h at rt (bottom).

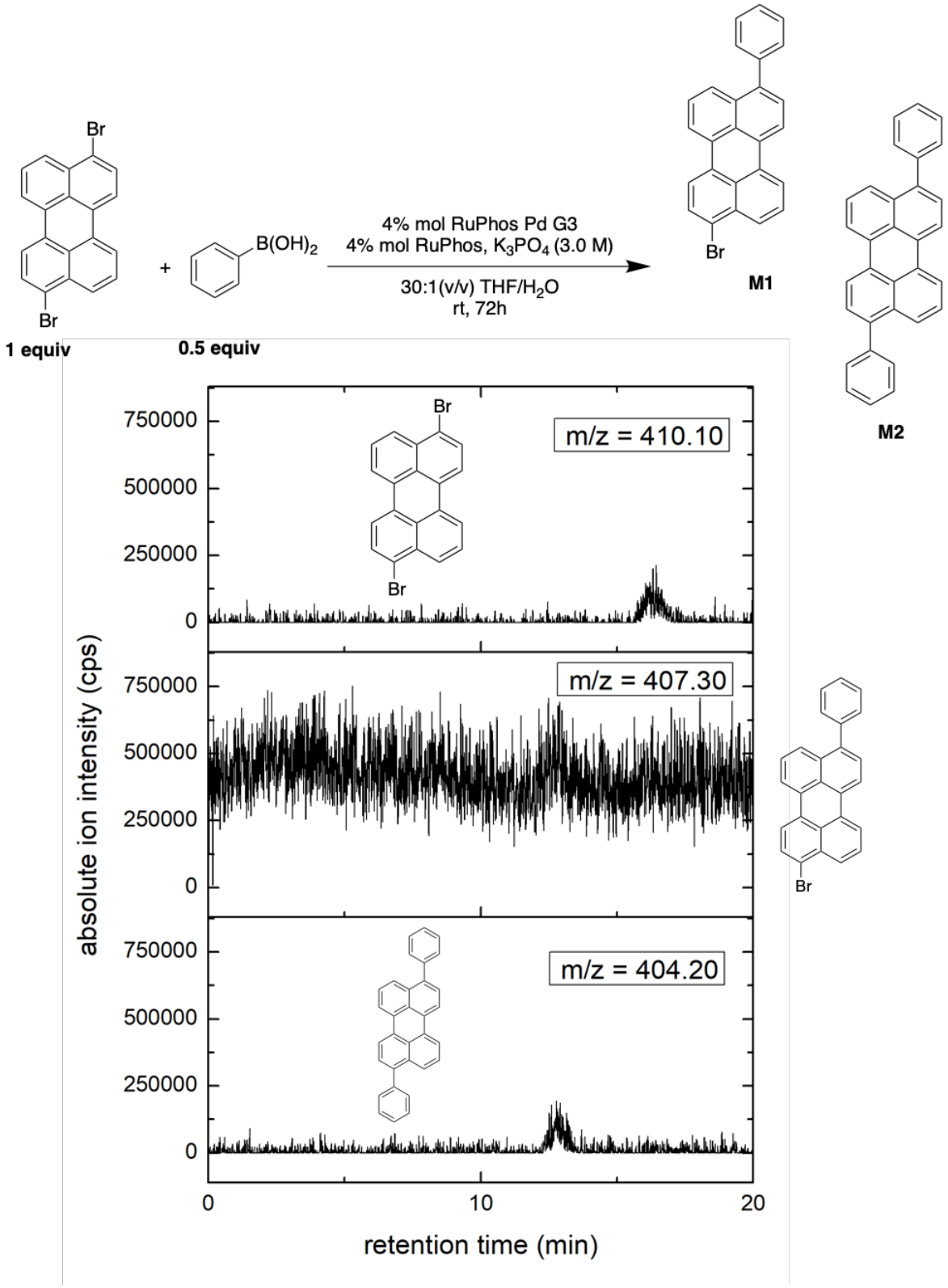

Figure 2.9. Reaction scheme of the Suzuki-Miyaura coupling between 3,9-dibromoperylene and phenylboronic acid using RuPhos Pd G3 as pre-catalyst (top). Extracted ion chromatogram of the reaction mixture after 72h at rt (bottom).

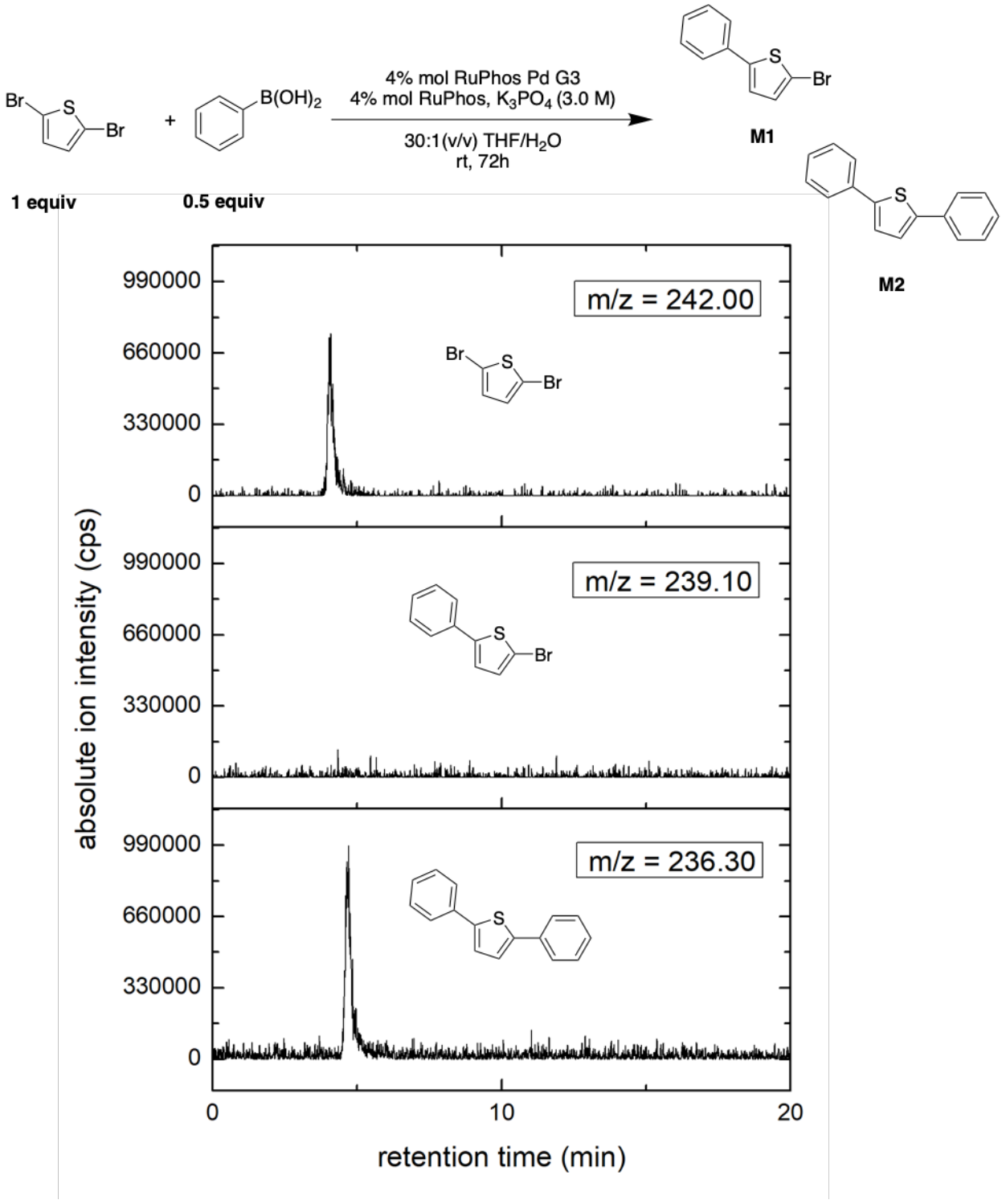

Figure 2.10. Reaction scheme of the Suzuki-Miyaura coupling between 2,5-dibromothiophene and phenylboronic acid using RuPhos Pd G3 as pre-catalyst (top). Extracted ion chromatogram of the reaction mixture after 72h at rt (bottom).

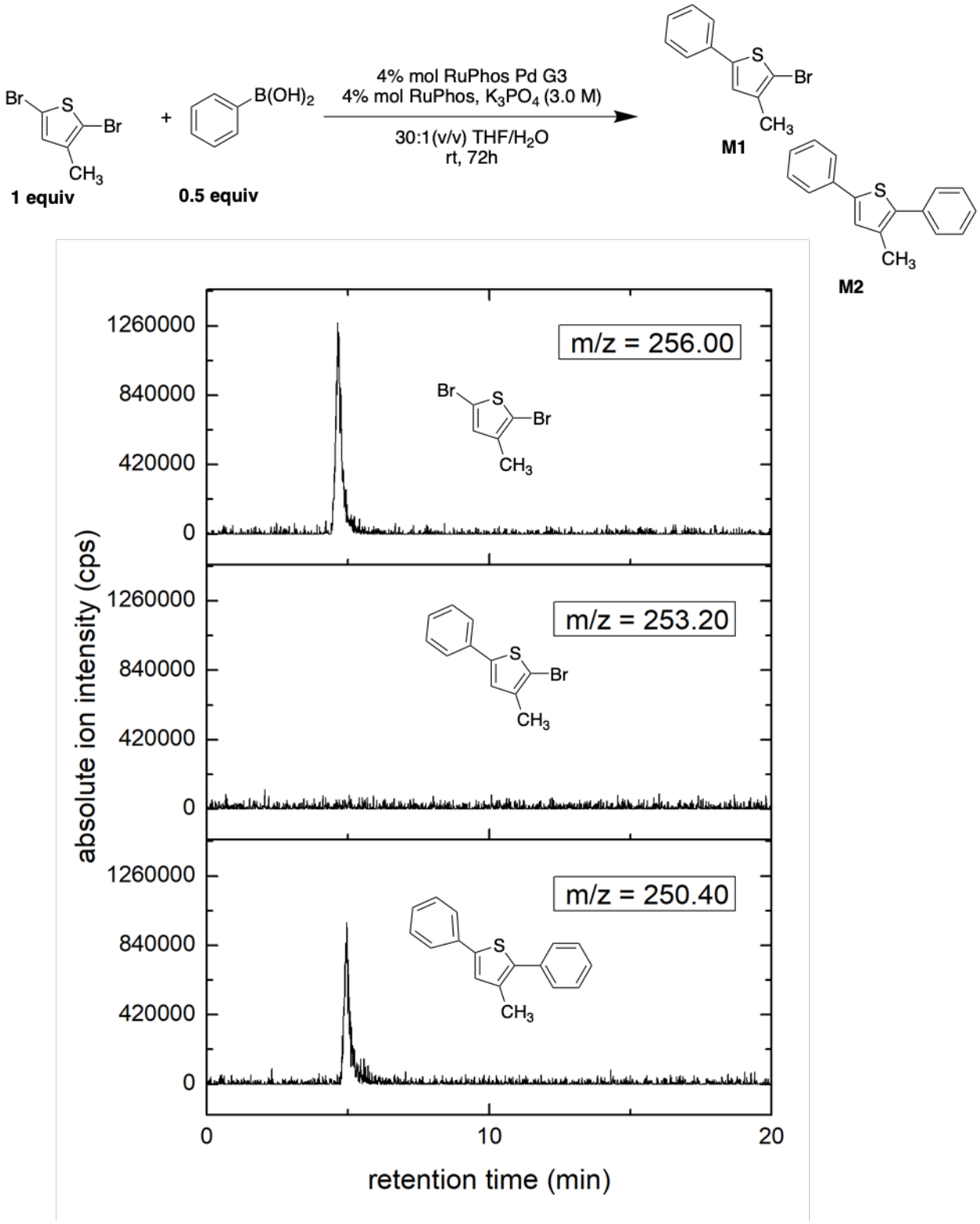

Figure 2.11. Reaction scheme of the Suzuki-Miyaura coupling between 3-methyl-2,5-dibromothiophene and phenylboronic acid using RuPhos Pd G3 as pre-catalyst (top). Extracted ion chromatogram of the reaction mixture after 72h at rt (bottom).

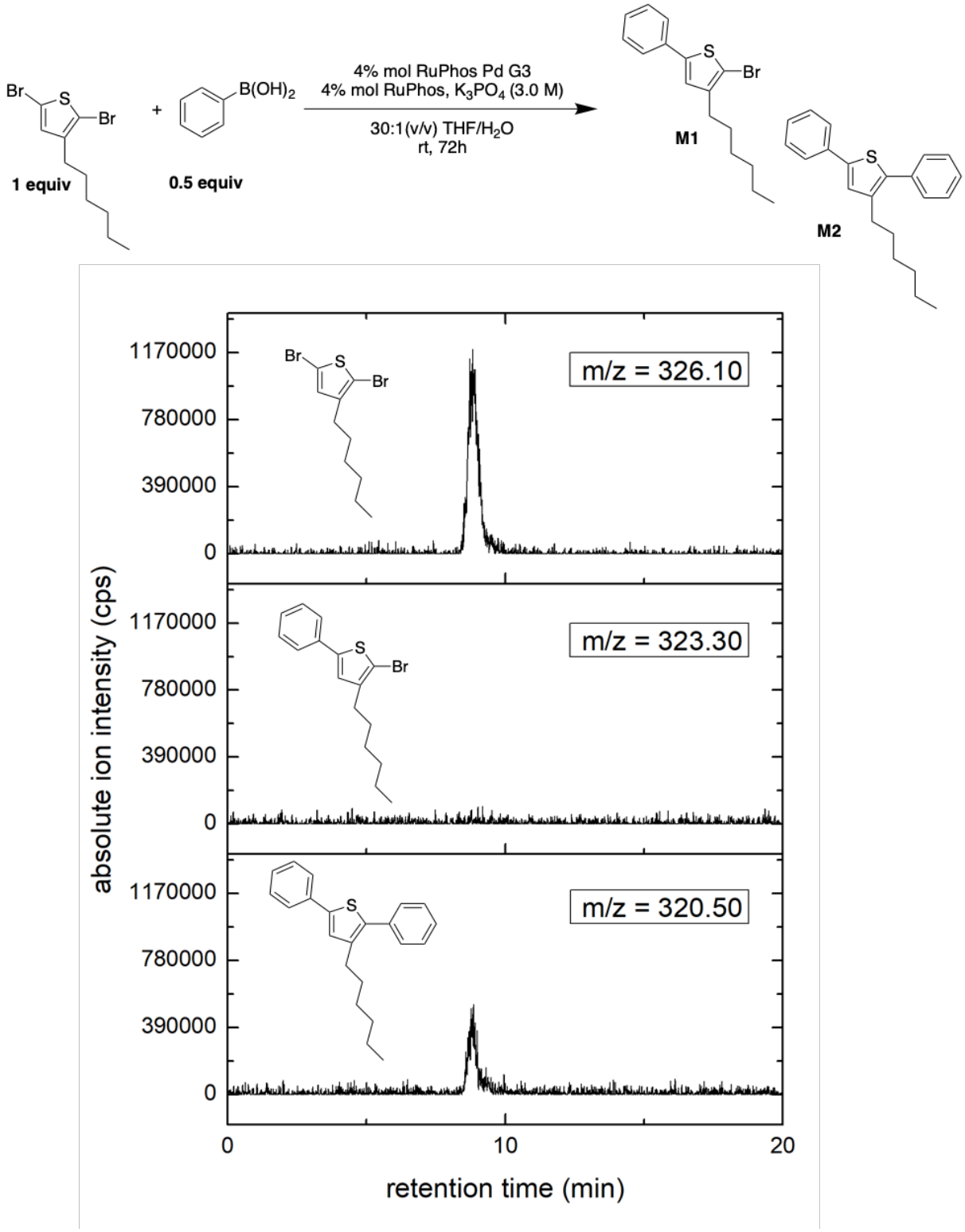

Figure 2.12. Reaction scheme of the Suzuki-Miyaura coupling between 3-hexyl-2,5-dibromothiophene and phenylboronic acid using RuPhos Pd G3 as pre-catalyst (top). Extracted ion chromatogram of the reaction mixture after 72h at rt (bottom).

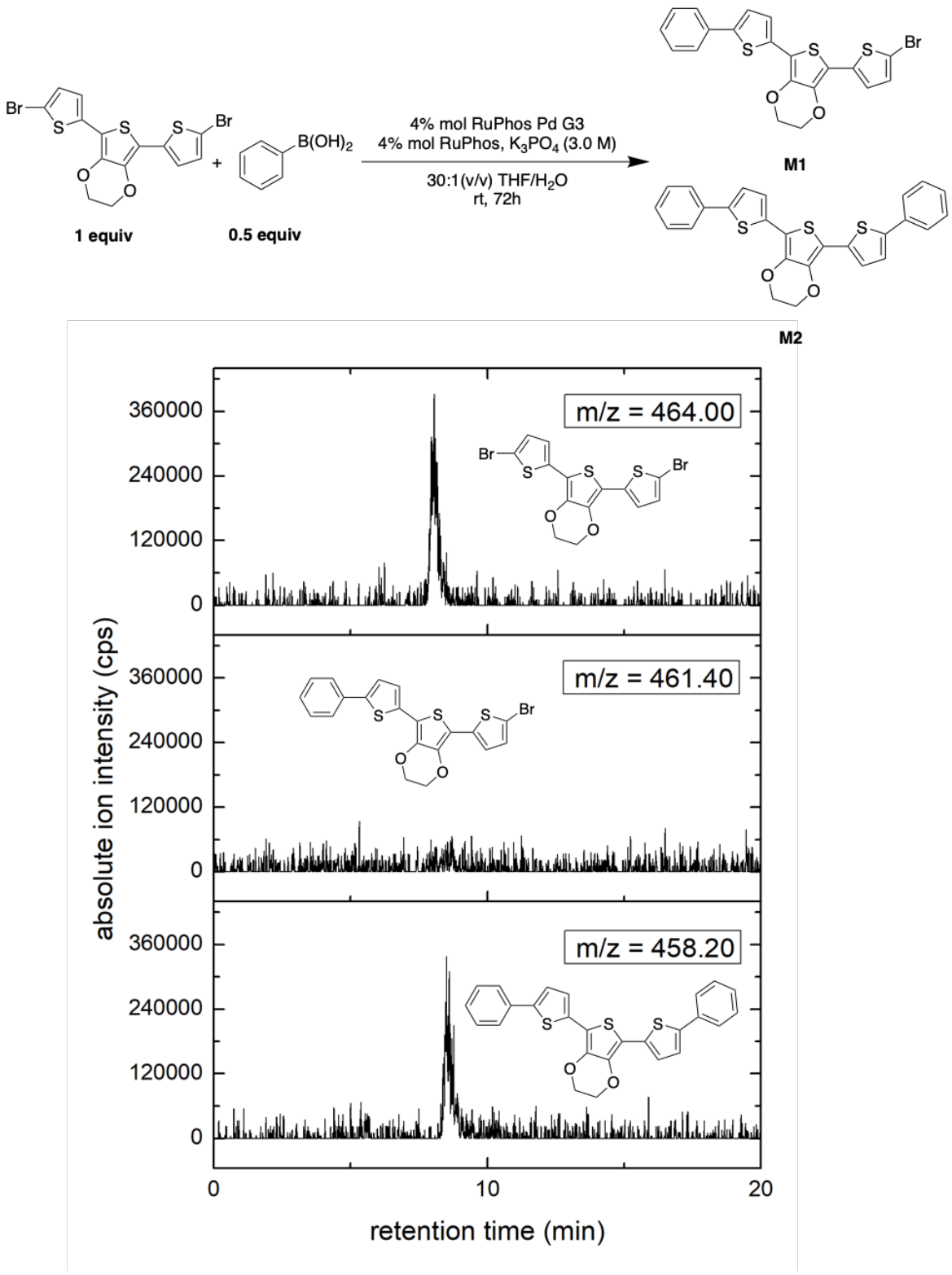

Figure 2.13. Reaction scheme of the Suzuki-Miyaura coupling between 2,5-di(5'-bromo-2'-thienyl)-3,4-ethylenedioxythiophene and phenylboronic acid using RuPhos Pd G3 as pre-catalyst (top). Extracted ion chromatogram of the reaction mixture after 72h at rt (bottom).

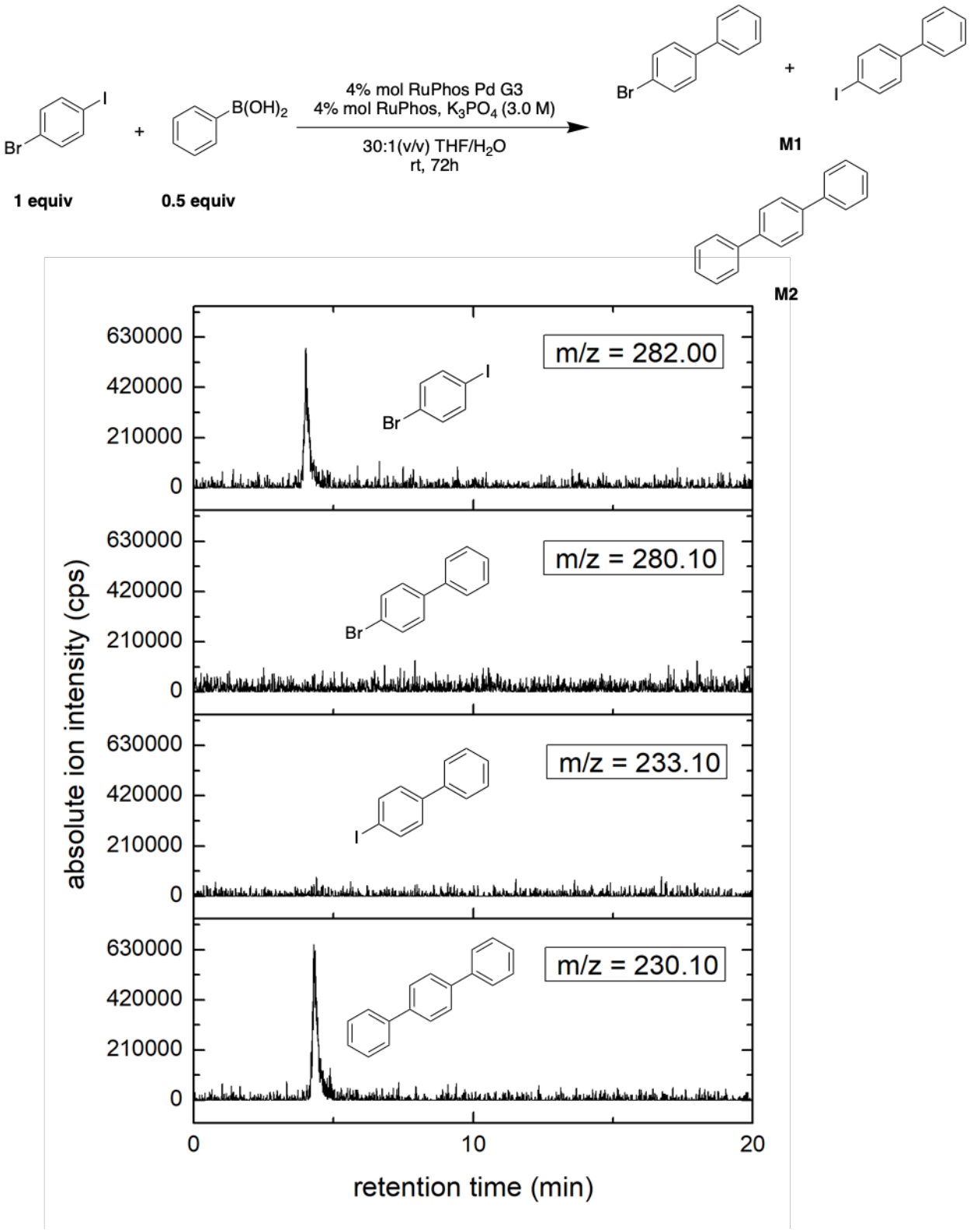

Figure 2.14. Reaction scheme of the Suzuki-Miyaura coupling between 1-bromo-4-iodobenzene and phenylboronic acid using RuPhos Pd G3 as pre-catalyst (top). Extracted ion chromatogram of the reaction mixture after 72h at rt (bottom).

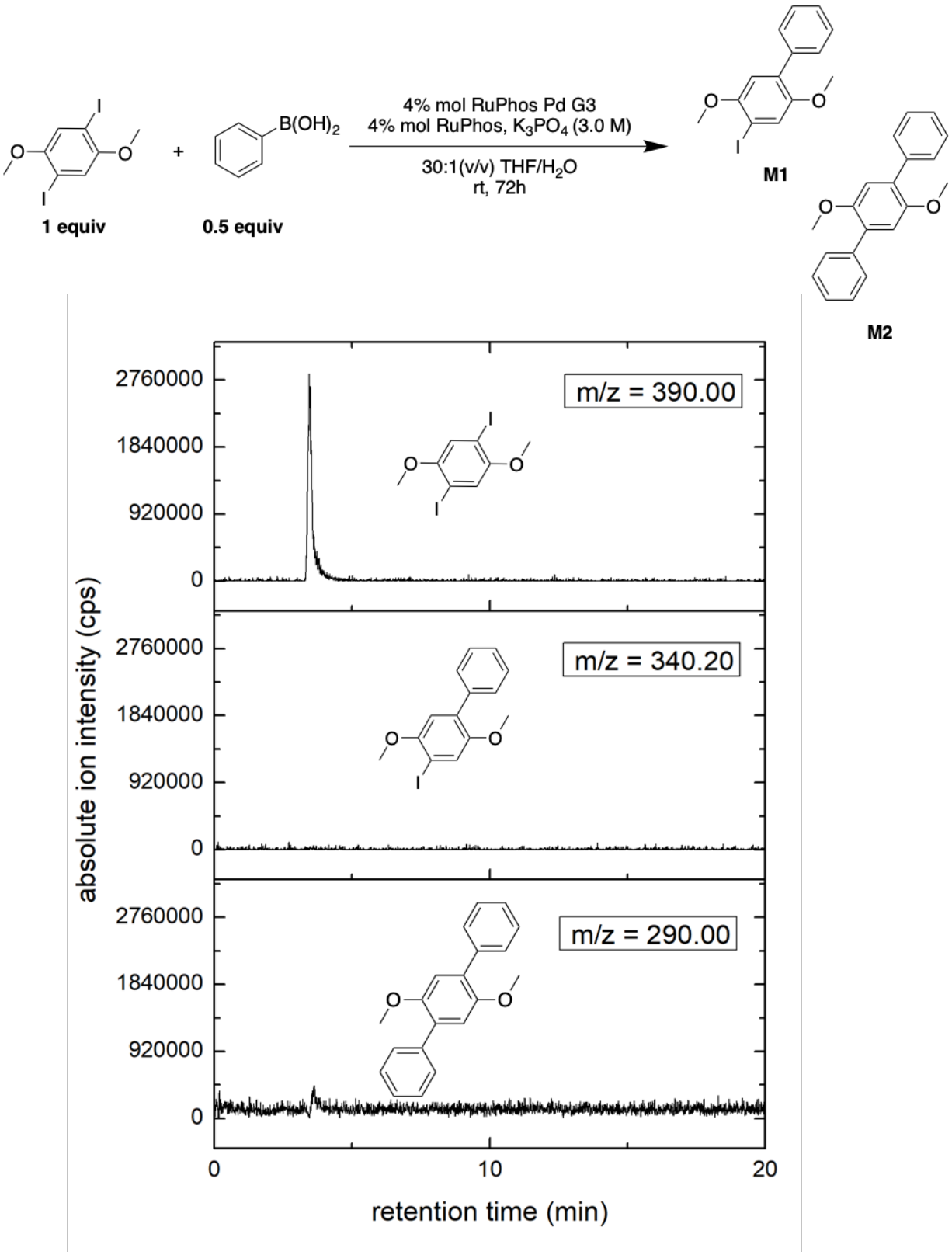

Figure 2.15. Reaction scheme of the Suzuki-Miyaura coupling between 2,5-methyloxy-1,4-diiodobenzene and phenylboronic acid using RuPhos Pd G3 as pre-catalyst (top). Extracted ion chromatogram of the reaction mixture after 72h at rt (bottom).

Even though 2,5-dialkyloxyphenylboronic acid monomers are typically used in SCTP reactions, the unexpected poor performance of 2,7-dibromo-9,9-di(6'methoxyhexyl)fluorene and 2,5-dimethyloxy-1,4-diiodobenzene (relative to their non-oxygenated analogs) indicated that oxygen atoms that are directly bonded to the π system or oxygen atoms installed on the solubilizing side chain have negative impacts on intramolecular catalyst-transfer mechanism.

2.2.3. Controlled Preparation of Poly(*p*-phenylene): Possible Theoretical Catalytic Pathways

The small molecule model experiments were conducted at room temperature to observe the highest potential for intramolecular catalyst-transfer. However, the initial SCTP polymerization studies were conducted at 45°C. This was necessary to accommodate for the slow hydrolysis rate of *N*-methyliminodiacetic acid (MIDA) boronates at ambient temperatures.

Yokozawa and co-workers first reported the preparation of poly(*p*-phenylenes) (PPPs) through SCTP of 4-iodo-2,5-dialkoxyphenylboronic acid, and using $Pd(^tBu_3)_2$ as the pre-catalyst.[16] In this study, we also found that 1,4-diiodo-2,5-dialkoxybenzene could undergo intramolecular catalyst-transfer at room temperature using RuPhos Pd G3 as the precatalyst. However, it's MIDA boronate analog did not produce an efficient SCTP polymerization reaction at 45°C (Figure 2.16).

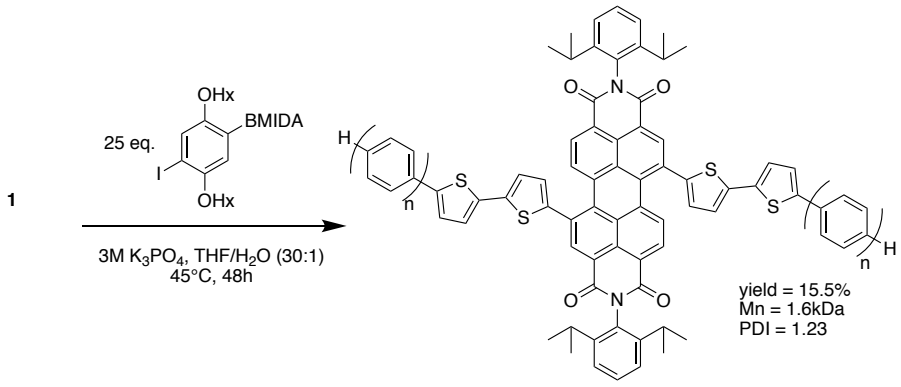

Figure 2.16. Suzuki-Miyaura catalyst-transfer polymerization of 4-iodo-2,5-dialkyoxy-phenylboronic acid MIDA ester at 45°C. [a]Polymerization reaction conditions: **1** (3.3μmol, 1 equiv), 4-iodo-2,5-dihexyloxyphenylboronic acid MIDA ester (89 μmol, 27 equiv), K_3PO_4 (0.77mmol, 3M), THF/H_2O (30:1). [b]Absolute molecular weight was measured by NMR. [c]M_w/M_n was determined by GPC calibrated using polystyrene standard and with THF as eluent at 40°C.

The inability of 4-iodo-2,5-dihexyloxyphenylboronic MIDA ester to undergo efficient controlled chain-growth at 45°C is also in agreement with Yokozawa's report, where they used 4-iodo-2,5-dihexyloxyphenylboronic acid pinacol ester and were compelled to lower the reaction temperature to -20°C in order to optimize the reaction. These results confirm that alkyloxy substituted phenylenes are not suitable for SCTP in these conditions.

All of the remaining phenylene monomers identified from the model reaction studies as potential candidates for externally initiated SCTP contain alkyl substituents as solubilizing groups. 4-bromo-2,5-dihexylphenylboronic acid MIDA ester **2** was chosen as a representative monomer for preparing poly(*p*-2,5-dialkylphenylenes) due to its expected solubility in THF/H_2O and ease of synthesis. Longer alkyl chain 1,4-dibromo-2,5-dialkylbenzenes are prone to precipitate during the lithium halogen exchange reaction at -78°C and were found to produce lower yields than 1,4-dibromo-2,5-dihexylbenzene.

Previously, Carrillo and co-workers reported that the theoretical stoichiometric ratio of H_2O to K_3PO_4 to MIDA boronate monomer in the SCTP of 5-bromo-4-hexylthiophene boronic acid MIDA ester **3** was 3:3:1.[17] They proposed that two equivalents of base are needed to hydrolyze MIDA protecting group, and the third was used to form the boronate anion under the assumption that the transmetalation proceeded through the reaction between $L_2ArPdBr$ and $BrArB(OH)_3K$ (the boronate pathway of Suzuki-Miyaura reaction). However, Burke later published comprehensive mechanistic studies demonstrating that the slow hydrolysis of MIDA boronates in THF and aqueous K_3PO_4 occurs predominately with H_2O and not hydroxide as the nucleophile in both hydrolysis steps of the reaction.[18] Therefore, these stoichiometries are not likely to be correct. Since Carrillo's report, there has also been strong evidence that the Suzuki-Miyaura coupling between $L_2ArPdOH$ and neutral phenylboronic acid (the oxo-palladium pathway) is orders of

magnitude faster than the reaction between $L_2ArPdBr$ and anionic $BrArB(OH)_3K$, suggesting when the two species exist in equilibrium that the oxo-palladium pathway would be dominant in the Pd-catalyzed Suzuki Miyaura reaction between aryl halides and phenylboronic acid.[19-23]

Based on these reports, the minimum theoretical stoichiometric ratio between H_2O : K_3PO_4 : BrArBMIDA in the Pd catalyzed SCTP of **2** should be 4:4:1 via the oxo-palladium pathway. One stochiometric equivalent of base is needed to form the active palladium hydroxo complex $L_2ArPdOH$ in the transmetalation step, and three are required to neutralize the side products produced per CTP catalytic cycle with MIDA boronate monomers. The side product *N*-methyliminodiacetic acid has a pK_{a1} of 2.81 and pK_{a2} of 10.18. Boric acid has a pK_a of 9.24, whereas the conjugate acid of K_3PO_4 has a pK_a of 12.67. Based on pK_a values, the neutralization of these side products occurs almost quantitatively in the presence of excess K_3PO_4.

Additionally, based on findings by Amatore and co-workers, ^{-}OH catalyzes the reductive elimination of $L_2ArPdArBr$ via a pentacoordinate Pd^{II} complex, and thus a catalytic concentration of ^{-}OH should be implemented in the reaction design to for transmetalation to be rate limiting.[21] To differentiate between the two palladium pathways, **2** was polymerized in typical SCTP conditions using 3.5 equivalents of base (entries 1-4, Table 2.1). A 3.5 : 1 molar ratio of K_3PO_4 : **2** was chosen in consideration of the boronate pathway and its stoichiometry, an excess of 0.5 equivalents of K_3PO_4 was employed as a catalyst for reductive elimination as proposed by Amatore. Carrillo also found that a large excess of water was necessary for successful Pd catalyzed SCTP of 5-bromo-4-hexylthiophene boronic acid MIDA ester. In the following experiments (entries 1-4, Table 2.1), the molar ratio of H_2O to **2** was 66. This amount is consistent with the 40-80 molar ratio of H_2O to monomer proposed by Carrillo and co-workers. Theoretically, if the boronate pathway was dominant, this stoichiometry should lead to an efficient reaction.

Alternatively, if the oxo-palladium pathway is the dominant catalytic pathway, then the expedient neutralization of K_3PO_4 is expected. The catalytic amount of ^-OH would also be exhausted, leading to a critical reduction in reaction rate before all the monomers are consumed. Ultimately, if the SCTP of **2** occurs via the oxo-palladium pathway, the sub-stoichiometric amount of base is expected to lead to a characteristic decrease of the M_n and yield via suppression of the polymerization rate relative to hydrodeboronation. Utilizing a 3.5 to 1 molar ratio of K_3PO_4 in typical SCTP conditions[9] utilized for the polymerization of **3**, the polymerization of **2** resulted in a low molecular weight, yield and moderate polydispersity. (Table 2.1, entry 1)

Table 2.1. Externally Initiated SCTP of 4-bromo-2,5-dihexylphenylboronic acid MIDA ester **2** using RuPhos supported Pd external initiator **1**.

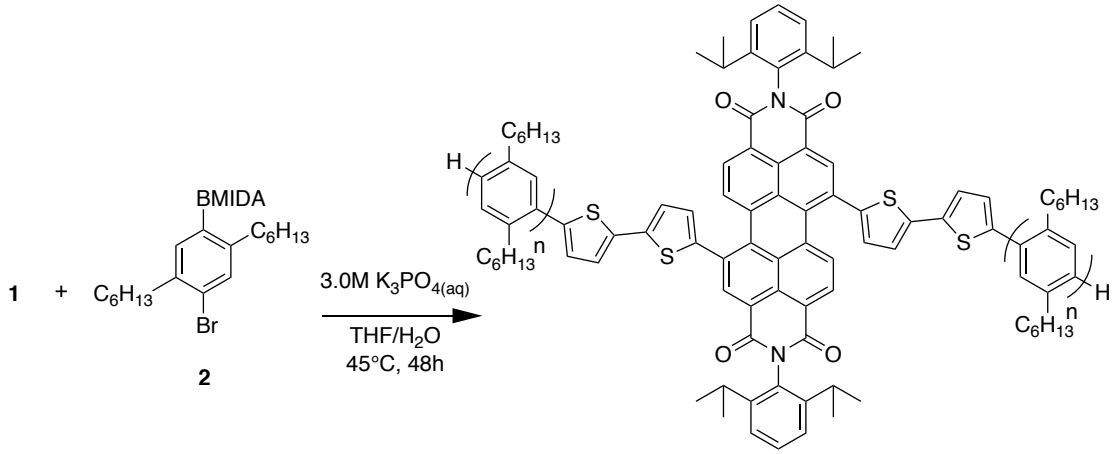

entry	THF (mL)	H_2O (mL)	M_n[b] (PDI[c])	yield[d] (%)	X_{H2O}
1	8	0.15	1.2k (1.31)	5.6%	0.08
2	4	0.15	1.8k (1.30)	8.0%	0.14
3	2	0.15	3.0k (1.21)	15.6%	0.25
4	1	0.15	3.6k (1.19)	46.6%	0.40

[a]Reaction conditions: **1** (3.3μmol, 1 equiv), K_3PO_4 (0.45mmol, 3.0M), $[\mathbf{2}]_0/[\mathbf{1}]_0 = 38$. [b]Absolute molecular weight was determined by quantitative NMR. [c]M_w/M_n was determined by GPC calibrated using polystyrene standard and with THF as eluent at 40°C. [d]Isolated yield after precipitation in acetone.

The utilization of MIDA boronates as protecting groups is beneficial because the slow release of $BrArB(OH)_2$ limits the overall rate of hydrodeboronation. In highly basic conditions, the buildup of transient unreacted $BrArB(OH)_2$ would readily result in hydrodeboronation via the Kuivila mechanism and would theoretically reduce both the M_n and yield in a correlated fashion via monomer degradation.[19-21] Vice versa, an increase in polymerization rate relative to hydrodeboronation would improve M_n and yield in the same correlated fashion. The characteristic low yield and M_n observed for entry 1 (Table 2.1) implied a slow polymerization rate relative to MIDA hydrolysis. To test this theory and to obtain better results, we conducted the next series of reactions with increased concentration in the THF phase in order to accelerate the polymerization (entries 2-4, Table 2.1). This resulted in the expected concurrent improvement of the molecular weight of PDCI-PPP up to 3.6 kDa, a narrowing of the polydispersity index from 1.31 to 1.19 and large increase in yield from 5.6% to 46.6%.

In the externally initiated polymerization of **2**, both oxidative addition and reductive elimination are assumed to be unimolecular processes. Since increasing the solute concentration in the THF phase of entries 1-4 resulted in accelerated reaction rate relative to hydrodeboronation (as indicated by higher molecular weight and yield), transmetalation was conjectured to be rate limiting.

Reducing the THF volume affects the kinetics of the reaction in two major ways. First, the concentrations of catalytic Pd centers and monomers are increased. This would theoretically increase the rate of polymerization up to 64 times from entry 1 to entry 4 (assuming that rate limiting transmetalation is an ideal bimolecular reaction between active catalytic species and monomer). Second, the lowering of THF volume also increases the water molar fraction which appears to be more impactful on the polymerization reaction. The water molar fraction (X_{H2O}) dictates water activity in the THF phase and increasing the water activity accelerates the MIDA

hydrolysis reaction.[18,22] Clearly, increasing the rate of MIDA hydrolysis relative to rate of polymerization would exacerbate hydrodeboronation, leading to lower yields and thus cannot be the reason for the improved results. Most critically, water activity strongly influences the equilibrium position of the ligand exchange reaction between $L_2ArPdOH$ and $L_2ArPdBr$.[23] In the oxo-palladium pathway, $L_2ArPdOH$ is reactive and $L_2ArPdBr$ is not. Because of this, their dynamic equilibrium concentration may be determining the average polymerization rate of Pd catalyzed SCTP reactions of boronic acid containing monomers. To understand the phenomenon observed in entry 1-4 (Table 2.1) and to conclude on the palladium catalytic pathway, a full understanding on how X_{H2O} and water activity affects the M_n, yield and polydispersity of PDCI-PPP prepared by SCTP is required.

2.2.4. Two Opposing Roles of Water Molar Fraction on the Oxo-Palladium Pathway

Kinetic studies by Amatore, Hartwig and others of base mediated Pd-catalyzed Suzuki-Miyaura reactions between aryl bromides and phenylboronic acid employing THF/H_2O as the solvent (between 50:1 and 10:1 (v:v) THF/H_2O ratio) and utilizing a 1 : 1 molar ratio of $L_2ArPdOH$ and Br^-, an increase of X_{H2O} has been reported to drive K_{eq} from 1 up to 9.3 favoring the formation of unreactive $L_2PdArBr$ as the dominate palladium species in solution.[23-28]

In the case of SCTP of bromo-substituted arene monomers, the solution concentration of Br^- is directly proportional to the average degree of polymerization due to Br^- being a side product of the catalytic cycle. At the beginning of the reaction (low DP) where the concentration of Br^- is low, implementing a high X_{H2O} in the reaction design is theoretically expected to increase the concentration of ^-OH in the THF phase and would drive the formation of the active $L_2ArPdOH$ even with a relatively high K_{eq} (determined by X_{H2O} shown by Hartwig) between the ligand exchange reaction of $L_2ArPdOH$ to $L_2ArPdBr$; thus increasing the polymerization rate at the

beginning of the reaction. However, increasing concentrations of Br^- due to catalytic turnover would cause a significant buildup of unreactive $L_2ArPdBr$ and attenuating the average polymerization rate as the reaction progresses. This dynamic equilibrium concentrations of $L_2ArPdOH$ and $L_2ArPdBr$ throughout the reaction progress would also result in polymer chain ends with a distribution of reactivities and conceivably result in broadening or narrowing of polydispersity as a function of X_{H2O} in basic conditions such was observed in Table 2.1, entry 1-4. Water's dual role in the ligand exchange reaction between the two palladium species may also be the reason for Carrillo and co-workers' finding that an excess of water is necessary for efficient polymerization of **3** using Pd supported by SPhos. But, at the same time, they found that further increasing X_{H2O} has harmful effects on the SCTP reaction. Overall, water activity can enhance and inhibit the average rate of transmetalation in Pd catalyzed SCTP reactions. To test this theory and contrast the effects of THF concentration versus water molar fraction on the M_n, yield and polydispersity, a series of reactions were conducted at varying water and THF volumes in the SCTP of **2** using **1** as the external initiator. (Table 2.2)

Table 2.2. Externally Initiated SCTP of 4-bromo-2,5-dihexylphenylboronic acid MIDA ester **2** at varying volumes of THF and water.

entry	THF (mL)	H_2O (mL)	M_n[b] (PDI[c])	yield[d]	X_{H2O}	[Pd] (μM)	$[K_3PO_4]/[\mathbf{2}]$
5	8	0.25	3.6k (1.27)	8.0%	0.12	0.82	6.00
6	1	0.15	7.0k (1.19)	59.2%	0.40	6.56	7.00[e]
7	8	0.42	3.1k (1.17)	20.0%	0.19	0.82	9.00
8	2	0.42	7.6k (1.16)	61.7%	0.48	3.28	9.00
9	4	0.63	6.8k (1.15)	70.1%	0.41	1.64	15.00
10	8	0.63	5.7k (1.16)	44.5%	0.26	0.82	15.00
11	16	0.63	3.7k (1.15)	27.1%	0.15	0.42	15.00

[a]Reaction conditions: **1** (3.3μmol, 1 equiv), K_3PO_4 (3.0 M), $[\mathbf{2}]_0/[\mathbf{1}]_0 = 38$. [b]Absolute molecular weight was determined by quantitative NMR. [c]M_w/M_n was determined by GPC calibrated using polystyrene standard and with THF as eluent at 40°C. [d]Isolated yield after precipitation in acetone. [e]6.0M K_3PO_4.

Entry 5 is notably different than entry 1 because of the higher base stoichiometry (6:1 K_3PO_4 : **2** in entry 5 vs 3.5:1 in entry 1) and slightly higher X_{H2O} (0.12 in entry 5 vs 0.08 in entry 1) which resulted in small improvements in molecular weight, polydispersity and yield after reprecipitation in acetone (3.6 kDa, PDI = 1.27, 8.0% yield). In this case, the improvements of entry 5 vs entry 1 are not likely due to increased X_{H2O} because entry 2 (with higher X_{H2O} of 0.14 vs 0.12 in entry 5) did not show these improvements. We repeated the most optimized reaction (entry 4) in the series of entry 1-4 with identical conditions except using 7:1 equivalents of K_3PO_4 : **2** instead of 3.5:1 (Table 2.2, entry 6). This resulted in doubling of the molecular weight up to 7.0 kDa and a significant increase of yield from 46.6% to 59.2%. These improvement in yield and molecular weight of entry 5 and 6 vs entry 1 and 4 respectively demonstrate that 3.5 molar equivalents of base relative to monomer is not optimal for the Pd catalyzed SCTP of **2**; rebutting the theoretical stoichiometry for the boronate pathway and supporting the oxo-palladium mechanism where at least 4 equivalents of K_3PO_4 relative to **2** is necessary for an efficient polymerization reaction. In conditions where the stoichiometric amount of base is insufficient, the low M_n and yield are hypothetically attributed to the formation of $L_2ArPdBr$ due to low ^-OH concentration.

Using at least 6 : 1 ratio of K_3PO_4 : **2**, increasing X_{H2O} from 0.12 to 0.26 by increasing the water volume and keeping THF volume constant (entry 5, 7 and 10) lead to characteristic improvements of M_n from 3.6 kDa to 5.7 kDa, polydispersity from 1.27 to 1.16 and yield from 8.0% to 44.5%. Likewise, increasing the X_{H2O} from 0.19 to 0.48 (entry 7 and entry 8) by changing the THF concentration while keeping volume of water constant also showed correlated improvements of the M_n from 3.1 kDa up to 7.6kDa, polydispersity from 1.17 to 1.16 and yield from 20.0% to 61.7%. These results show that the improved polymerization reaction from entries 1-4 is not due to the increased concentration of solutes in the THF phase, but from increasing the water molar

fraction. This refutes the hypothesis that reaction between $L_2ArPdOH$ and $BrArB(OH)_2$ due to low concentration in the THF phase is limiting the overall rate of polymerization via transmetalation. It should be noted that the molar quantities of K_3PO_4 in entries 5-11 must be increased as the volume of water increases to maintain the concentration of 3.0 M K_3PO_4 in the aqueous phase. Additional to its role as a base, K_3PO_4 also acts as a strong electrolyte which lowers the water activity in THF, slowing down the rate of MIDA hydrolysis that is vital for an efficient SCTP reaction.

To gain further insight into the behavior of rate limiting step, a series of SCTP polymerization reactions of **2** was conducted at relatively high X_{H2O} (between 0.15 and 0.41) and varying amounts of THF up to 16mL (entries 9-11). Even at this dilute concentration of 0.42 μM of palladium centers (16 mL THF, entry 11), the polymerization reactions produced remarkable results for the controlled synthesis of poly(*p*-2,5-dihexylphenylene) (M_n = 3.7kDa, PDI = 1.15, yield = 27.1%) and adhering to the theory proposed herein. Entries 9-11 displayed a decrease in yield and M_n with increasing THF volume (and decreasing X_{H2O}) and again demonstrated how water molar fraction is fundamentally tied to the reagent stoichiometries and polymerization results. Entries 5-11 show that changing the quantities of THF and H_2O affects the reaction only through X_{H2O}, and that increasing X_{H2O} in these conditions results in enhancement of the M_n, yield and polydispersity significantly.

From these initial studies, it is apparent that the minimum X_{H2O} observed for the 3.0M K_3PO_4 mediated externally initiated SCTP of **2** using **1** must be greater than 0.15 (entry 11) in order to produce a narrow polydispersity (PDI < 1.2) of polymer chains. Implementing even higher water molar fractions up to 0.48 dramatically improve M_n and yield of poly(*p*-phenylenes) presumably deriving from more efficient formation of catalytically active $L_2ArPdOH$. This is contingent on a

sufficient molar amount of K_3PO_4 relative to the **2**, which is proposed to be at least the theoretical minimum stoichiometry of 4:1. The concentration of Pd species in solution leading to successful externally initiated SCTP can be as low as 0.42 μM, and the low concentration of palladium centers does not appear to be limiting the polymerization rate. These observations are consistent with rate limiting process involving the equilibrium exchange reaction between $L_2ArPdOH$, Br^-, $L_2ArPdBr$ and ^-OH. The premises are integrated into the proposed catalytic cycle via the oxo-palladium pathway illustrated in Figure 2.17. Such a mechanism of SCTP polymerization of MIDA boronates and associated catalytic cycle has never been postulated.

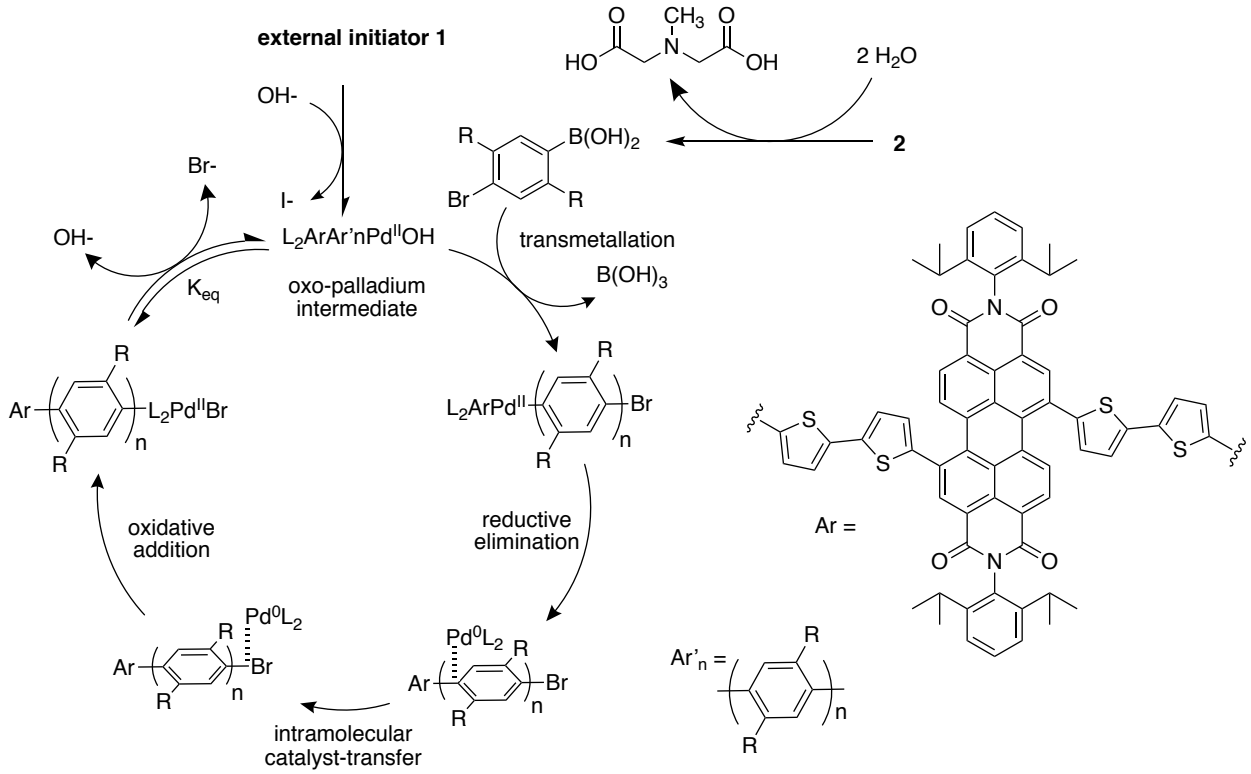

Figure 2.17. Proposed catalytic cycle for the Externally Initiated Suzuki-Miyaura Catalyst-Transfer Polymerization of 4-bromo-2,5-dihexylphenylboronic acid MIDA ester **2** initiated by **1** via the Oxo-Palladium Pathway.

In this proposed catalytic cycle, the external initiator **1** becomes activated through ligand exchange reaction of ^-OH with I^- centered on the Pd^{II} precatalytic species to generate the oxo-

palladium intermediate. I^- is less nucleophilic than Br^- and has a smaller K_{eq} in the equilibrium reaction between the Oxo-Pd intermediate and ArL_2PdX, therefore iodine derived external initiators are theoretically expected to better form Oxo-Pd intermediate and result in more efficient initiation than initiators with aryl bromide precursors.[23] **2** is converted to the free boronic acid via the slow mechanism of MIDA boronate hydrolysis, and the by-product *N*-methyliminodiacetic acid is deprotonated by 2 equivalents of K_3PO_4. The neutral boronic acid undergoes transmetalation with the oxo-palladium intermediate and boric acid is produced as a side product, consuming another equivalent of K_3PO_4. Following fast reductive elimination, intramolecular catalyst-transfer and oxidative addition steps, the subsequent conversion of ArL_2PdBr to ArL_2PdOH by hydroxide ligand exchange reaction produces Br^- as a side product and regenerates the oxo-palladium complex.

An important question remains: which is the rate determining step? The reaction rate is seemingly affected by the equilibrium between ArL_2PdBr and the oxo-Pd intermediate; strongly suggesting that neither of the transmetalation, oxidative addition, reductive elimination nor intramolecular catalyst-transfer itself is limiting the average rate of polymerization. Practically (for controlling the overall polymerization rate), the ligand exchange reaction of ^-OH and ArL_2PdBr to form ArL_2PdOH seems to be the rate limiting step. This hypothesis is supported by the observed influence of the Br^- anion on the polymerization rate, which is not participating in any of the elementary catalytic processes.

Alternatively, the rate of MIDA hydrolysis of **2** could be rate limiting. It's slow formation certainly warrants consideration as the rate limiting step. The two mechanisms would show different rate kinetics. If the formation of the oxo-palladium intermediate from ArL_2PdBr was rate limiting, it should show a zero-order reaction in excess base because the concentration of Pd

centers and the pH of the THF phase can be assumed to be constant. If MIDA hydrolysis was rate limiting, then a first-order kinetics is expected proportional to the concentration of **2**. It would progressively slow down as the monomer is depleted. Initial studies of the rate kinetics showed a zero-order reaction, showing a linear dependency of the molecular weight vs time, but more experiments were needed to confirm this result.

2.2.5. Capturing Br^- using Ag^+: Enhancement of the M_n, Polydispersity and Yield

Halides play opposing roles in the boronate and oxo-palladium pathways. In the boronate pathway, the halide anion increases the reaction rate through L_2ArPdX species which undergoes transmetalation with the anionic boronate monomer. In the oxo-palladium pathway, halides drive the formation of inactive L_2ArPdX. The results obtained from the polymerization study strongly suggests that Br^- plays an antagonistic role, thus favoring the oxo-palladium pathway.

We hypothesized that the polymerization could be further enhanced by removing Br^- from solution. Ag^+ readily reacts with Br^- to form AgBr and has been used in small molecule Suzuki coupling for accelerating reactions. Thus, SCTP of **2** was conducted in the presence of various silver(I) salts to enhance the polymerization reaction results (Table 2.3). The use of Ag^+ to accelerate Suzuki-Miyaura reaction rate was pioneered by Kishi et al.[27] Ag^+ can react with Br^- and ^-OH to form AgBr and Ag_2O respectively. In basic conditions, Ag^+ is expected to form Ag_2O almost quantitatively and reduce the availability of reactive ions in solution. As so, the equilibrium reaction between aqueous Ag^+ and Ag_2O must be considered in order to integrate this strategy effectively. For the following reactions (entries 12 to 24), AgOAc and Ag_2SO_4 were chosen because of their limited solubility in H_2O, which was hypothesized to slowly form in-situ Ag_2O with a significant surface area.

Table 2.3. Externally Initiated SCTP of 4-bromo-2,5-dihexylphenylboronic acid MIDA ester **2** using AgOAc and Ag_2SO_4 as bromide capturing agents.

entry	THF (mL)	H_2O (mL)	M_n[b] (PDI[c])	yield (%)	X_{H2O}	Ag^+ (equiv)	$[K_3PO_4]/[\mathbf{2}]$	temp (°C)	time (h)
12[g]	8	0.25	8.8k (1.13)	31.2%	0.12	AgOAc (1)	12	45°C	48
13[g]	8	0.25	9.8k (1.14)	33.6%	0.12	Ag_2SO_4 (1)	12	45°C	48
14[g]	8	0.5	9.3k (1.15)	39.8%	0.22	AgOAc (1)	24	45°C	48
15[g]	8	0.5	9.8k (1.16)	34.8%	0.22	Ag_2SO_4 (1)	24	45°C	48
16[g]	8	0.25	6.8k (1.17)	50.1%	0.12	Ag_2SO_4 (1)	6	45°C	48
17	8	0.25	7.5k (1.21)	60.6%	0.12	Ag_2SO_4 (2)	11	rt	96
18	8	0.25	7.5k (1.18)	60.9%	0.12	Ag_2SO_4 (2)	13	rt	96
19	8	0.45	6.9k (1.16)	71.8%	0.20	Ag_2SO_4 (2)	12	rt	96
20	8	0.75	7.5k (1.14)	67.8%	0.30	Ag_2SO_4 (2)	20	rt	96
21	8	1.2	6.5k (1.12)	52.9%	0.40	Ag_2SO_4 (2)	32	rt	96
22	16	0.5	8.4k (1.16)	86.4%	0.12	Ag_2SO_4 (2)	13	rt	96
23	8	0.25	5.7k (1.16)	59.7%	0.12	Ag_2SO_4 (2)	13	rt	66
24	8	0.25	7.9k (1.17)	74.0%	0.12	Ag_2SO_4 (2)	13	rt	91

[a]Reaction conditions: $[K_3PO_4] = 3.0M$, $[\mathbf{2}]_0/[\mathbf{1}]_0 = 29$. [b]Absolute molecular weight was determined by quantitative NMR. [c]M_w/M_n was determined by GPC calibrated using polystyrene standard and -with THF as eluent at 40°C. [d]Isolated yield after precipitation in acetone. [e]5.0M K_3PO_4. [f]6.0M K_3PO_4. [g]$[\mathbf{2}]_0/[\mathbf{1}]_0 = 45$.

Using 1 molar equivalent of AgOAc (entry 12, 14) or Ag_2SO_4 (entry 13, 15) relative to **2** resulted in narrow polydispersity at X_{H2O} between 0.12 and 0.22; and significantly higher M_n (up to 9.8 kDa, theoretical M_n= 10.4 kDa) than previously obtained. This showed the compatibility of AgOAc and Ag_2SO_4 in SCTP conditions and also affirmed the innocent nature of acetate and sulfate counter-anions. Using 1 equivalent of silver salt relative to **2** and at $X_{H2O} = 0.12$, Ag_2SO_4 (entry 15) produced higher M_n (9.8 kDa) PDCI-PPP than AgOAc (8.8 kDa, entry 14). Ag_2SO_4 contains double the amount of Ag^+ per mole of reagent versus AgOAc and this demonstrated that silver(I) salts are not effective in stoichiometric amounts relative to the monomer. At $X_{H2O} = 0.22$ however (entry 14), AgOAc produced a higher molecular weight polymer (9.3 kDa) than it did in conditions with $X_{H2O} = 0.12$, and this implied that water volume affects the availability of Ag^+

significantly. Both silver salts demonstrated excellent compatibility and reaction enhancement capabilities. Due to its more uniform effects in varying X_{H2O}, Ag_2SO_4 was selected for further studies.

Next, we repeated entry 5 with exact reaction conditions except adding 1 molar equivalent of Ag_2SO_4 relative to the monomer (entry 16). In previous conditions, narrow polydispersity PDI < 1.2 was only obtained at $X_{H2O} > 0.15$. Along with results from entry 12 and 13, entry 16 confirmed silver's polymerization rate enhancing abilities and produced PDCI-PPP with consistently better polydispersity (PDI = 1.13 - 1.17, $X_{H2O} = 0.12$) relative to entry 5 (PDI = 1.27, $X_{H2O} = 0.12$). The improvement can only be rationalized from the oxo-Pd pathway where the removal of Br^- in the beginning of reaction would result in a more uniform initiation step, deriving from a higher concentration of $L_2ArPdOH$ vs $L_2ArPdBr$. Also, adding Ag_2SO_4 improved the M_n and yield from 3.6 kDa in entry 5 to 6.8 kDa in entry 16, and yield from 8.0% in 50.1%.

The molecular weight of PDCI-PPP prepared from entry 16 using 6 : 1 molar ratio of K_3PO_4 to **2** was lower than entry 12 and 13 using 12 : 1 molar ratio of K_3PO_4 to **2**. In this case, Ag_2SO_4 is likely acting as a Brønsted acid in the hydrolysis reaction to form Ag_2O, consuming ^-OH and reducing the stoichiometry of the base below the necessary amount for the polymerization reaction. Therefore, additional stoichiometric amount of K_3PO_4 was added in following reactions to allow for efficient silver mediated SCTP reaction to occur. For PDCI-PPP polymers with $M_n > 9$ kDa, precipitation was observed during the extraction process using $CHCl_3$/brine as organic and aqueous phases and led to lower yields for entry 12-15.

A final reaction optimization series of SCTP of **2** was conducted using Ag_2SO_4, in various relative amounts of THF, H_2O and K_3PO_4. Using the knowledge gained in previous studies, the objective of experiments in entries 17 – 25 is to obtain ideal silver mediated SCTP conditions.

Along this route, the reactions were conducted at room temperature to reduce intermolecular chain-transfer process, but this increased the reaction time dramatically. Two equivalents of Ag_2SO_4 was utilized, and therefore additional stoichiometric amount of K_3PO_4 was also increased. Due to precipitates observed at higher molecular weights (entries 12 – 15), the theoretical molecular weight for reactions 17 - 25 was lowered to 8.1 kDa. Two identical reactions were conducted to obtain the total reaction time at X_{H2O} = 0.12 (entry 23, 24). At 66h, the entry 23 reached a yield of 59.7% and molecular weight 5.7 kDa (70% of the theoretical molecular weight). At 91h, the second identical reaction (entry 24) reached 74% yield and 7.9 kDa (97% theoretical molecular weight). Therefore, the reaction time was estimated to be 4 days at 0.12 water molar fraction and at room temperature.

Next, additional molar quantity of base was added (to accommodate for the acidic nature of Ag^+) by increasing the aqueous concentration of K_3PO_4 to 5.0M (entry 17) and 6.0 M (entry 18). Using 5.0 M and 6.0 M K_3PO_4 produced similar results, producing PDCI-PPP with molecular weight up to 7.5 kDa (93% of the theoretical M_n), with similar yields of 61% and PDI 1.18-1.21. In ideal controlled polymerization systems, the % theoretical M_n (observed M_n / theoretical M_n × 100%) is an effective intrinsic indicator of reaction progress. The molar quantities of base can also be added by increasing the volume of H_2O while maintaining 3.0 M concentration of K_3PO_4. Concurrently, this increased the water molar fraction to 0.20 (entry 19), 0.30 (entry 20) and 0.40 (entry 21). Increasing X_{H2O} again improved the polydispersity proportionally from 1.16 in entry 19 to 1.12 in entry 21, which is attributed to the increased formation of ArL_2PdOH vs ArL_2PdBr. Surprisingly, the yield decreased as the water molar fraction increased in stark contrast to entries 9-11 where the increasing X_{H2O} resulted in higher yields.

In the theory proposed here, the increase in X_{H2O} plays a beneficial role in driving the formation of ArL_2PdOH versus ArL_2PdBr. But at the same time, increasing X_{H2O} raises the pH and results in monomer degradation (via formation of $BrArB(OH)_3K$, a precursor to hydrodeboronation via the Kuivila mechanism[19-21]). When a significant amount of Br^- is present (with no Ag^+ added), increasing X_{H2O} battles the negative effects of Br^-, thus enhances the polymerization rate, M_n, yield, and polydispersity. But in the absence of Br^-, the beneficial effects of increasing X_{H2O} are neutralized because the equilibrium between the oxo-palladium and palladium halide species is already being boosted by Ag^+. Then, only the negative effects of increasing X_{H2O} can be observed. Thus, the dual effects of increasing X_{H2O} materialize as two different results in silver and non-silver mediated SCTP. This process explains why the best polymerization reaction results in silver mediated SCTP are obtained at lower X_{H2O}, because it reduces the rate of hydrodeboronation. PDCI-PPP polymers in entries 19-21 reached a maximum % theoretical M_n of 92% (entry 20).

The molar amounts of base relative to **2** could also be added by scaling up the entire reaction (adding THF, H_2O and K_3PO_4) while maintaining the molar quantities of the initiator **2**, and monomers **5** (entry 22); relative to entry 16. This allowed the reaction to maintain a low X_{H2O} of 0.12. These conditions produced the best results, reaching the highest yield of 86.4%, a quantitative % theoretical M_n and narrow polydispersity of 1.16.

Applying the optimized silver mediated SCTP conditions just obtained, a series of PDCI-PPP were prepared with increasing degree of polymerization up to 50 (Table 2.4). A control reaction was conducted without silver to contrast its effects at room temperature (entry 31). The polymers were prepared with excellent yields and consistently low polydispersity. The number averaged molecular weight of the polymers were plotted to show a linear dependence versus feed ratio $[\mathbf{2}]_0/[\mathbf{1}]_0$ (Figure 2.18), demonstrating excellent controlled chain-growth behavior.

Ag^+ does not seem to be totally innocent. Although the M_n and yield are dramatically enhanced versus the control in entry 31, the polydispersity is actually lower without silver. Albeit, the silver reactions still demonstrated narrow polydispersity indexes of PDI < 1.2 (entry 25-30). Amatore has described a similar effect where the cations of bases used in Suzuki coupling has been shown to coordinate to the oxygen lone pair on the oxo-palladium complex, making it inactive towards transmetalation.[26] Ag^+ is also an oxophilic Lewis acid, and it would be logical that it can behave in the same way. This is likely to be the reason for the increased polydispersity in entries 25-30. A constant concentration of silver would statistically deactivate a portion of the oxo-palladium complexes via Amatore's proposed mechanism.

Table 2.4. Preparation of PDCI-PPP_n with various degrees of polymerization via silver mediated SCTP.

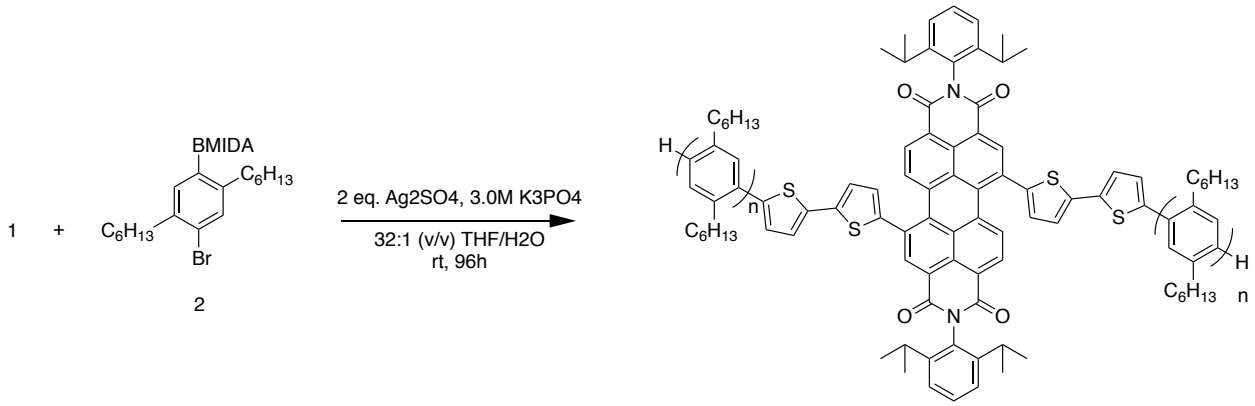

entry	M_n[b] (PDI[c])	yield[d] (%)	$[\mathbf{2}]_0/[\mathbf{1}]_0$
25	4.9k (1.19)	80.9%	17
26	5.7k (1.16)	71.5%	20
27	6.7k (1.19)	72.4%	25
28	7.8k (1.18)	71.7%	30
29	10.0k (1.17)	57.8%	40
30	12.5k (1.20)	71.6%	50
31[e]	3.4k (1.09)	12.6%	25

[a]Reaction conditions: $[K_3PO_4]$ = 3.0 M, rt, 96h. [b]Absolute molecular weight was determined by quantitative NMR. [c]M_w/M_n was determined by GPC calibrated using polystyrene standard and with THF as eluent at 40°C. [d]Isolated yield after precipitation in acetone. [e]No Ag_2SO_4 was added.

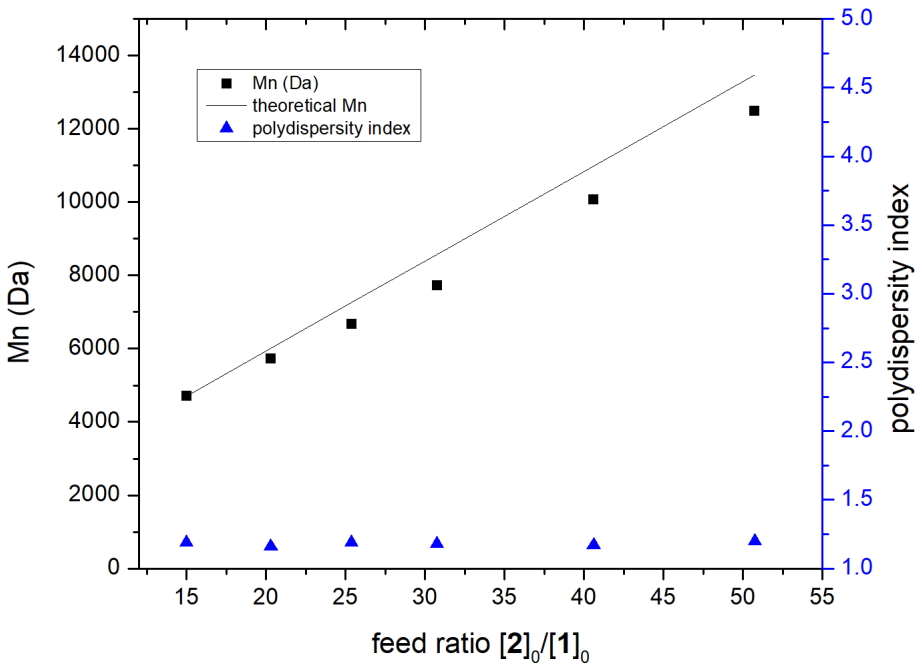

Figure 2.18. M_n vs feed ratio ($[\mathbf{2}]_0/[\mathbf{1}]_0$) of PDCI-$PPP_n$ polymers prepared by silver mediated Suzuki-Miyaura Catalyst-Transfer Polymerization.

And similar to how the dynamic equilibrium between ArL_2PdBr and ArL_2PdOH can effect polydispersity because of their relative reactivities, it's probable that the equilibrium between the free oxo-palladium complex and the silver ligated oxo-palladium complex could also result in a statistical distribution of chain-end reactivities; giving rise to a polydispersity phenomenon observed in entries 25-31.

2.2.6. Photophysical Properties of PDCI-PPP Polymers With Varying Molecular Weight

PDCI-PPP polymers having varying degree of polymerizations from 15 to 50 were characterized by UV-VIS absorbance and photoluminescence spectroscopy (Figure 2.19). The absorption spectra of all PDCI-PPP polymers in this series were essentially identical, with the bands significantly red-shifted relative to the free PDCI, which indicated increased π-conjugation due to phenylene being electronically coupled to PDCI. λ_{max} of the short wavelength emission shifted

from 338 to 365 nm, λ_{max} of the S_0 to S_2 transition shifted from 466 to 495 nm, and the lowest energy S_0 to S_1 transition was red shifted from 613 to 645 nm. The polymers were essentially nonfluorescent. Interestingly, the expected emission band around 400 nm expected of poly(*p*-phenylene) was not observed in PDCI-PPP_{15}, but became progressively more intense as the degree of polymerization of the polymer chain increased up to 50. This indicated an efficient quenching process of the PPP excited state energy by PDCI charge-transfer complex. As the chain length increases, the energy transfer may become less efficient and some of the excited state energy would be fluorescently emitted by the more distant chromophores situated on PPP. In the emission spectra, the NIR band is also dramatically red-shifted from the 775 nm emission of the free PDCI core to 860 nm in the PDCI-PPP polymer series.

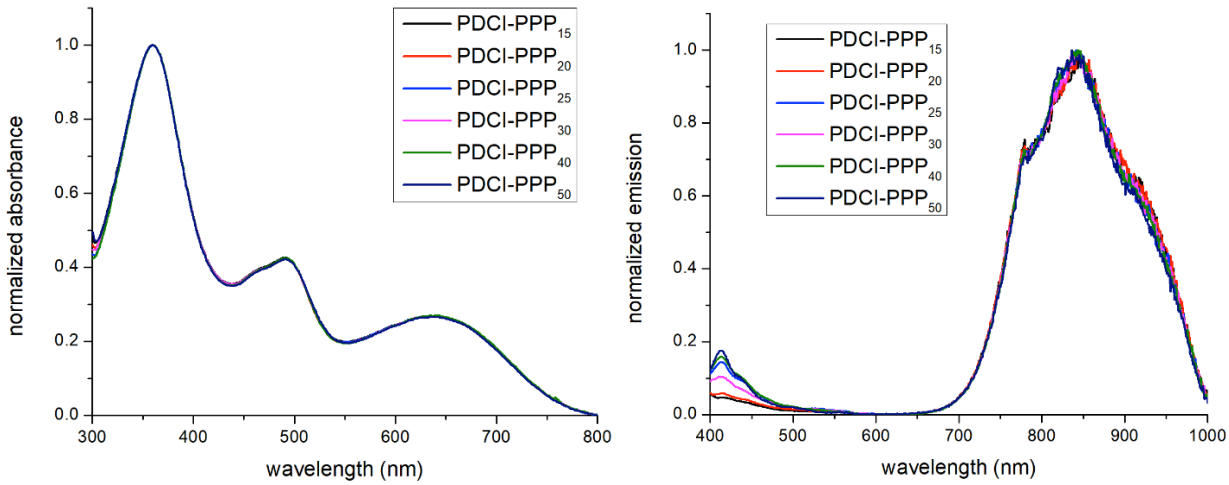

Figure 2.19. UV-Vis absorbance (left) and emission spectra (right) of PDCI-PPP_n

2.2.7. Silver Mediated Externally Initiated SCTP for Preparing Poly(9,9-dioctylfluorene)s

Poly(2,5-dialkylphenylene)s and poly(9,9-dialkylfluorene)s (PFs) are chemically very similar, having alkylated solubilizing groups installed on a conjugated backbone composed of benzene rings. Therefore, 7-bromo-9,9-diocytylfluorene boronic acid MIDA ester **4** was synthesized and a series of PDCI-PF polymers having various theoretical molecular weights were prepared to test if

the optimized silver mediated SCTP was transferrable to preparing poly(9,9-dioctylfluorene) (Table 2.5). A control reaction was also conducted without silver (entry 37). PDCI-PF prepared by silver mediated SCTP demonstrated controlled chain-growth character up to 14.9 kDa and resulted in a modest yield and narrow polydispersity (Figure 2.20). The photophysical properties of PDCI-PF series having various theoretical molecular weights were characterized by UV-VIS Absorbance and photoluminescence spectroscopy. (Figure 2.21)

Table 2.5. Preparation of PDCI-PPP_n with various molecular weights by silver mediated SCTP.

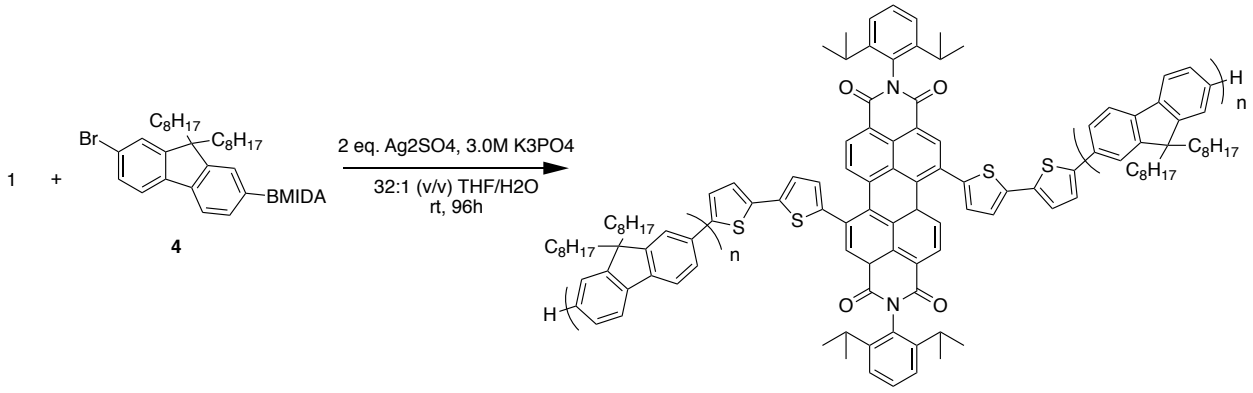

entry	M_n (PDI)	yield (%)	$[\mathbf{4}]_0/[\mathbf{1}]_0$	QY
32	3.5k (1.41)	41.7%	8	24.0%
33	5.6k (1.40)	36.6%	16	71.7%
34	9.5k (1.57)	43.0%	24	110.0%
35	11.1k (1.53)	47.8%	32	156.6%
36	14.9k (1.49)	37.4%	40	161.8%
37[e]	2.4k (1.13)	12.80%	16	-

[a]Reaction conditions: [K_3PO_4] = 3.0 M, rt, 96h. [b]Absolute molecular weight was determined by quantitative NMR. [c]M_w/M_n was determined by GPC calibrated using polystyrene standard and with THF as eluent at 40°C. [d]Isolated yield after precipitation in acetone. [e]No Ag_2SO_4 was added.

The control reaction also showed similar results in comparison to the control reaction of PDCI-PPP polymers where it had lower molecular weight, yield, but more narrow polydispersity (entry 37). The absorbance spectra of PDCI-PF_n was heavily influenced by PF chain length. Unlike PDCI-PPP where the absorption is dominated by the PDCI core (or related charge-transfer

complex), the absorbance by polyfluorene becomes more intense as the degree of polymerization is increased. The PDCI-PF was much more fluorescent and demonstrated up to an unprecedented 160% photoluminescence quantum yield (last column in Table 2.5), where the short wavelength and NIR bands demonstrated an approximately 1:1 ratio of PL quantum yields.

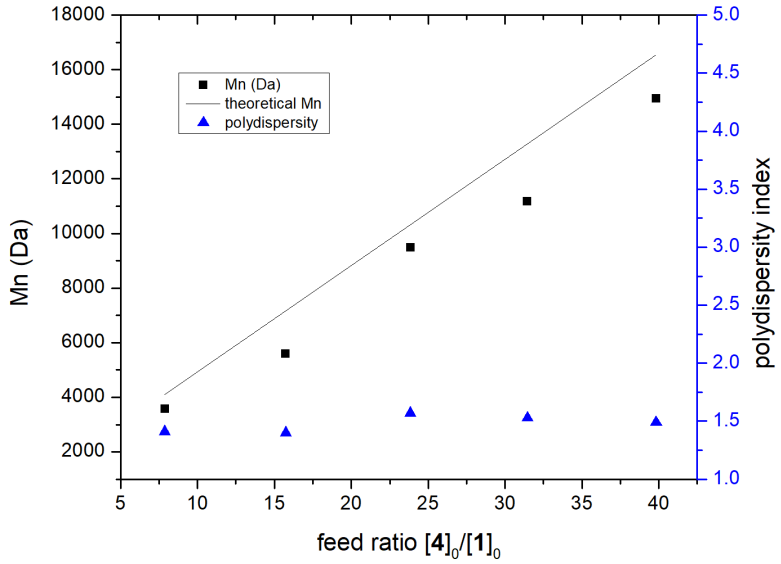

Figure 2.20. M_n vs feed ratio ($[\mathbf{4}]_0/[\mathbf{1}]_0$) of PDCI-$PF_n$ polymers prepared by silver mediated Suzuki-Miyaura Catalyst-Transfer Polymerization.

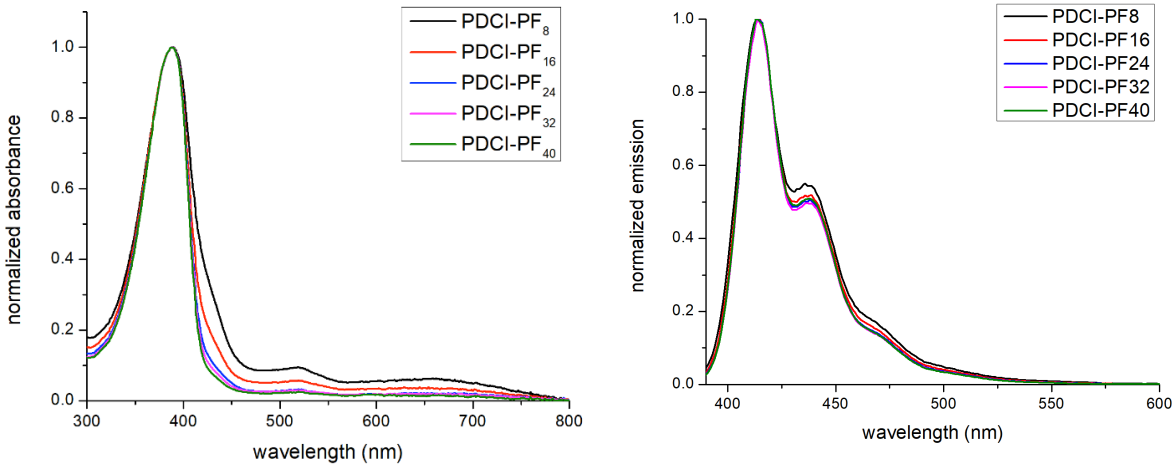

Figure 2.21. UV-Vis absorbance (left) and emission spectra (right) of PDCI-PF_n

The photoluminescence quantum yield varied proportionally from 11.9% in the case of PDCI-PF_8, 35.8% for PDCI-PF_{16}, 55.3% for PDCI-PF_{24}, 74.0% for PDCI-PF_{32} to 81.2% for PDCI-PF_{40}. Strong intramolecular energy transfer is expected via the Förster mechanism since the emission λ_{max} of PF overlaps with the absorption λ_{max} of the PDCI charge transfer complex (Figure 2.1). PDCI is expected to significantly quench PF emission and the chain-length dependent fluorescence quantum yield shows a highly efficient energy transfer taking place.

2.2.8. Externally Initiated Controlled Polymerization for Preparing Poly(3-hexylthiophenes)

The successful preparation of PDCI-$P3HT_n$ did not require the use of silver. A series of PDCI-P3HT polymers were prepared with degree of polymerization varying from 20 to 100. External initiation using **1** resulted in PDCI-P3HT with controlled molecular weight, excellent yields and modest polydispersity (Table 2.6). The PDCI-$P3HT_n$ polymers were characterized by UV-Vis absorbance and photoluminescence spectroscopy (Figure 2.22). PDCI-$P3HT_n$ series displayed a strong correlation between the molecular weight of the polymers and their PL quantum yield (Table 2.6), where the quantum yield progressed from 4.9% to 24.8% going from PDCI-$P3HT_{20}$ to PDCI-$P3HT_{100}$. The observed trend further demonstrates the quenching effect of PDCI core (or likely an associated charge-transfer state) and also shows effective energy transfer from P3HT to low energy PDCI. PDCI-$P3HT_n$ displayed a broad absorbance, owing to the dynamic conformational subunits caused by twisting and kinking of the polymer chains. The PL spectra of PDCI-P3HT was far more blue-shifted vs PDCI-PPP and PDCI-PF with an emission band λ_{max} of 575 nm. A slight vibronic structure is also observed with an emission band appearing around 630 nm.

Table 2.6. Controlled molecular weight series of PDCI-PT_n prepared by SCTP without silver.

entry	M_n (PDI)	Yield (%)	$[\mathbf{4}]_0/[\mathbf{1}]_0$	QY
38	4.0k (1.21)	65.0%	20	4.9%
39	7.7k (1.23)	82.7%	40	2.4%
40	11.4k (1.29)	88.1%	60	12.4%
41	14.0k (1.40)	92.3%	80	15.2%
42	17.0k (1.45)	83.8%	100	24.8%

[a]Reaction conditions: [K_3PO_4] = 3.0 M, 45°C, 48h. [b]Absolute molecular weight was determined by quantitative NMR. [c]M_w/M_n was determined by GPC calibrated using polystyrene standard and with THF as eluent at 40°C. [d]Isolated yield after precipitation in acetone.

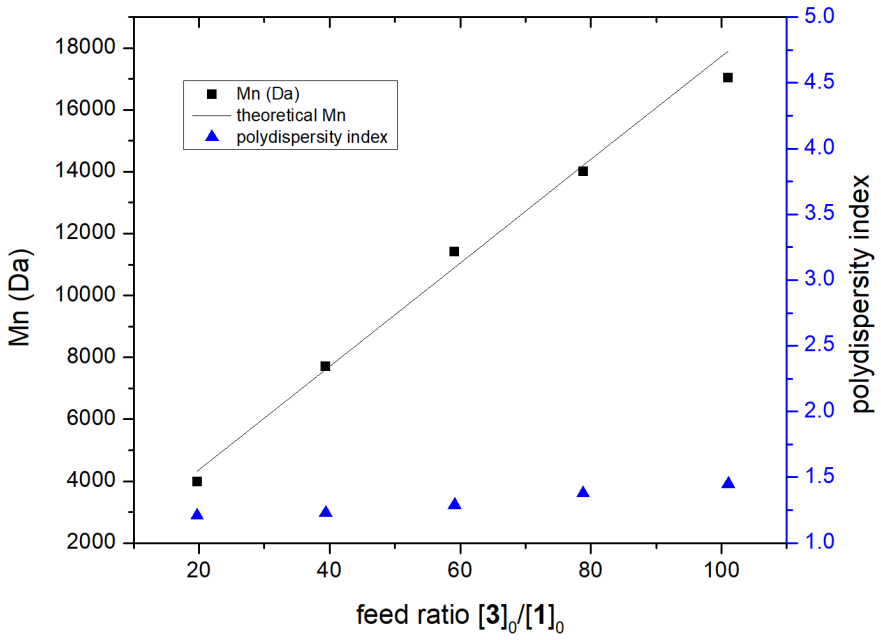

Figure 2.22. M_n vs feed ratio ($[\mathbf{3}]_0/[\mathbf{1}]_0$) of PDCI-P3$HT_n$ polymers prepared by silver mediated Suzuki-Miyaura Catalyst-Transfer Polymerization.

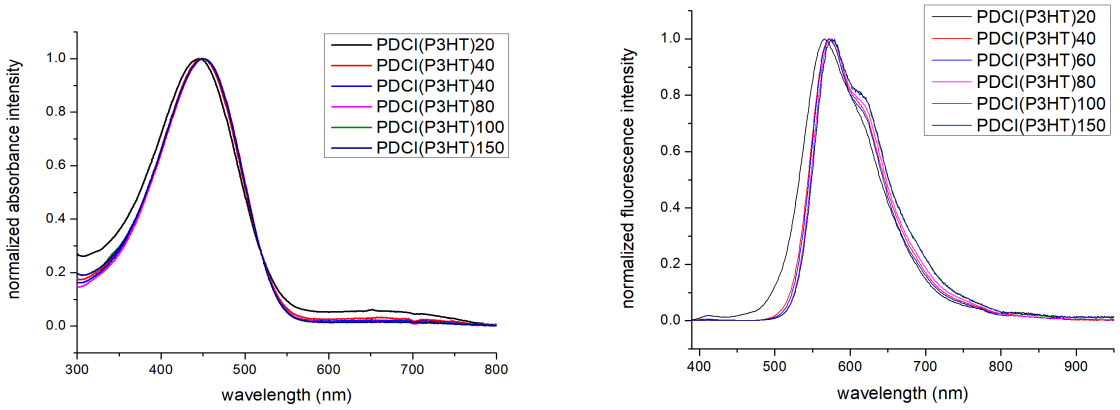

Figure 2.23. UV-Vis absorbance (left) and emission spectra (right) of PDCI-P3HT$_n$

The shortest chain-length PDCI-P3HT$_{20}$ had a blue-shifted absorbance and also emission bands versus PDCI-P3HT$_{40\text{-}100}$. This is expected because of the symmetry of PDCI-P3HT having two short 10 repeating unit P3HT on each side of the chain instead of a single 20-unit polymer chain and thus the conjugation path length for these units is much shorter than expected for 20 repeating unit of typical P3HT. The PDCI absorbance is also more pronounced in PDCI-P3HT$_{20}$ versus the other polymer samples, demonstrating that polythiophene has a significant molecular weight dependent extinction coefficient relative to the PDCI core (unlike PDCI-PPP where the absorption was dominated by PDCI). These experiments show that the donor-acceptor polymers prepared by externally initiated SCTP are well-defined, highly precise platforms for studying the structure dependent properties of conjugated polymers. PDCI was shown to be an effective energy acceptor and exhibits interesting and novel behavior when incorporated into conjugated polymer backbones.

2.3 Conclusion

Suzuki-Miyaura Catalyst Transfer Polymerization is still a technique at its infancy with few reports able to produce robust methodologies broadly applicable for preparing various classes of conjugated polymers. This evidence-based study on the SCTP mechanism revealed several novel fundamental processes that will likely have a lasting impact in conjugated polymer research. First, overwhelming evidence has been provided in support of the oxo-palladium (rather than boronate) pathway to be in operation for Pd SCTP. Second, the unequivocal role of water was elucidated to show two opposing effects on the M_n, yield and polydispersity of conjugated polymers prepared by SCTP. Third, the influential role of Br^- was discovered to seriously hamper the rate SCTP reactions. Fourth, based on the proposed mechanism, a synthetic solution utilizing silver was developed and integrated into the optimized SCTP methodology. These principles were combined to demonstrate controlled chain-growth preparation of P3HT, PPP and PF.

2.4 References

(1) Leone, A. K.; Mueller, E. A.; McNeil, A. J. The History of Palladium-Catalyzed Cross-Couplings Should Inspire the Future of Catalyst-Transfer Polymerization. *J. Am. Chem. Soc*. **2018**, 140, 15126-15139.

(2) Ego, C.; Marsitzky, D.; Becker, S.; Zhang, J.; Grimsdale, A. C.; Müllen, K.; MacKenzie, J. D.; Silva, C.; Friend, R. H. Attaching Perylene Dyes to Polyfluorene: Three Simple, Efficient Methods for Facile Color Tuning of Light-Emitting Polymers. *J. Am. Chem. Soc.* **2003**, 125, 437-443.

(3) Becker, K.; Lupton, J. M. Efficient Light Harvesting in Dye-Endcapped Conjugated Polymers Probed by Single Molecule Spectroscopy. *J. Am. Chem. Soc.* **2006**, 128, 6468-6479.

(4) Xia, J.; Sanders, S. N.; Cheng, W.; Low, J. Z.; Liu, J.; Campos, L. M.; Sun, T. Singlet Fission: Progress and Prospects in Solar Cells. *Adv. Mater.* **2017**, 29, 1601652.

(5) Ramanan, C.; Smeigh, A. L.; Anthony, J. E.; Marks, T. J.; Wasielewski, M. R. Competition between Singlet Fission and Charge Separation in Solution-Processed Blend Films of 6,13-Bis(triisopropylsilylethynyl)pentacene with Sterically-Encumbered Perylene-3,4:9,10-bis(dicarboximide)s. *J. Am. Chem. Soc.* **2012**, 134, 386-397.

(6) Kosaka, K.; Uchida, T.; Mikami, K.; Ohta Y.; Yokozawa, T. Amphos Pd-Catalyzed Suzuki-Miyaura Catalyst-Transfer Condensation Polymerization: Narrower Dispersity by Mixing the Catalyst and Base Prior to Polymerization. *Macromolecules* **2018**, 51, 364-369.

(7) Leone, A. K.; McNeil, A. J. Matchmaking in Catalyst-Transfer Polycondensation: Optimizing Catalysts based on Mechanistic Insight. *Acc. Chem. Res.* **2016**, 49, 2822-2831.

(8) Leone, A. K.; Mueller, E. A.; McNeil, A. J. The History of Palladium-Catalyzed Cross-Couplings Should Inspire the Future of Catalyst-Transfer Polymerization. *J. Am. Chem. Soc.* **2018**, 140, 15126-15139.

(9) Seo, K.-B.; Lee, I. H.; Lee, J.; Choi, I.; Choi. T.-L A Rational Design of Highly Controlled Suzuki-Miyaura Catalyst-Transfer Polycondensation for Precision Synthesis of Polythiophenes and Their Block Copolymers: Marriage of Palladacycle Precatalysts with MIDA-Boronates. *J. Am. Chem. Soc.* **2018**, 140, 4335-4343.

(10) Lutz, J. P.; Hannigan, M. D.; McNeil, A. J. Polymers Synthesized via Catalyst-Transfer and Their Applications. *Coord. Chem. Rev.* **2018**, 376, 225-247.

(11) Chen, S.; Liu, Y.; Qiu, W.; Sun, X.; Ma, Y.; Zhu, D. Oligothiophene-Functionalized Perylene Bisimide System: Synthesis, Characterization, and Electrochemical Polymerization Properties. *Chem. Mater.* **2005**, 17, 2208-2215.

(12) Byun, H. Y.; Chung, I. J.; Shim, H.-K.; Kim, C. Y. Optoelectronic and Photophysical Properties of Polyfluorene Blends as Side-Chain Length and Shape. *Macromolecules* **2004**, 37, 6945-6953.

(13) Remmers, M.; Müller, B.; Martin, K.; Räder, H.-J. Poly(*p*-phenylene)s: Synthesis, Optical Properties, and Quantitative Analysis with HPLC and MALDI-TOF Mass Spectrometry. *Macromolecules* **1999**, 32, 1073-1079.

(14) Murphy, C. B.; Zhang, Y.; Troxler, T.; Ferry,V.; Martin, J. J.; Jones, W. E. Probing Förster and Dexter Energy-Transfer Mechanisms in Fluorescent Conjugated Polymer Chemosensors. *J. Phys. Chem. B.* **2004**, 108, 1537-1543.

(15) Zhang, H.-H.; Xing, C.-H.; Hu, Q.-H. Controlled Pd(0)/*t*-Bu_3-P-Catalyzed Suzuki Cross-Coupling Polymerization of AB-Type Monomers with PhPd(*t*-Bu_3P)I or $Pd_2(dba)_3$/*t*-Bu_3-P/ArI as the Initiator. *J. Am. Chem. Soc.* **2012**, 134, 13156-13159.

(16) Yokozawa, T.; Kohno, H.; Ohta, Y.; Yokoyama, A. Catalyst-Transfer Suzuki-Miyaura Coupling Polymerization for Precision Synthesis of Poly(*p*-phenylene). *Macromolecules* **2010**, 43, 7095-7100.

(17) Carrillo, J. A.; Ingleson, M. J.; Turner, M. L. Thienyl MIDA Boronate Esters as Highly Effective Monomers for Suzuki-Miyaura Polymerization Reactions. *Macromolecules* **2014**, 48, 979-986.

(18) Gonzalez, J. A.; Ogba, O. M.; Morehouse, G. F.; Rosson, N.; Houk, K. N.; Leach, A. G.; Cheong, P. H.-Y.; Burke, M. D.; Lloyd-Jones, G. C. MIDA Boronates are Hydrolysed Fast and Slow by Two Different Mechanisms. *Nat. Chem.* **2016**, 8, 1067-1075.

(19) Kuivila H. G.; Reuwer, J. F.; Mangravite, J. A. Electrophilic Displacement Reactions. *Can. J. Chem.* **1963**, 41, 3081-3090.

(20) Cox, P. A.; Leach, A. G.; Campbell, A. D.; Lloyd-Jones, G. C. Protodeboronation of Heteroaromatic, Vinyl and Cyclopropyl Boronic Acids: pH-Rate Profiles, Autocatalysis, and Disproportionation. *J. Am. Chem. Soc.* **2016**, 128, 9145-9157.

(21) Cox, P. A.; Reid, M.; Leach A. G.; Campbell, A. D.; King, E. J. Base-Catalyzed Aryl-$B(OH)_2$ Protodeboronation Revisited: From Concerted Proton Transfer to Liberation of a Transient Aryl Anion. *J. Am. Chem. Soc.* **2017**, 139, 13156-13165.

(22) Pinder, K. L. Activity of Water in Solution with Tetrahydrofuran. *J. Chem. Eng. Data* **1973**, 18, 275-277.

(23) Carrow, B. P.; Hartwig, J. F. Distinguishing Between Pathways for Transmetalation in Suzuki-Miyaura Reactions. *J. Am. Chem. Soc.* **2011**, 133, 2116-2119.

(24) Amatore, C.; Le Duc, G.; Jutand, A. Mechanism of Palladium-Catalyzed Suzuki-Miyaura Reactions: Multiple and Antagonistic Roles of Anionic "Bases" and Their Countercations. *Chem. Eur. J.* **2013**, 19, 10082-10093.

(25) Amatore, C.; Jutand, A.; Duc, G. L. Kinetic Data for the Transmetalation/Reductive Elimination in Palladium-Catalyzed Suzuki-Miyaura Reactions: Unexpected Triple Role of Hydroxide Ions Used as Base. *Chem. Eur. J.* **2011**, 17, 2492-2503.

(26) Amatore, C.; Jutand A.; Le Duc, G. Mechanistic Origin of Antagonist Effects of Usual Anionic Bases (OH^-, CO_3^{2-}) as Modulated by Their Countercations (Na^+, Cs^+, K^+) in Palladium-Catalyzed Suzuki-Miyaura Reactions. *Chem. Eur. J.* **2012**, 18, 6616-6625.

(27) Uenishi, J.-C.; Beau, J.-M.; Armstrong, R. W.; Kishi, Y. Dramatic Rate Enhancement of Suzuki Diene Synthesis: Its Application to Palytoxin Synthesis. *J. Am. Chem. Soc.* **1987**, 109, 4756-4758.

(28) Smith, M. B.; Michi, J. Singlet Fission. *Chem. Rev.* **2010**, 110, 6891-6939.

(29) Kasai, Y.; Tamai, Y.; Ohkita, H.; Benten, H.; Ito S. Ultrafast Singlet Fission in a Push-Pull Low- Bandgap Polymer Film. *J. Am. Chem. Soc.* **2015**, 15980-15983.

(30) Hu, J.; Ku, K.; Shen, L.; Wu, Q.; He, G.; Wang, J.-Y.; Pei, J.; Xia, J.; Sfeir, M. Y. New Insights Into the Design of Conjugated Polymers for Intramolecular Singlet Fission. *Nat. Commun.* **2018**, 9, 2999.

CHAPTER 3. TUNABLE NANOSTRUCTURES OF DONOR-ACCEPTOR NANOPARTICLES BY EXTERNALLY INITIATED KUMADA CATALYST-TRANSFER DISPERSION POLYMERIZATION

3.1. Introduction

Recently, there has been a growing interest in utilizing surfactant-free donor-acceptor conjugated polymer nanoparticles (CPN) for organic electronic devices such as organic light emitting diodes, organic field effect transistors and organic photovoltaic cells.[1-10] Integrating CPNs into the active layers of organic electronic devices allows for the optoelectronic properties to be engineered separately from the thin-film construction. Donor-acceptor CPNs are prepared by reprecipitation or miniemulsion methods[11-12] and their material properties[13-15] can be tailored by varying the polymer concentration during the preparation process; resulting in nanoparticles of different sizes and properties. Alternatively, the relative molar ratios of donor-acceptor blends can be adjusted prior to nanoparticle formation to modify the microstructure within (such as morphology and average distance between donor and acceptor domains).[16-21] But these methods don't allow for controlling the properties of primary nanostructures such as chain-conformation and average conjugation path lengths to any significant degree.

Using ultrasonication is a major drawback for both reprecipitation and miniemulsion techniques. The heat and cavitation bubbles caused by high energy ultrasound waves completely alter the polymer self-assembly process and disallow for using temperature as a synthetic parameter for tuning CPN properties.[22-27] For example, Luscombe and Pozzo have recently demonstrated that ultrasonication triggers the self-assembly of poly(3-hexylthiophene) into nanofibers even in good solvents such as chlorobenzene or chloroform.[28] Therefore, an ability to prepare CPN's without sonication to control the temperature-dependent self-assembly process would be an important fundamental approach for making CPNs with precise and tunable properties.

Herein, donor-acceptor polythiophene nanoparticles with tunable photophysical properties are prepared by externally initiated Kumada Catalyst-Transfer dispersion polymerization. The CPNs are prepared without sonication or surfactants in THF. An electron deficient perylenedicarboximide (PDCI) was utilized as precursor to the Ni(dppp) based external initiator and was covalently integrated into the polymer; forming a donor-acceptor system. The reaction temperature was found to affect the average conjugation path length of polythiophene chain segments that are kinetically trapped within the supramolecular assembly. Subsequently, the polythiophene fluorescence λ_{max} from these chromophores can be controlled and alters the Förster energy transfer efficiency towards PDCI. The kinetically trapped conformations revert back to a common structure upon heating at 310°C. In addition to providing a synthetic handle on conjugated polymer self-assembly process affording various tunable photophysical properties, PDCI-PTh particles were investigated by X-ray powder diffraction (XRD), small-angle X-ray scattering (SAXS), small-angle neutron scattering(SANS), high-resolution scanning electron microscopy (SEM) experiments to provide more details on the structure of donor-acceptor nanoparticles on multiple length-scales.

Polythiophene is an ideal model system to study nanoparticle structure formation by controlled polymerization because of the abundance of structural characterization data, predictable self-assembly behavior and compatibility with transition metal catalyzed polymerization methods. For polythiophene synthesis, Kumada Catalyst-Transfer Polymerization (CTP) is well-established for its quasi-living chain-growth nature and its ability to produce polythiophenes.[29-32] The controlled chain-growth nature of Kumada CTP was discovered independently by McCullough[33] and Yokozawa[34] in 2004. Kumada type CTP reactions were used to polymerize thiophene Grignard monomers in this study which led to polythiophenes. We also employed an efficient preparation

of the external initiator using $Ni(dppp)_2$ as the pre-catalyst; a method previously reported by our group.[35]

PDCI is an electron-deficient π-conjugated fluorophore which can form various supramolecular assemblies[36-38] and donor-acceptor complexes with electron-rich molecules[39] (e.g. thiophene). Thus, depending on the reaction conditions, externally initiated PDCI catalyst can result in various initial supramolecular assemblies which can direct CTP towards different PDCI-PTh macromolecular mesoscale systems.

3.2 Results and Discussion

3.2.1. Preparation of the Regioisomerically Pure External Initiator

Classical bromination of perylenetetracarboxylic dianhydride **1** (Scheme 3.1) produces a mixture of constitutional and regioisomers which are practically inseparable because of their low solubility.[40] Although some researchers have debated[41] that the difference in photophysical properties of these isomers are insignificant, its crystallinity and self-assembly properties of the donor-acceptor polymers will be affected by the regioregularity of the central initiating core. We therefore decided to pursue isomerically pure starting materials. In 2014, Sengupta et al. reported[42] a four-step preparation of regioisomerically pure 1,7-dibrominated PDCI via a tetrabutyl ester intermediate which could be readily purified in five days. Utilizing this method, the synthesis began with perylenetetracarboxylic dianhydride **1** (Scheme 3.1), which was converted into a perylene tetrabutyl ester **2** using a 1:1(v/v) mixture of butanol and bromobutane. DBU was utilized as a strong organic base. Bromination of **2** afforded a 3:2 ratio of 1,7- and 1,6-dibrominated regioisomers **3a** and **3b**, respectively. The 1,7-dibrominated product **3a** was isolated with a 27% recovery by recrystallization in a mixture of acetonitrile and dichloromethane.

Scheme 3.1. Preparation of External Catalytic Initiator for Kumada Catalyst-Transfer Dispersion Polymerization.

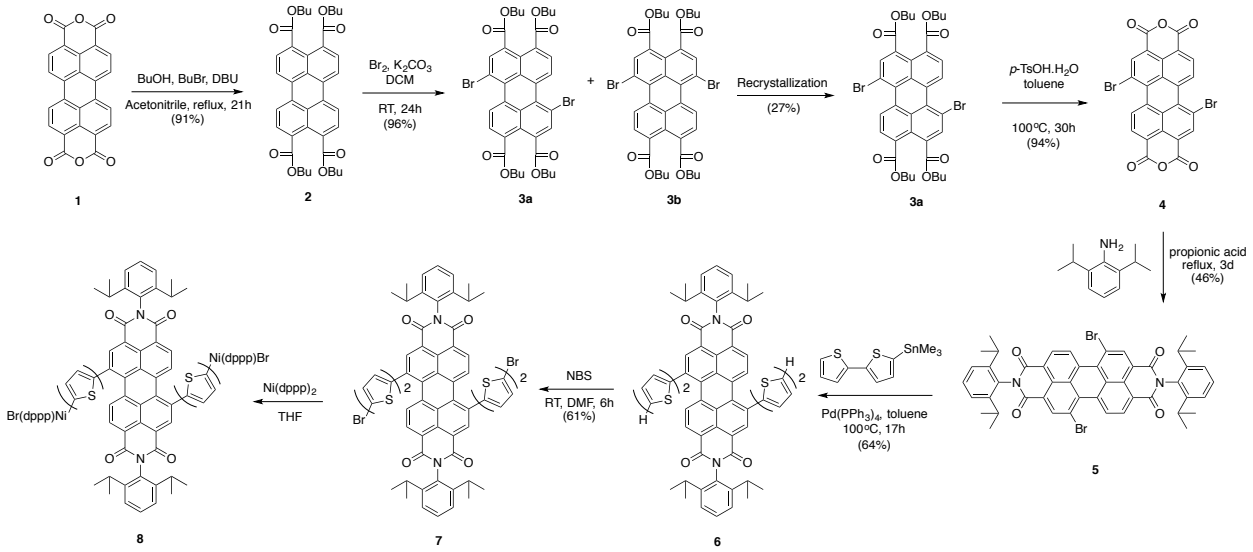

Hydrolysis of the isomerically pure tetrabutyl ester **3a** yielded the isomerically pure **4**. Its structure was confirmed by NMR in D_2SO_4. The ^1H NMR spectrum showed a single regioisomer and high purity of compound **4**. Isomerically pure **4** was condensed with 4-bromo-2,6-diisopropylaniline to yield perylenedicarboximide **5**. Following a typical Stille coupling and subsequent NBS bromination, the small molecule precursor **7** was obtained. A solution of the external initiator **8** is produced upon mixing of precursor **7** with an excess of $Ni(dppp)_2$ in THF. The external initiator **8** was freshly prepared prior to each polymerization reaction.

3.2.2. Morphology of PDCI-PTh Prepared at -10°C to 22°C: Characterization by SEM

Preparation of PDCI-PTh nanoparticles begins with a 50 mM solution of 5-bromo-2-thienylchloromagnesium monomer which was made by mixing 2,5-dibromothiophene with a sub-stoichiometric amount of ^{i}PrMgCl. Because of its mono-functionality and relatively high reactivity versus the target Grignard monomer, excess ^{i}PrMgCl will cause chain termination in this KCTP system. Nanoparticles are formed when a solution **8** (1 mol% relative to the monomer) is introduced to the Grignard solution under air-free conditions and at various temperatures. After

five minutes, the reaction was quenched using 6.0M HCl to neutralize the Grignard monomer and the resulting polymer suspension was isolated and washed repeatedly with chloroform and methanol via centrifugation. The obtained nanoparticles were dried in vacuum and could be resuspended in a variety of solvents including water, methanol, chloroform, and 1,2-dichlorobenzene.

$CHCl_3$ suspensions of PDCI-PTh produced at 22°C, 7°C, 0°C and -10°C (PDCI-$PTh_{22°C}$, PDCI-$PTh_{7°C}$, PDCI-$PTh_{0°C}$ and PDCI-$PTh_{-10°C}$) were drop-casted onto a copper substrate for scanning electron microscopy (SEM). SEM reveals that PDCI-$PTh_{22°C}$ particles have an irregular, and jagged shape. As the reaction temperature is lowered, KCTP produced larger PDCI-PTh particle diameters and the morphology became progressively disk-like (Figures 3.1-3.4). The number averaged diameter of PDCI-$PTh_{22°C}$ is 234 ± 26 nm. The odd morphology of PDCI-PTh nanoparticles was unexpected because CPNs prepared by reprecipitation (a similar CPN forming process) generally form spherical particles which minimize the material's surface area in contact with the solvent; and the solvophobic effect is the dominant driving force for particle self-assembly by reprecipitation.[11] The higher surface area morphology of disk-shaped particles versus forming spheres is entropically unfavorable in this regard. Nanoparticle that are not single-crystals are typically made of smaller primary units, and the tendency to form disk-like structures at length scale >100 nm point to the existence of sheet-like primary particles that would be necessary to direct hierarchal self-assembly towards two-dimensional morphology. At -10°C, finer sheet structures are observed protruding at the surface of the particles, forming distinct edges and supporting the hypothesis that the sheet-like primary structures are directing hierarchal self-assembly at longer length-scales. Gravimetric analysis and study of the supernatant after centrifugation showed a percent conversion of 53%, while the remaining solute in the supernatant

contained quenched monomer (42% recovery) and unreacted dibromothiophene. 2,5-dibromothiophene is not expected to cause chain-transfer in CTP reactions.[40]

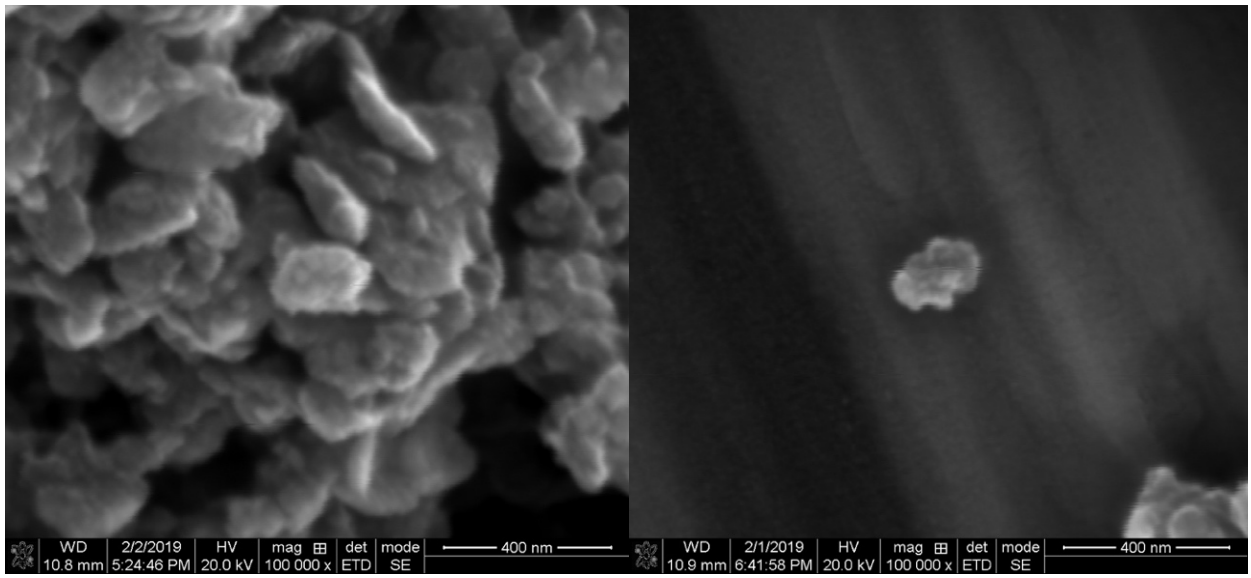

Figure 3.1. SEM images of PDCI-PTh nanoparticles prepared by Kumada Catalyst-Transfer Dispersion Polymerization at 22°C.

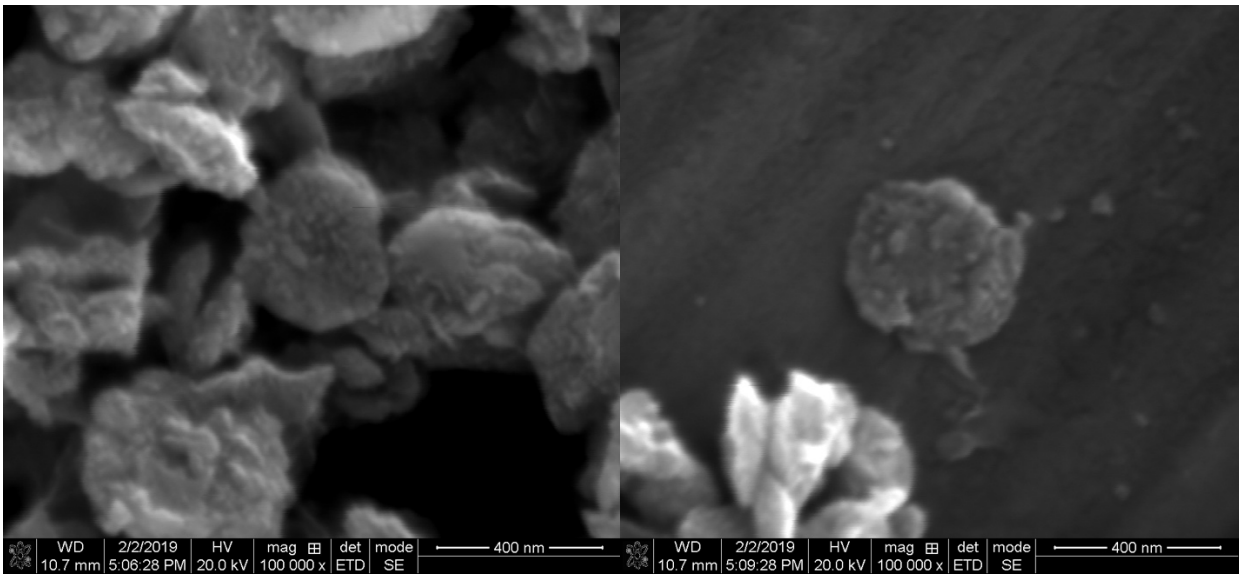

Figure 3.2. SEM images of PDCI-PTh nanoparticles prepared by Kumada Catalyst-Transfer Dispersion Polymerization at 7°C.

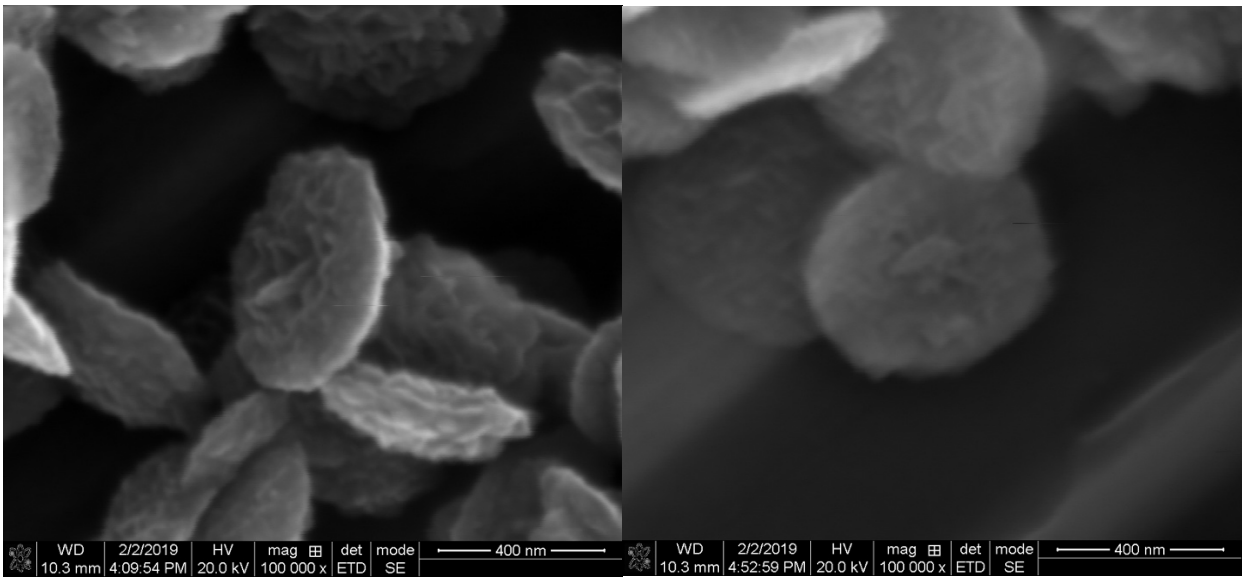

Figure 3.3. SEM Images of PDCI-PTh nanoparticles prepared by Kumada Catalyst-Transfer Dispersion Polymerization at 0°C.

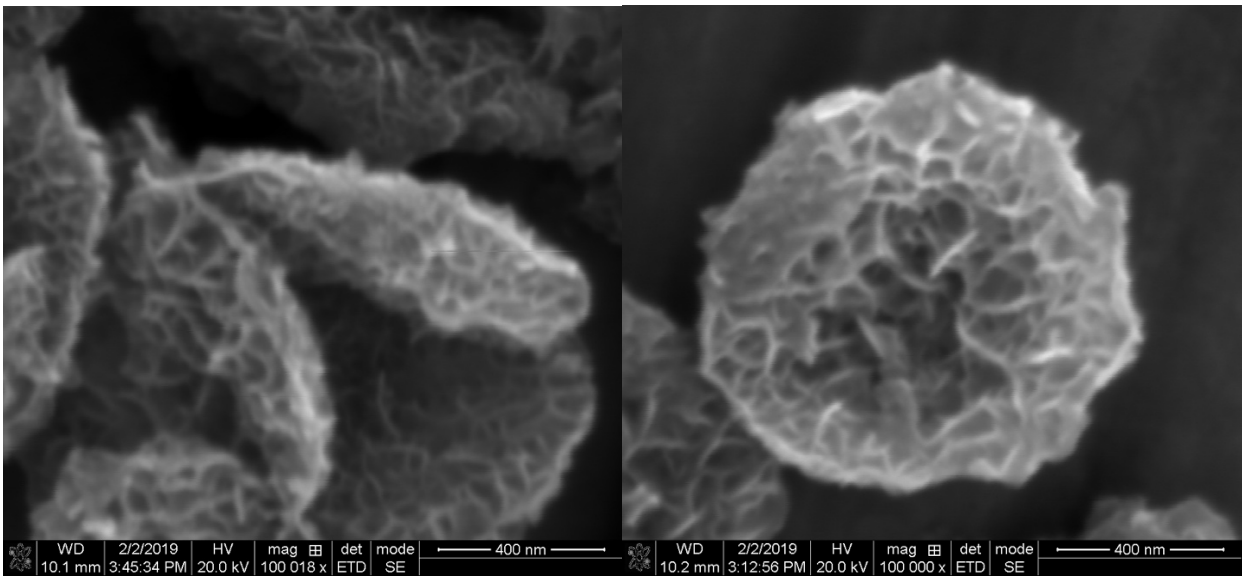

Figure 3.4. SEM images of PDCI-PTh nanoparticles prepared by Kumada Catalyst-Transfer Dispersion Polymerization at -10°C.

3.2.3. Effects of Polymerization Temperature on the Photophysical Properties of PDCI-PTh Nanoparticles

The polymerization reaction temperature had a dramatic effect on the photophysical properties of resulting PDCI-PTh nanoparticles. PDCI-PTh nanoparticles produced between -10ºC and 22ºC

displayed broad absorption spectra with λ_{max} of 625nm (Figure 3.5). The disordered twisting of the polythiophene polymer backbone in the polymer supramolecular assemblies can result in a statistical distribution of chromophores (termed conformational subunits) with different electronic structures; resulting in a wide absorption spectra.[41-43] PDCI-PTh$_{7°C}$, PDCI-PTh$_{0°C}$ and PDCI-PTh$_{-10°C}$ produced a more disordered absorption spectra versus the PDCI-PTh$_{22°C}$, presumably due to the lower reaction temperature trapping polythiophene chains into non-equilibrium conformations.

The emission spectra of PDCI-PTh$_{22°C}$, PDCI-PTh$_{7°C}$, PDCI-PTh$_{0°C}$ and PDCI-PTh$_{-10°C}$ displayed a broad emission from 400 – 950 nm with definitive dependence on the polymerization temperature (Figure 3.6). Albeit, these come from different excited states species responding to the change of polymerization reaction temperature in different ways. Notably, the short wavelength emission band (λ_{max} between 450 nm and 500 nm) of the PDCI-PTh nanoparticle series (Figure 3.6) showed a dramatic red-shift with decreasing temperature. PDCI-PTh nanoparticles produced at lower reaction temperatures are expected to result in segments of polythiophene chains with more planar conformations, resulting in longer conjugation path length. This would explain red shift of PDCI-PTh particles emission (λ_{max} between 450-500 nm) as reaction temperature decreases as observed in Figure 3.6.

There is also a reaction temperature dependent trend in the emission intensity of the PDCI core at λ_{max} = 775 nm relative to the short wavelength thiophene emission bands. The absorbance and emission spectra of the PDCI core is taken separately using the starting materials and confirmed the assignment of the PDCI-PTh nanoparticle emission at λ_{max} = 775 nm (Figure 3.7). An excitation spectrum of PDCI-PTh$_{22°C}$ revealed that the origin of emission at λ_{max} = 775 nm (Figure 3.8) comes from absorption at 340 nm, and the shape of the excitation spectra is identical to the absorption of PDCI in Figure 3.7 (showing characteristic absorption maxima at both 340 nm and

460 nm). This further supports that the 775 nm emission band of the PDCI-PTh nanoparticle series originates from PDCI.

Unlike polythiophene, PDCI chromophore is not subject to conformation-dependent electronic structures and is expected to have a constant absorption wavelength λ_{max} = 340 nm and emission at λ_{max} = 775 nm (Figure 3.7). Indeed, the emission wavelength at λ_{max} = 775 nm of the PDCI-PTh remained constant for PDCI-PTh produced at various reaction temperatures. A significant overlap of the donor emission band and the acceptor absorbance band is a critical requirement for efficient dipole-induced dipole coupling needed for Förster energy transfer. Consequently, this characteristic of a constant absorbance wavelength in the acceptor but a variable emission wavelength of the donor affords a mechanism for tuning of the Förster energy transfer efficiency.

If Förster energy transfer is taking place from higher energy polythiophene conformational subunits to PDCI, intensity of the 775 nm emission band would be dramatically affected by the fluorescence wavelength of polythiophene. As the reaction temperature is decreased, the red shift of polythiophene conformational subunits may cause depletion of available energy donors that are able to undergo Förster energy transfer. Thus, for lower reaction temperatures, reduced energy transfer is expected to occur from polythiophene to the PDCI chromophore as it was observed in emission intensity of the 775 nm emission band in Figure 3.6.

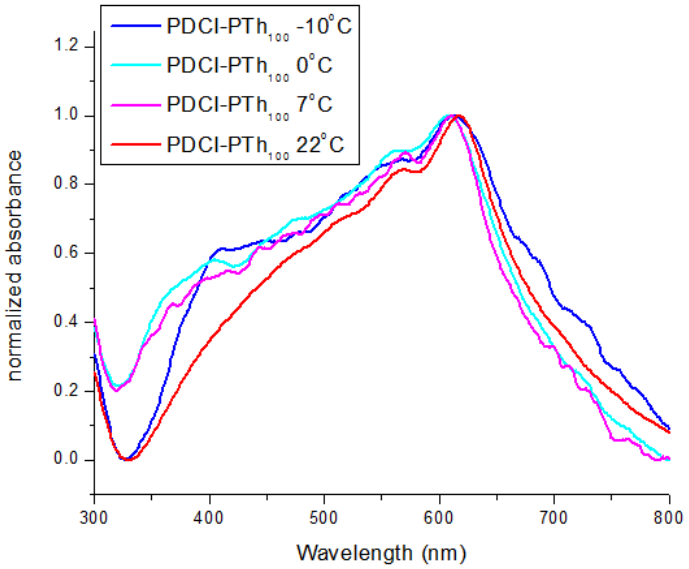

Figure 3.5. UV-Vis absorbance spectra of PDCI-PTh particles prepared between -10°C and 22°C by Kumada Catalyst-Transfer Dispersion Polymerization.

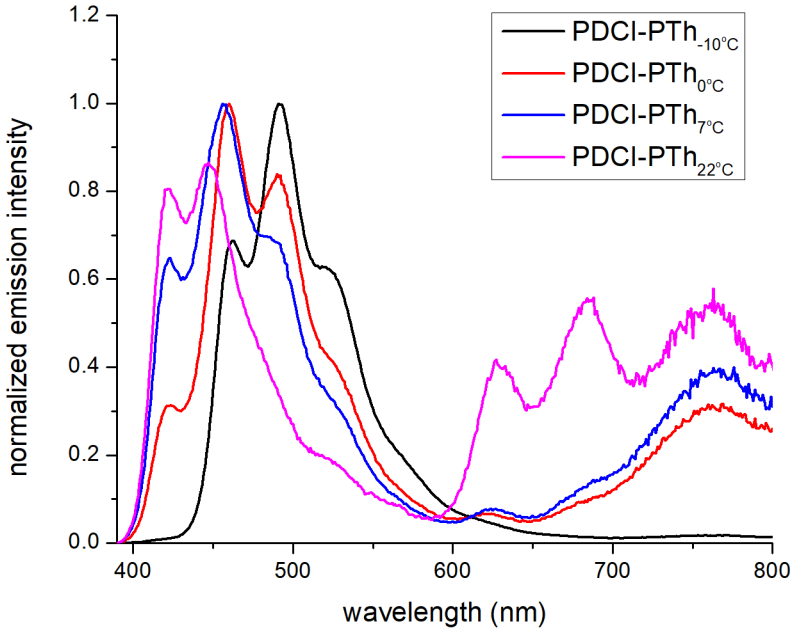

Figure 3.6. Emission spectra of PDCI-PTh particles prepared between -10°C and 22°C by Kumada Catalyst-Transfer Dispersion Polymerization.

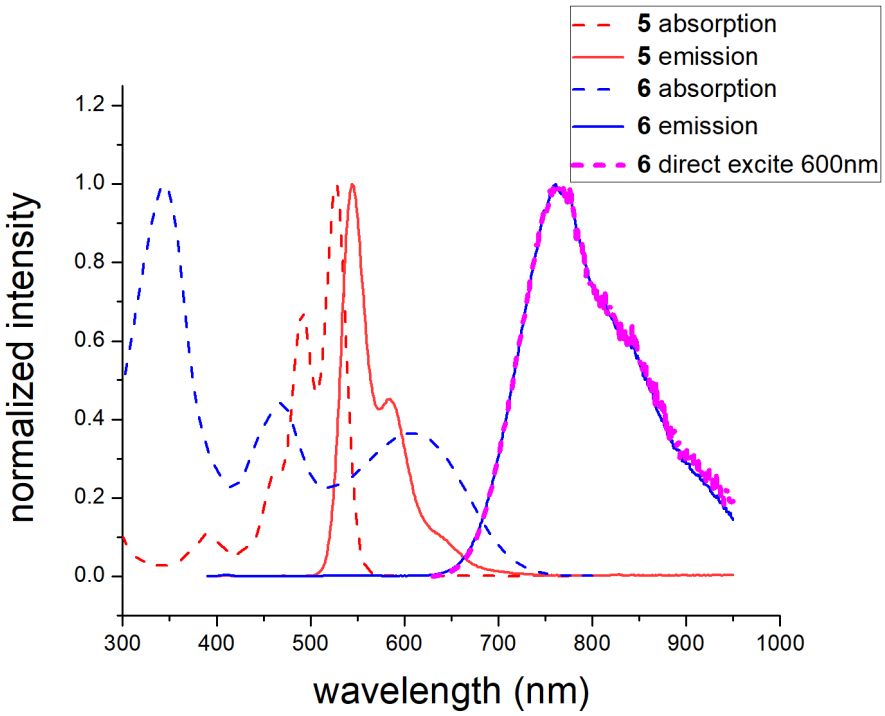

Figure 3.7. UV-Vis absorbance and emission spectra of PDCI precursor **5** and **7**.

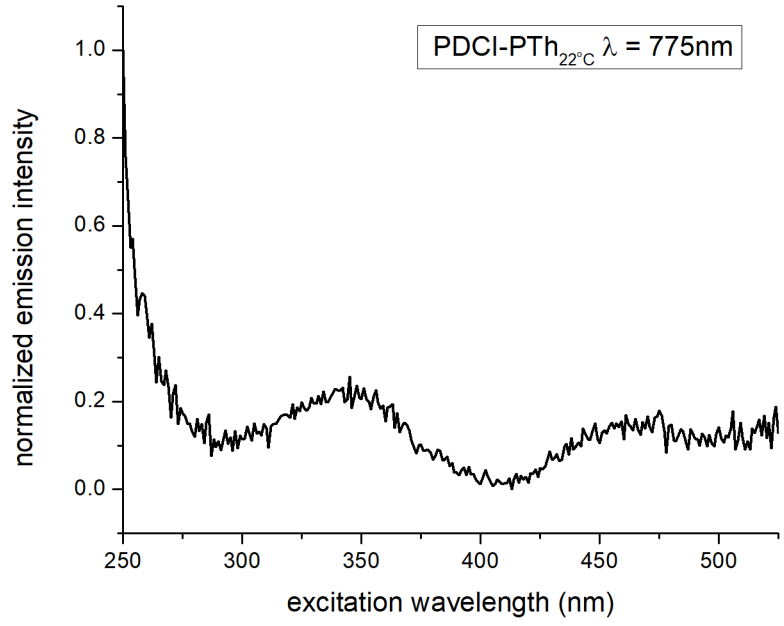

Figure 3.8.Excitation spectra acquired at λ_{max} = 775 nm emission bands of PDCI-PTh$_{22°C}$.

The conformation of polythiophene chains within the PDCI-PTh mesoscopic self-assemblies are shown herein to depend on reaction temperature, which affects the average polythiophene conformational subunit emission λ_{max}. The NIR emission bands at 775 nm was shown to correlate to the polythiophene emissions λ_{max}. Thus, the photophysical properties of PDCI-PTh nanoparticles have been demonstrated here to be highly dependent on reaction temperature, affecting the conjugation path length of polythiophene conformational subunits and subsequently altering the energy-transfer efficiency to PDCI via Förster mechanism.

3.2.4. Kinetically Trapped Polythiophene Chains in PDCI-PTh$_{22°C}$ and PDCI-PTh$_{0°C}$

The control over PDCI-PTh particles' energy transfer behavior and photophysical properties rely on the hypothesis that the reaction temperature causes the formation of kinetically trapped conformational states. To test this idea, PDCI-PTh$_{22°C}$ and PDCI-PTh$_{0°C}$ were heated in an inert atmosphere at high temperature to allow for thermodynamically driven rearrangement of the polythiophene segments into a common supramolecular structural state. First, PDCI-PTh$_{22°C}$ was characterized by differential scanning calorimetry (DSC) to identify possible thermal transitions (Figure 3.10).

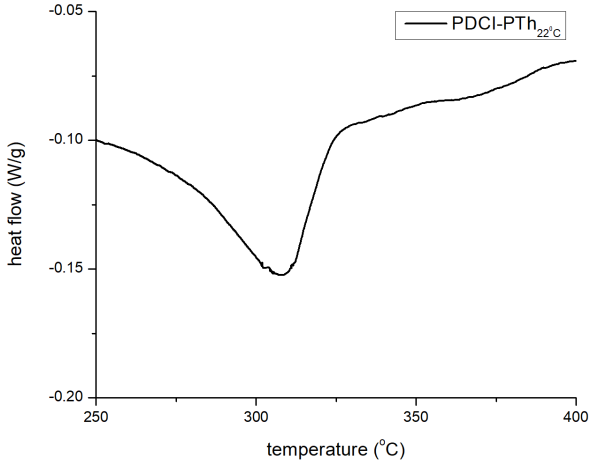

Figure 3.9. PDCI-PTh$_{22°C}$ characterized by Differential Scanning Calorimetry.

DSC showed an endothermic transition around 310°C and thus this temperature was used for heating experiments. The absorbance and fluorescence of PDCI-PTh$_{22°C}$ and PDCI-PTh$_{0°C}$ before and after heating at 310°C is shown in Figure 3.11.

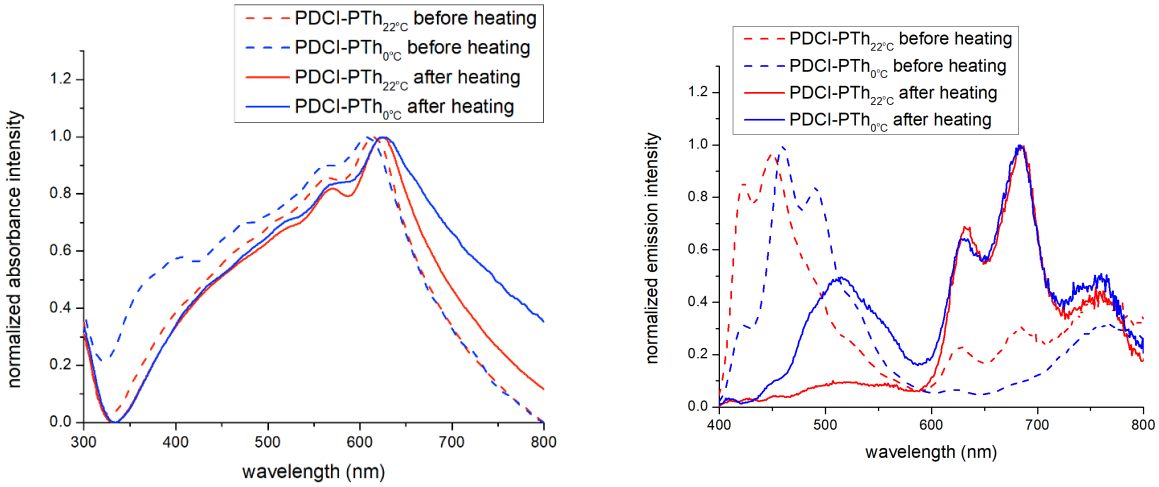

Figure 3.10. UV-Vis absorbance (left) and emission spectra (right) of PDCI-PTh$_{22°C}$ and PDCI-PTh$_{0°C}$ before and after heating at 310°C.

Expectedly, heating transformed the absorbance and emission spectra of PDCI-PTh$_{22°C}$ and PDCI-PTh$_{0°C}$ towards a similar pattern, indicating a rearrangement of the polymer chain towards a common and more delocalized supramolecular structural state. In the absorbance spectra, the relative number of higher energy transition states (associated to more twisted polythiophene chains) decreased, while the longer wavelength absorbance increased (Figure 3.11, left), indicating the conversion of polythiophene segments with shorter conjugation path lengths into longer ones. This is expected as the DSC showed an endothermic transition at 310°C, implying that PDCI-PTh particles absorbed heat for a chemical process. The emission spectra also changed dramatically upon heating. After heating, the emission spectra of both PDCI-PTh$_{22°C}$ and PDCI-PTh$_{0°C}$ are perfectly superimposed within the range 600 – 800 nm (Figure 3.11, right), and the short wavelength emission λ_{max} between 450 nm become redshifted in comparison to the pre-heated, kinetically trapped states. This also indicates that the short wavelength emission coming from λ_{max}

= 450nm for PDCI-PTh$_{22°C}$ and PDCI-PTh$_{0°C}$ are derived from segments of polythiophene conformational subunits which are converted into chains with longer conjugation length by heating. PDCI-PTh$_{0°C}$ had a characteristic decrease in the shortwave emission with concomitant increase in emission in the range 600 – 700 nm which are assigned to as the crystalline domains of semicrystalline polythiophene.

These experiments provide strong support that the lower temperature reactions produce segments of polythiophene chains with more planar and longer conjugation path lengths; resulting in tunable photophysical properties of primary nanostructures. At the same time, the lower reaction temperature does not allow polythiophene chains to rearrange into more crystalline supramolecular structures (involving more than one polythiophene chain) that are more delocalized.

3.2.5. Small Angle X-ray Scattering and X-ray Powder Diffraction

The internal structure of PDCI-PTh nanoparticles was characterized by X-ray and neutron scattering experiments. X-ray Powder Diffraction (XRD) describes the molecular packing of the polymer chains. PDCI-PTh$_{22°C}$ was chosen for comprehensive structural studies due to the more rich photophysical characteristics observed in its photoluminescence spectra. PDCI-PTh$_{22°C}$ showed typical XRD diffraction for crystalline polythiophenes and this type of pattern has been shown in literature to come from herringbone type packing of polythiophene.[49-50] The broad peak at 2Θ = 2.5-7.7° is indicative of the amorphous regions of polythiophene while the sharp Bragg peaks are assigned to crystalline domains. Therefore, the PDCI-PTh$_{22°C}$ was shown to be a highly ordered semi-crystalline material. The semi-crystalline nature of PDCI-PTh$_{22°C}$ observed by XRD agrees with the distribution of chromophores assigned as segmented polythiophene chains and crystalline polythiophene observed by the emission spectra in Figure 3.6. XRD showed no other, alternative types of nanostructures or packing conformations.

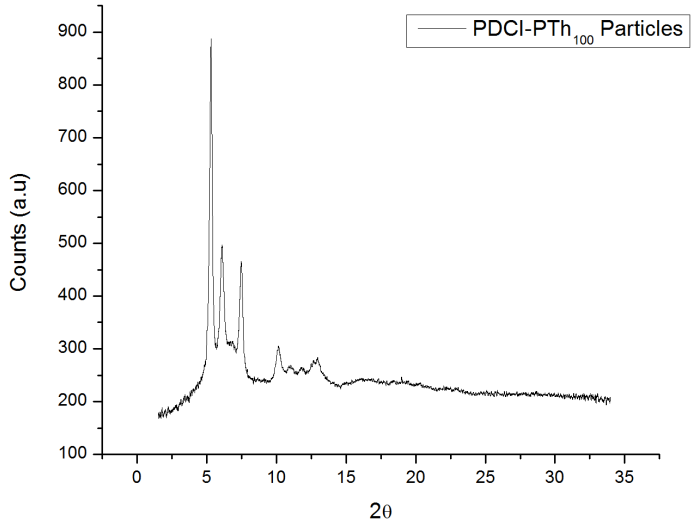

Figure 3.11. X-ray Powder Diffraction Pattern of PDCI-$PTh_{22°C}$.

PDCI-$PTh_{22°C}$ was also characterized by small angle X-ray scattering (SAXS). The crystalline domains of polythiophene are expected to be significantly denser than the amorphous components and would manifest as high contrast in the x-ray scattering length density (SLD). Thus, the SAXS pattern is expected to reveal the nanostructure of the crystalline polythiophene relative to the lesser dense amorphous polythiophene. At medium q range between 0.1 and 0.02 $Å^{-1}$, the slope of -2.67 is indicative of a planar sheet like structure such as to the one proposed upon analysis of the SEM data, and it is also expected because of the known sheet like self-assembled structures of polythiophene. Beyond q = 0.02 $Å^{-1}$, aggregation of the primary nanostructures is apparent by the increased slope to -3.7. The q = 0.02 $Å^{-1}$ is associated with the length of 31.4 nm and is assigned to a single size dimension of the primary nanostructure, presumably the sheet thickness.

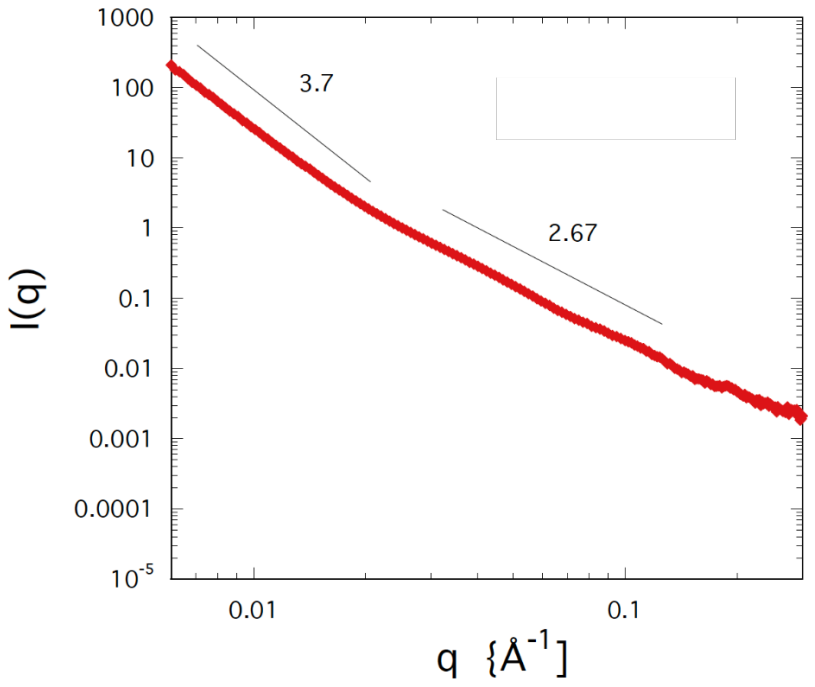

Figure 3.12. Small-angle X-ray Scattering curve of PDCI-PTh$_{22°C}$

3.2.6. Small-Angle Neutron Scattering Experiments

Neutrons are an ideal tool to differentiate and elucidate the structure of a multiple component nanostructure composed of light elements. Unlike X-rays which interact with the electron cloud (and can be used to differentiate between areas of different electron density), neutrons communicate with the atomic nuclei which results in greater sensitivity for elements such as carbon, hydrogen and nitrogen. Additionally, the scattering length density (SLD) of individual chemical components can be matched with the SLD of the solvent via isotopic labeling, absolving their contrast and scattering signal. In this way, the signal contributions from individual components can be highlighted while attenuating the signal from other chemical species (such as differentiating between PDCI and PTh nanostructures). PDCI-PTh$_{22°C}$ and PDCI-PTh$_{0°C}$ particles were suspended in either protonated (h)1,2-dichlorobenzene or deuterated (d)1,2-dichlorobenzene for SANS analysis.

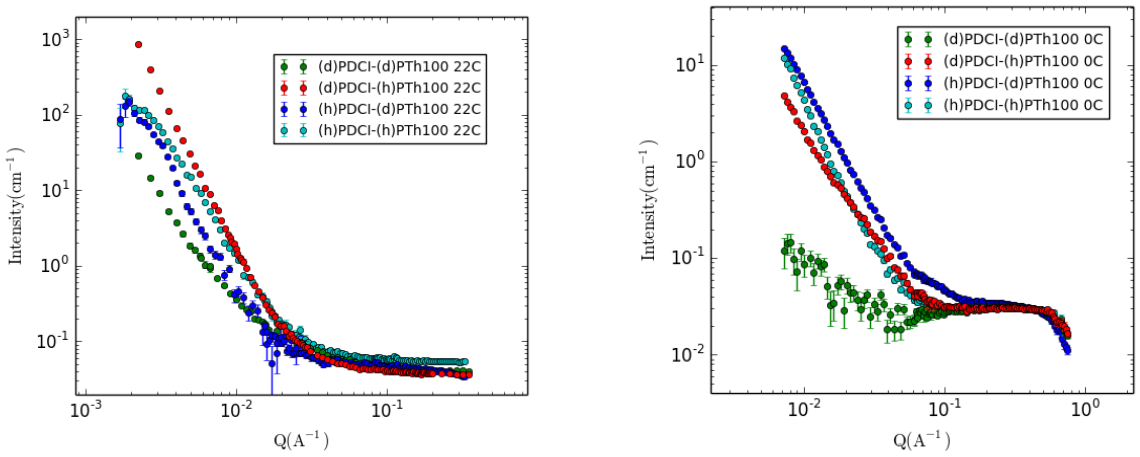

Figure 3.13. Small-angle neutron scattering curves of PDCI-PTh synthesized at 22ºC (left), PDCI-PTh at 0ºC (right).

For these experiments, nanoparticles with deuterated and protonated PDCI and PTh units were synthesized, and referred to here as (*d*)PDCI, (*h*)PDCI, (*d*)PTh and (*h*)PTh. All the (*d/h*)PDCI-PTh particles exhibited a power law scattering at below q = 0.02 Å^{-1} and this derives from the aggregation of primary nanostructures with a characteristic size of 31.4 nm such as observed in SAXS studies. This is assigned to thickness of polythiophene sheet nanostructures. The intensity I(Q) is proportional to the square of the SLD contrast. Because of the low contrast between (*d*)PDCI (SLD = 4.43) (*d*)PTh (SLD=4.81) with the solvent (SLD = 4.59), (*d*)PDCI and (*d*)PTh is not expected to contribute significantly to scattering signal above the incoherent scattering background (green traces, Figure 3.14). The SLD of (*d*)PTh was measured experimentally using a control sample (*d*)PTh nanoparticles that do not contain PDCI component. Protonated components: (*h*)PDCI (SLD=1.79) and (*h*)PTh (SLD = 2.48) are expected to result in more than 4 times stronger signal to noise ratio in comparison to their deuterated counterparts. Therefore, only sub-structures containing (*h*)PDCI or (*h*)PTh are assumed to affect scattering data.

SAXS and SEM provided strong supporting evidence that polythiophenes form sheet-like primary structures that drive the self-assembly of higher order mesoscopic assemblies. The nanostructure of PTh was investigated using (*d*)PDCI-(*h*)PTh nanoparticles prepared at 22°C and 0°C. Both samples showed power law scattering below q = 0.02 $Å^{-1}$ and did not show definite scattering slopes that can be measured quantitatively by SANS. This demonstrated that the polythiophene nanostructures had poor SLD contrast with its environment in the supramolecular assembly. Whereas in SAXS, the increased physical density of the crystalline PTh domains produced a stronger scattering signal (versus MeOH as solvent). The increased density of crystalline domains of PTh (vs amorphous domains) in SANS actually lowers the signal. Because the solvent's SLD is 4.59 and the protonated PTh's SLD is 2.48, higher PTh density will increase the SLD proportionally, lowering the contrast with the solvent and resulting in less signal to noise ratio versus the amorphous regions of polythiophene.

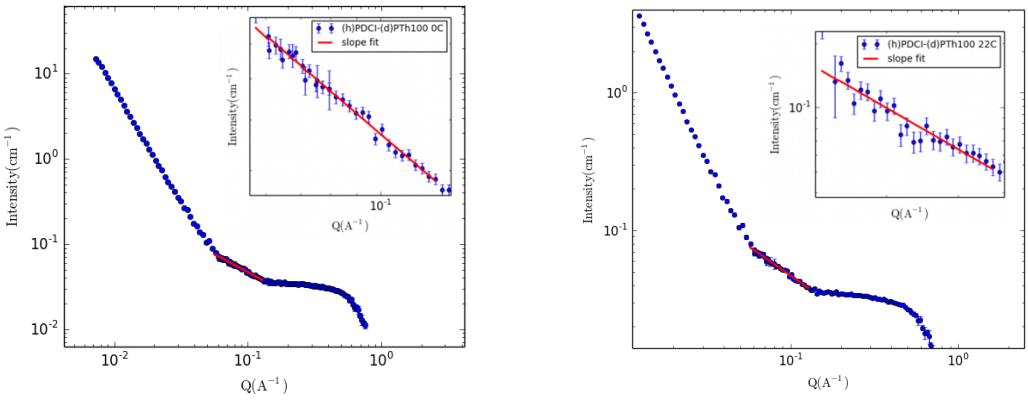

Figure 3.14. Porod slope of (h)PDCI-(d)PTh prepared at 0°C and 22°C. I(Q) ~ q^(-0.86) for (h)PDCI-(d)$PTh_{0°C}$ and I(Q) ~ q^(-1.04) for (h)PDCI-(d)$PTh_{22°C}$, indicated a 1D structure.

However, protonated PDCI, deuterated polythiophene (*h*)PDCI-(*d*)PTh prepared at 0ºC and (*h*)PDCI-(*d*)PTh prepared at 22ºC showed distinct features by SANS. The I(Q) was proportional to q^(-0.86) for (h)PDCI-(d)$PTh100_{0°C}$ and I(Q) was proportional to q^(-1.0) for (h)PDCI-

(d)$PTh_{22^{o}C}$ between q = 0.006 and 0.15 which strongly indicated a 1D object for PDCI sub-structure in the supramolecular structure (Figure 3.15). Perylene has often been reported to form 1D supramolecular structures in literature.[36-39.] However, the photoluminescence spectra showed that PDCI-PTh nanoparticles exhibited similar NIR emission behaviors as the free PDCI precursor in Figure 3.7, which indicates that the PDCI core is electronically separated from other molecules. Therefore, PDCI is not expected to exist in strongly associated complexes with other PDCI molecules (such as H or J aggregates). More likely, the PDCI may be forming 1D structures due to the living character of KCTP reaction and the 2D symmetry of polythiophene self-assembled structures. As so, PDCI is expected to be randomly distributed in the PDCI-PTh nanoparticles except being forced into 1D structures by the supramolecular assembly of polythiophene 2D structures.

3.3 Conclusion

In conclusion, we described the first example of preparing donor-acceptor conjugated polymer nanoparticles by externally initiated Kumada Catalyst-Transfer dispersion polymerization. The approach allows for using reaction temperature to fine-tune the photophysical properties of conjugated polymer nanoparticles, which affects the conformations of polythiophene and their emission wavelength; also altering their ability to transfer energy efficiently to PDCI. Changing the reaction temperature allowed for tuning emission wavelength of PDCI-PTh nanoparticles between 400-600 nm, and also allows for adjusting NIR emission intensity bands at 775 nm. The obtained particles were dispersible in H_2O and a variety of organic solvents without dissolving. Extensive structural characterization studies revealed polythiophene sheet-like nanostructures, which can drive the hierarchical self-assembly at larger length scales, whereas PDCI chromophore formed loosely correlated 1D structures. This method represents a novel fundamental approach for

tuning the properties of donor-acceptor conjugated polymer nanoscale systems and affords a new surfactant- and sonication-free way to engineering materials for organic electronic devices.

3.4 References

(1) Marks, M.; Holmes, N. P.; Sharma, A.; Pan, X.; Chowdhury, R.; Barr, M. G.; Fenn, C.; Griffith, M. J.; Feron, K.; Kilcoyne, A. L. D.; Lewis, D. A.; Andersson, M. R.; Belcher, W. J.; Dastoor, P. C. Building Intermixed Donor-Acceptor Architectures for Water-Processable Organic Photovoltaics. *Phys. Chem. Chem. Phys.* **2019**, 21, 5705-5715.

(2) Xie, C.; Heumüller, T.; Gruber, W.; Tang, X.; Classen, A.; Schuldes, I.; Bidwell, M.; Späth, A.; Fink, R.; Unruh, T.; McCulloch, I.; Li, N.; Brabec, C. J. Overcoming Efficiency and Stability Limits in Water-Processing Nanoparticular Organic Photovoltaics by Minimizing Microstructure Defects. *Nat. Commun.* **2018**, 5335.

(3) Park, E.-J.; Erdem, T.; Ibrahimova, V.; Nizamoglu, S.; Demir, H. V.; Tuncel, D. White-Emitting Conjugated Polymer Nanoparticles With Cross-Linked Shell for Mechanical Stability and Controllable Photomertric Properties in Color-Conversion LED Applications. *ACS Nano* **2011**, 4, 2483-2492.

(4) Herrera, M.; Abdul-Moqueet, M.; Mahmoud, M. A. Conjugated Polymer Nanoparticles Having Modified Band Gaps Assembled into Nano- and Micropatterned Organic Light-Emitting Diodes. *ACS Appl. Nano Mater.* **2019**, 2, 577-585.

(5) Vohra, V. Can Polymer Solar Cells Open the Path to Sustainable and Efficient Photovoltaic Windows Fabrication? *Chem. Rec.* **2019**, 19, 1166-1178.

(6) Almyahi, F.; Andersen, T. R.; Cooling, N.; Holmes, N. P.; Fahy, A.; Barr, M. G.; Kilcoyne, D.; Belcher, W.; Dastoor, P. C. Optimization, Characterization and Upscaling of Aqueous Solar Nanoparticle Inks for Organic Photovoltaics Using Low-Cost Donor:Acceptor Blend. *Org. Electron.* **2018**, 52, 71-78.

(7) Jana. B.; Ghosh, A.; Patra, A. Photon Harvesting in Conjugated Polymer-Based Functional Nanoparticles. *J. Phys. Chem. Lett.* **2017**, 8, 4608-4620.

(8) Colberts, F. J. M.; Wienk, M. M.; Janssen,m R. A. J. Aqueous Nanoparticle Polymer Solar Cells: Effects of Surfactant Concentration and Processing on Device Performance. *ACS Appl. Mater. Interfaces* **2017**, 9, 13380-13389.

(9) Cho, J.; Yu, S. H.; Chung, D. S. Environmentally Benign Fabrication Processes for High-Performance Polymeric Semiconductors. *J. Mater. Chem. C.* **2017**, 5, 2745-2757.

(10) Zhou, X.; Belcher, W.; Dastoor, P. Solar Paint: From Synthesis to Printing. *Polymers* **2014**, 6, 2832-2844.

(11) Pecher, J.; Mecking, S. Nanoparticles of Conjugated Polymers. *Chem. Rev.* **2010**, 110, 6260-6279.

(12) Landfester, K. Miniemulsion Polymerization and the Structure of Polymer and Hybrid Nanoparticles. *Angew. Chem. Int. Ed.* **2009**, 48, 4488-4507.

(13) Arias, A. C.; MacKenzie, J. D.; Stevenson, R.; Halls, J. J. M.; Inbasekaran, M.; Woo, E. P.; Richards, D.; Friend, R. H. Photovoltaic Performance and Morphology of Polyfluorene Blends: A Combined Microscopic and Photovoltaic Investigation. *Macromolecules* **2001**, 34, 6005-6013.

(14) Ferron, T.; Waldrip, M.; Pope, M.; Collins, B. A. Increased Charge Transfer State Separation via Reduced Mixed Phase Interface In Polymer Solar Cells. *J. Mater. Chem. A.* **2019**, 7, 4536-4545.

(15) Ozel, I. O.; Ozel, T.; Demir, H. V.; Tuncel, D. Non-Radiative Resonance Energy Transfer in Bi-Polymer Nanoparticles of Fluorescent Conjugated Polymers. *Opt. Express* **2010**, 670-672.

(16) Al-Mudhaffer, M. F.; Griggith, M. J.; Feron, K.; Nicolaidis, N. C.; Cooling, N. A.; Zhou, X.; Holdsworth, J.; Belcher, W. J.; Dastoor, P. C. The Origin of Performance Limitations in Miniemulsion Nanoparticulate Organic Photovoltaic Devices. *Sol. Energy Mater. Sol. Cells* **2018**, 175, 77-88.

(17) Jindal, A; Kotani, H.; Kushida, S.; Saeki, A.; Kojima, T.; Yamamoto, Y. Significant Enhancement of Hole Transport Ability in Conjugated Polymer/Fullerene Bulk Heterojunction Microspheres. *ACS Appl. Polym. Mater.* **2019**, 1, 118-123.

(18) Gärtner, S.; Christmann, M.; Sankaran, S.; Röhm, H.; Prinz, E.-M.; Penth, F.; Pütz, A.; Türeli, A. E.; Penth, B.; Baumstümmler, B.; Colsmann, A. Eco-Friendly Fabrication of 4% Efficient Organic Solar Cells from Surfactant-Free P3HT:ICBA Nanoparticle Dispersions. *Adv. Mater.* **2014**, 26, 6653-6657.

(19) Parrenin, L.; Laurans, G.; Pavlopoulou, E.; Fleury, G.; Pecastaings, G.; Brochon, C.; Vignau, L.; Hadziioannou, G.; Cloutet, E. Photoactive Donor-Acceptor Composite Nanoparticles Dispersed in Water. *Langmuir* **2017**, 33, 1507-1515.

(20) Wu, C.; Zheng, Y.; Szymanski, C.; McNeill, J. Energy Transfer in a Nanoscale Multichromophoric System: Fluorescent Dye-Doped Conjugated Polymer Nanoparticles. *J. Phys. Chem. C* **2008**, 112, 1772-1781.

(21) Tuncel, D.; Demir, H. V. Conjugated Polymer Nanoparticles. *Nanoscale* **2010**, 2, 484-494.

(22) Henson, Z. B.; Müllen, K.; Bazan, G. C. Design Strategies for Organic Semiconductors Beyond the Molecular Formula. *Nat. Chem.* **2012**, 699-704.

(23) Suslick, K. S. Sonochemistry. *Science* **1990**, 247, 1439-1445.

(24) Li-Destri, G.; Tuccitto, N.; Livio, P. A.; Messina, G. M. L.; Pithan, L.; Marletta, G. Energy-Sustained Reversible Nanoscale Order and Conductivity Increase in Polymer Thin Films. *Polymer* **2018**, 153, 344-353.

(25) Xu, H.; Zeiger, B. W.; Suslick, K. S. Sonochemical Synthesis of Nanomaterials. *Chem. Soc. Rev.* **2013**, 42, 2555.

(26) Bang, J. H.; Suslick, K. S. Applications of Ultrasound to the Synthesis of Nanostructure Materials. *Adv. Mater.* **2010**, 22, 1039-1059.

(27) Suslick, K. S.; Hyeon, T.; Fang, M. Nanostructured Materials Generated by High-Intensity Ultrasound: Sonochemical Synthesis and Catalytic Studies. *Chem. Mater.* **1996**, 8, 2172-2179.

(28) Xi, Y.; Li, D. S.; Newbloom, G. M.; Tatum, W. K.; O'Donnell, M.; Luscombe, C. K.; Pozzo, L. D. Sonocrystallization of Conjugated Polymers with Ultrasound Fields. *Soft Matter* **2018**, 4, 4963-4976.

(29) Yokozawa, T.; Ohta, Y. Transformation of Step-Growth Polymerization into Living Chain-Growth Polymerization. *Chem. Rev.* **2016**, 116, 1950-1968.

(30) Bryan, Z. J.; Mcneil, A. J. Controlled Synthesis of Fully π-Conjugated Donor–Acceptor Block Copolymers Using a Ni(II) Diimine Catalyst. *Macromolecules* **2015**, 48, 7385-7395.

(31) Kiriy, A.; Senkovskyy, V.; Sommer, M. Kumada Catalyst-Transfer Polycondensation: Mechanism, Opportunities, and Challenges. *Macromol. Rapid Commun.* **2011**, 32, 1503, 1517.

(32) Yokozawa, Y.; Yokoyama, A. Chain-Growth Condensation Polymerization for the Synthesis of Well-Defined Condensation Polymers and π-Conjugated Polymers. *Chem. Rev.* **2009**, 109, 5595-5619.

(33) Sheina, E. E.; Liu, J. S.; Iovu, M. C.; Laird, D. W.; McCullough, R. D. Chain Growth Mechanism for Regioregular Nickel-Initiated Cross-Coupling Polymerizations. *Macromolecules* **2004**, 37, 3526-3528.

(34) Yokoyama, A.; Miyakoshi, R.; Yokozawa, T. Chain-Growth Polymerization for Poly(3-hexylthiophene) with a Defined Molecular Weight and a Low Polydispersity. *Macromolecules* **2004**, 37, 1169-1171.

(35) Chavez, C. A.; Choi, J.; Nesterov, E. E. One-Step Simple Preparation of Catalytic Initiators for Catalyst-Transfer Kumada Polymerization: Synthesis of Defect-Free Polythiophenes. *Macromolecules* **2014**, 47, 506-516.

(36) Guo, Z.; Zhang, X.; Wang, Y.; Li, Z. Supramolecular Self-Assembly of Perylene Bisimide Derivatives Assisted by Various Groups. *Langmuir* **2019**, 35, 342-358.

(37) Sahoo, D et al. Hierarchical Self-Organization of Perylene Bisimides into Supramolecular Spheres and Periodic Arrays Thereof. *J. Am. Chem. Soc.* **2016**, 138, 14798-14807.

(38) Chen, S.; Slattum, P.; Wang, C.; Zang, L. Self-Assembly of Perylene Imide Molecules into 1D Nanostructure: Methods, Morphologies, and Applications. *Chem. Rev.* **2015**, 11967-11998.

(39) Marty, R. et al. Hierarchically Structured Microfibers of "Single Stack" Perylene Bisimide and Quaterthiophene Nanowires. *ACS Nano* **2013**, 7, 8498-8508.

(40) Würthner, F.; Stepanenko, V.; Chen, Z.; Saha-Moller, C. R.; Kochner, N.; Stalke, D. Preparation and characterization of regioisomerically pure 1,7-disubstituted perylene bisimide dyes. *J. Org. Chem.* **2004**, 69, 7933-7939.

(41) Handa, N. V.; Mendoza, K. D.; Shirtcliff, L. D. Syntheses and Properties of 1,6 and 1,7 Perylene Diimides and Tetracarboxylic Dianhydrides. *Org. Lett.* **2011**, 17, 4724-4727.

(42) Sengupta, S.; Dubey, R. K.; Hoek, R.-W. M.; van Eeden, S.-P. P.; Gunbas, D. D.; Grozema, F. C.; Sudholter, E.-J. R.; Jager, W. F. Synthesis of Regioisomerically Pure 1,7-Dibromoperylene-3,4,9,10-tetracarboxylic Acid Derivatives. *J. Org. Chem.* **2014**, 79, 6655-6662.

(43) Bryan, Z. J.; McNeil, A. J. Conjugated Polymer Synthesis via Catalyst-Transfer Polycondensation (CTP): Mechanism, Scope, and Applications. *Macromolecules* **2013**, 46, 8395-8405.

(44) Lee, S. J.; Lee, J. M.; Cheong, I. W.; Lee, H.; Kim, J. H. A Facile Route of Polythiophene Nanoparticles via Fe^{3+}-Catalyzed Oxidative Polymerization in Aqueous Medium. *J. Polym. Sci. Part A: Polym. Chem.* **2008**, 46, 2097-2108.

(45) Bässler, H. Charge Transport in Disordered Organic Photoconductors. *Phys. Stat. Sol.* **1993**, 175, 15.

(46) Fichou, D. Structural Order in Conjugated Oligothiophenes and Its Implications on Opto-Electronic Devices. *J. Mater. Chem.* **2000**, 10, 571-588.

(47) Wasserberg, D.; Marsal, P.; Meskers, S. C. J.; Janssen, R. A. J.; Beljonne, D. Phosphorescence and Triplet State Energy of Oligothiophenes. *J. Phys. Chem. B* **2005**, 109, 4410-4415.

(48) Rentsch, S.; Yang, J. P., Paa, W.; Birckner, E.; Schiedt, J.; Weinkauf, R. Size Dependence of Triplet and Singlet States of α-Oligothiophenes. *Phys. Chem. Chem. Phys.* **1999**, 1, 1707-1714.

(49) Mo, Z.; Lee, K. B.; Kobayashi, M.; Heeger, A. J.; Wudl, F. X-ray Scattering from Poly(thiophene): Crystallinity and Crystallographic Structure. *Macromolecules* **1985**, 18, 1972-1977.

(50) Isz, S.; Weissbuch, I.; Kjaer, K.; Bouwman, W. G.; Als-Nielsen, J.; Palacin, S.; Ruaudel-Teixier, A.; Leiserowitz, L.; Lahav, M. Crystalline Mono- and Multilayer Self-Assemblies of Oligothiophene at the Air-Water Interface. *Chem. Eur. J.* **1997**, 3, 6.

CHAPTER 4. EXPERIMENTAL SECTION

4.1. General Considerations

All reactions were performed under an atmosphere of dry nitrogen (unless mentioned otherwise). Column chromatography was performed on silica gel (Sorbent Technologies, 60 Å, 40-63 μm) slurry packed into glass columns. Tetrahydrofuran (THF) and *N*,*N*-dimethylformamide (DMF) were dried by passing through activated alumina and molecular sieves, respectively, using a PS-400 Solvent Purification System from Innovative Technology, Inc. The water content of the solvents was periodically controlled by Karl Fischer titration (using a DL32 coulometric titrator from Mettler Toledo). Isopropylmagnesium chloride (2.0 M solution in THF) was purchased from Acros Organics, all other reagents and solvents were obtained from Sigma-Aldrich and Alfa Aesar and used without further purification. Organometallic reagents were titrated with salicylaldehyde phenylhydrazone prior to use.[1] UV-Visible absorption spectra were recorded on Agilent Cary 5000 and Varian Cary 50 spectrophotometers. Fluorescence studies were carried out using a PTI QuantaMaster4/2006SE spectrofluorimeter. ^{1}H NMR spectra were recorded at 400 MHz and are reported in ppm downfield from tetramethylsilane; ^{31}P NMR spectra were obtained at 162 MHz and are reported in ppm relative to 80% aqueous H_3PO_4 as external standard. Ultrasonication was carried out using a Branson Sonifier 450 (400 W nominal power) operating at 70% power. GPC analysis of polymers was performed with Agilent 1100 chromatograph equipped with two PLgel 5 μm MIXED-C and one PLgel 5 μm 1000 Å columns connected in series, using THF as a mobile phase, and calibrated against polystyrene standards. SEM Images were obtained on a Quanta 3D DualBeam FEG-FIB-SEM instrument. (accelerating voltage of 20 kV). SEM samples were dropcasted from $CHCl_3$ suspensions onto copper substrates. Samples for Total Ion Count Mass Spectrometry were analyzed on a Shimadzu LCMS-8045 system. The column used was a

Shimadzu C18 1.8 μm particle size of dimensions 50 x 4.6 mm. Mobil phases A and B were water and acetonitrile, respectively, each containing 0.1% formic acid. The analytical conditions consisted of: gradient, 95% B (20 min); flow rate, 0.20 mL/min; column temperature, 40°C; detection, APCI(+) and APCI(-); nebulizing gas, N2 at 2 L/min; drying gas, N2 at 10 L/min; heating gas, air at 10 L/min; probe voltage, 4.5 kV (+) and -3.5 kV (-); interface temperature, 220°C; DL temperature, 250°C; heating block temperature, 400°C.

4.2. Synthetic Details

Perylene-3,4,9,10-tetracarboxylic tetrabutylester (**3-2**). 71.19mL BuOH and 1,8-diazabicyclo[5.4.0]undec-7-ene (23.69g, 155.6 mmol) was added to a suspension of commercially available perylene-3,4,9,10-tetracarboxylic dianhydride (15.26g, 38.9 mmol) in 500 mL acetonitrile. The reaction mixture was allowed to stir at 60°C for 1 hour before 71.0 mL of 1-bromobutane was added and brought up to reflux conditions to stir for 24 hours. After cooling to room temperature, the suspension was poured into 1 L ice cold deionized H_2O. The precipitate was filtered and dried overnight at 60°C in vacuo to yield 23.07g (91%) orange solid. ^{1}H NMR ($CDCl_3$, 400MHz) δ8.31 (d, 4H), 8.05 (d, 4H), 4.33 (t, 8H), 1.81-1.74 (m, 8H), 1.55-1.43 (m, 8H), 0.99 ppm (t, J = 7.4 Hz, 12H)

1,7-dibromo-Perylene-3,4,9,10-tetracarboxylic tetrabutylester (**3-3a**). To a 1L round bottom flask was added **3-2** (23.07g, 35.34 mmol), K_2CO_3 (11.47g, 83.04 mmol) and 285 mL DCM. Br_2 (23.04mL, 447.4 mmol) was added dropwise via addition funnel. After 22h, the reaction mixture was quenched with sat. 20% (w/v) $Na_2S_2O_3$ pentahydrate in deionized H_2O. The crude mixture was transferred to a separatory funnel, extracted with DCM and washed several times with deionized water. The organic layer was dried over Na_2SO_4 and concentrated to yield 27.45g red

viscous product which was dissolved in a minimal amount of dichloromethane (ca. 38mL) then subsequently 610 mL acetonitrile was slowly added. The solution was allowed to sit for 2-3 days to recrystallize. After 3 days, the crystals were filtered and recrystallized again according to the same procedure. After the 2nd recrystallization, the product was filtered, washed with ice cold acetonitrile then dried *in vacuo* at 60°C to yield 8.23g (28.8%) orange solid. ^{1}H NMR ($CDCl_3$, 400MHz) δ8.95 (d, *J* = 8.0Hz, 2H), 8.29 (s, 2H), 8.10 (d, *J* = 8.0 Hz, 2H), 4.36-4.32 (m, 8H), 1.82-1.74 (m, 8H), 1.54-1.45 (m, 8H), 1.02-0.97 ppm (m, 12H).

1,7-dibromoperylene-3,4,9,10-tetracarboxylate dianhydride (**3-4**). *p*-Toluenesulfonic acid monohydrate (9.10g 47.9mmol) was added to a solution of regioisomerically pure **3a** (7.76g, 9.57mmol) in 250 mL toluene. The reaction mixture was brought up to 100°C. After 48h, the reaction was allowed to cool to room temperature before it was filtered and dried overnight at 60°C in vacuo. The crude solid was then refluxed in $CHCl_3$ for 8 hours, filtered and washed with $CHCl_3$ to obtain the final product 4.93g (94%) red solid. ^{1}H NMR (D_2SO_4, 400MHz) δ9.70 (d, *J* = 8.32 Hz, 2H), 9.03 (s, 2H), 8.81 (d, *J* = 8.36 Hz).

***N*,*N*'-Di(2,6-diisopropylphenyl)-1,7-dibromoperylene-3,4,9,10-tetracarboxylic bisimide** (**3-5**). 2,6-diisopropylaniline (3.55g, 20.02 mmol) was added to a suspension of compound **3-4** (1.0g 1.82mmol) in 25mL of propionic acid and brought to reflux. Let stir 3 days. The reaction was cooled slightly and filtered hot into a 2L filter flask containing 500 mL ice cold deionized H_2O. Saturated $NaHCO_3$ was added until the acid is neutralized. Then the product was extracted with EtOAc, washed several times with sat. $NaHCO_3$ and deionized water, then dried over Na_2SO_4 and concentrated in vacuo. The crude product was purified by column

chromatography on silica gel (eluent: CH_2Cl_2 to hexanes (5:1)) to afford 723mg (46%) of red powder. ^{1}H NMR ($CDCl_3$, 400MHz) δ9.56 (d, J = 8.12 Hz, 2H), 9.02 (s, 2H), 8.80 (d, J = 8.12 Hz, 2H), 7.52 (t, J = 7.8 Hz, 2H), 7.36 (d, J=7.8 Hz, 4H), 2.77-2.70 (m, 4H), 1.19-1.18 (m, 24H). R_f = 0.32.

2-(2'-thienyl)-5-(trimethylstannyl)thiophene. Bithiophene (3.33, 20.02 mmol) was dissolved in 35mL dry THF under an inert atmosphere and cooled to -78°C. Subsequently, 13.55 mL of 1.6M *n*-BuLi in hexanes (21.67 mmol) was added dropwise. The solidified reaction mixture was warmed to room temperature slowly over 30 minutes, and then cooled again to -78°C. Afterwards, trimethyltinchloride (4.38g, 22.02 mmol) was added and the reaction mixture was allowed to stir overnight warming up to room temperature. The reaction was quenched with deionized H_2O, then THF was removed in vacuo. The crude product was extracted using DCM and washed several times with deionized H_2O and brine. The organic layer was dried over Na_2SO_4 and concentrated in vacuo to yield 5.55 g (84%) of a green oil and used without further purification. ^{1}H NMR ($CDCl_3$, 400MHz) δ7.29-7.27 (m, 1H), 7.22-7.20 (m, 1H), 7.19-7.16 (m, 1H), 7.10-7.08 (m, 1H), 7.03-7.00 (m, 1H), 0.45-0.35 (m, 9H).

***N,N'*-Di(2,6-diisopropylphenyl)-1,7-di(2,2'bithien-5-yl)perylene-3,4,9,10-tetracarboxylate bisimide** (**3-6**). Compound **3-5** (670mg, 0.77 mmol), 2-(2'-thienyl)-5-(trimethylstannyl)thiophene (955mg, 2.90 mmol), $Pd(PPh_3)_4$ (15mg, 0.013 mmol), and 90 mL of dry toluene was added to a dry Shlenk flask in air-free conditions and heated to 100°C. Stir overnight. Subsequently, the solvent was removed in vacuo and the crude product was separated by column chromatography using a short plug of silica gel (eluent: CH_2Cl_2 – hexanes (3:2)) to

yield 554mg (65%) of a black solid. ^{1}H NMR ($CDCl_3$, 400MHz) δ8.76 (d, *J* = 8.0 Hz, 2H), 8.48 (t, *J* = 9.7 Hz, 2H), 8.36 (d, *J* = 8.0 Hz, 2H), 7.65 – 6.94 (m, 16H), 2.88 – 2.64 (m, 4H), 1.40 – 0.96 ppm (m, 24H). R_f = 0.29.

***N,N*'-Di(2,6-diisopropylphenyl)-1,7-di(5'-bromo-2,2'-bithien-5-yl)perylene-3,4,9,10-tetracarboxylate bisimide** (**3-7**)**.** To a solution of **3-6** (550mg, 0.53 mmol) in 50mL of anhydrous DMF was added *N*-bromosuccinimide (188mg, 1.06mmol). The reaction was allowed to stir for 6 hours. Subsequently, the reaction mixture was transferred to a separatory funnel and the product was extracted with ethyl acetate. The organic layer was washed several times with deionized H_2O, brine, dried over Na_2SO_4 and concentrated in vacuo. The crude product was purified by recrystallization in boiling heptane (ca. 20mL) until dissolved and cooling to room temperature. The product was isolated by filtration to yield 386mg black solid. (61%) ^{1}H NMR ($CDCl_3$, 400MHz) δ8.77 (s, 2H), 8.43 (d, *J* = 8.12Hz, 2H), 8.38 (d, *J* = 8.12 Hz, 2H), 7.50 (t, *J* = 7.88 Hz, 2H), 7.34 (d, *J* = 7.8 Hz, 4H), 7.31 (d, *J* = 3.72 Hz, 2H), 7.19 (d, *J* = 3.72, 2H), 7.01 (d, *J* = 3.84 Hz, 2H), 6.98 (d, *J* = 3.84 Hz, 2H), 2.78-2.71 (m, 4H), 1.19-1.16 (m, 24H).

Catalytic Initiator (**3-8**). Compound **3-7** (50mg, 0.04 mmol) and $Ni(dppp)_2$ (110 mg, 0.12 mmol) was dissolved in dry THF (10 mL) and stirred in glovebox for 3 hours. The 4.18mM solution was used as is.

PDCI-PTh nanoparticles. Isopropylmagnesium chloride (0.21 mL of 1.62M solution in THF) was added dropwise to a solution of 2,5-dibromothiophene (100 mg, 0.41 mmol) in 8 mL dry THF at 0°C and in air-free conditions to generate the Grignard monomer solution. After 90

minutes, 1 mL of 4.18mM catalytic initiator solution is injected promptly under ultrasonication and allowed to sheer for 10 minutes. Subsequently the reaction mixture was quenched in 24mL of 0.1M solution of HCl in MeOH. The solid suspension was isolated by centrifugation at 3500 RPM for 15 minutes. The resulting particles were washed repeatedly by re-suspending in 25%(v/v) $CHCl_3$ in MeOH and centrifugation until the supernatant is clear. The resulting solids were dried *in vacuo* to yield 22.38 mg (58%) maroon powder.

2,6-diisopropylaniline-d_{19}. To a high pressure Parr reactor was added 56 g 2,6-diisopropylaniline, 5.6g 10% wt. palladium on carbon, 5.6g 10% wt. platinum on carbon, and 650mL of D_2O. The Parr reactor was flushed with hydrogen gas for 15 minutes before it was sealed and heated to 150°C, reaching 180 PSI and allowing to stir for 72 hours. After cooling to room temperature, the crude slurry was filtered and the product was extracted from the filtrate using dichloromethane. The organic layer was dried over $MgSO_4$ and concentrated *in vacuo* to yield 29g (46%) of a light brown oil.

***N*,*N*'-Di(2,6-diisopropylphenyl-d_{17})-1,7-dibromoperylene-3,4,9,10-tetracarboxylic bisimide.** 2,6-diisopropylaniline-d_{19} (7.76g, 39.52 mmol) was added to a suspension of regioisomerically pure **3-4** (4.35g, 7.9 mmol) in propionic acid (150 ml) and brought to reflux to stir for 3 days. After cooling to room temperature, the reaction was poured into 1L of ice cold deionized H_2O and neutralized with sat. $NaHCO_3$. Then, the product was extracted using EtOAc, dried over $MgSO_4$, and the solvent was removed *in vacuo* to yield a crude solid which was purified by column chromatography (eluent: Hx – DCM (3:4)) to yield 1.57g red solid. The

percent deuteration of alkyl protons in 2,6-diisopropylaniline 92%, 50% in the *meta*- position and 10% in the *para*- position due to hydrodebromination. R_f=0.15

***N,N'*-Di(2,6-diisopropylphenyl-d_{17})-1,7-di(2,2'bithien-5-yl)perylene-3,4,9,10-tetracarboxylate bisimide**. In a dry Schlenk flask, *N*,*N*'-Di(2,6-diisopropylphenyl-d_{17})-1,7-dibromoperylene-3,4,9,10-tetracarboxylic bisimide (1.57g, 1.74 mmol), 2-(2'-thienyl)-5-(trimethylstannyl)thiophene (1.70g, 5.16 mmol) and $Pd(PPh_3)_2Cl_2$ (80mg, 0.11 mmol) were dissolved in anhydrous toluene (175 mL) under air-free conditions, sealed, heated to 100°C, and allowed to stir 18h. Subsequently, the solvent was removed *in vacuo* and the product was purified by column chromatography on silica gel (eluent DCM – Hx (3:2)) to afford 733 mg (39.3%) black solid. R_f=0.3

***N,N'*-Di(2,6-diisopropylphenyl-d_{17})-1,7-di(5'-bromo-2,2'-bithien-5-yl)perylene-3,4,9,10-tetracarboxylate bisimide**. *N*-bromosuccinimide (243mg, 1.366 mmol) was added stepwise over 10 minutes to a solution of *N,N'*-Di(2,6-diisopropylphenyl-d_{17})-1,7-di(2,2'bithien-5-yl)perylene-3,4,9,10-tetracarboxylate bisimide (733 mg, 0.68 mmol) in DMF. After 3 hours, the reaction mixture was transferred to a separatory funnel and extracted using EtOAc. The organic layer was washed several times with deionized H_2O, brine, and dried over $MgSO_4$ before the solvent was removed *in vacuo*. The crude solid was recrystallized by boiling in heptane until dissolved and slowly cooling back to room temperature. The suspension was filtered and dried *in vacuo* to yield 310 mg (36%) black powder.

(*d*)PDCI catalytic initiator. *N,N*'-Di(2,6-diisopropylphenyl-d_{17})-1,7-di(5'-bromo-2,2'-bithien-5-yl)perylene-3,4,9,10-tetracarboxylate bisimide (130 mg, 0.11 mmol), $Ni(dppp)_2$ (286 mg, 0.32 mmol) and 26 mL of dry THF was mixed together and allowed to stir 3 hours. The 4.18 mM solution was used as prepared.

(*d*)PDCI-(*h*)PTh_{100} nanoparticles. 0.69 mL of 1.62M Isopropylmagnesium chloride (1.12 mmol) was added dropwise to a solution of 2,5-dibromothiophene (300 mg, 1.24 mmol) in 24 mL dry THF at 0°. After 90 minutes, 3 mL of the 4.18 mM (*d*)PDCI dinickel catalytic initiator was injected promptly at the decided reaction temperature. Subsequently, the reaction was quenched in 1 mL of 6.0M HCl solution in MeOH and concentrated by centrifugation at 5000 RPM for 15 minutes. The supernatant was removed and the resulting pellet was washed repeatedly by re-suspending the particles in 25%(v/v)$CHCl_3$ solution in MeOH and concentrating by centrifugation to yield 28 mg (24%) maroon powder.

(*d*)PDCI-(*d*)PTh_{100} nanoparticles. (*d*)PDCI-(*d*)PTh_{100} particles were prepared in the same way as (*d*)PDCI-(*h*)PTh_{100} except using 300 mg (1.23 mmol) of 2,5-dibromothiophene-d_2 yielding 25 mg (22%) maroon powder.

PDCI(PdRuPhosI)$_2$ External Initiator (2-1). RuPhos (244mg, 0.624 mmol, 3 eq), RuPhos Pd G3 95% (307.9mg, 0.367mmol, 2.10 eq), K_3PO_4 (380mg, 1.83 mmol), **3-7** (225.8mg, 0.175mmol, 1 eq) was added to a 20 mL scintillation vial with 0.8 mL H_2O and 8 mL dry THF. The reaction was heated to 50°C, for 1.5h. After, the reaction was allowed to cool to room temperature, and the organic layer was precipitated into 5:1 hexanes:THF. The solids were

collected by centrifugation in inert atmosphere. The crude powder was dissolved in dry THF and reprecipitated again in 5:1 hexanes:THF to result in a brown powder.

General procedure for preparing conjugated polymers using 2-1 as the external initiator. To a 20 mL scintillation vial was added **2-1** (9.64mg, 0.0039mmol), K_3PO_4 (320mg, 1.5mmol), silver sulfate (78mg, 0.25 mmol), 14mL THF and 0.5 mL H_2O. Mix until K_3PO_4 dissolves. After, add the monomer as a solution in 2 mL THF). Stir for 96 hr at room temperature.

PDCI-PPP. Following the general procedure, 55mg of 4-bromo-2,5-dihexylphenylboronic acid MIDA ester (0.114 mmol, 29 eq) was added to the solution of external initiator. After 96h, the reaction was quenched with 3 mL 6N HCl and extracted using $CHCl_3$. The organic layer was washed with brine and deionized H_2O repeatedly. The organic layer was dried over sodium sulfate and concentrated in vacuo. The crude polymer was dissolved in minimal amount of $CHCl_3$ and reprecipitated in acetone. The precipitates were collected by centrifugation and washed repeatedly with acetone and MeOH to yield a green solid (27.8mg, 86% yield).

PDCI-PF. Following the general procedure, 32.2 mg of 7-bromo-9,9-dioctylfluorene-2-lboronic acid MIDA ester (0.0515 mmol, 13.2 eq) was added to the solution of external initiator. After 96h, the reaction was quenched with 3 mL 6N HCl and extracted using $CHCl_3$. The organic layer was washed with brine and deionized H_2O repeatedly. The organic layer was dried over sodium sulfate and concentrated in vacuo. The crude polymer was dissolved in minimal amount of $CHCl_3$ and reprecipitated in acetone. The precipitates were collected by centrifugation and washed repeatedly with acetone and MeOH to yield a green solid (11.2mg, 46.4% yield).

PDCI-PT. Silver sulfate was not used for preparing PDCI-PT. Otherwise, following the general procedure, 50 mg of 2-bromo-3-hexylthiophene-5-boronic acid MIDA ester (0.124 mmol, 31.4 eq) was added to the solution of external initiator. After 96h, the reaction was quenched with 3 mL 6N HCl and extracted using $CHCl_3$. The organic layer was washed with brine and deionized H_2O repeatedly. The organic layer was dried over sodium sulfate and concentrated in vacuo. The crude polymer was dissolved in minimal amount of $CHCl_3$ and reprecipitated in acetone. The precipitates were collected by centrifugation and washed repeatedly with acetone and MeOH to yield a green solid (21.4mg, 86.5% yield).

4.3. References

(1) Love, B. E.; Jones, E. G. The Use of Salicylaldehyde Phenylhydrazone as an Indicator for Titration of Organometallic Reagents. *J. Org. Chem.* **1999**, 64, 3755-3756.

APPENDIX A: PERMISSIONS

Title: Advances in Living Anionic Polymerization: From Functional Monomers, Polymerization Systems, to Macromolecular Architectures

Author: Akira Hirao, Raita Goseki, Takashi Ishizone

Publication: Macromolecules

Publisher: American Chemical Society

Date: Mar 1, 2014

LOGIN

If you're a copyright.com user, you can login to RightsLink using your copyright.com credentials.

Already **a RightsLink user** or want to learn more?

PERMISSION/LICENSE IS GRANTED FOR YOUR ORDER AT NO CHARGE

This type of permission/license, instead of the standard Terms & Conditions, is sent to you because no fee is being charged for your order. Please note the following:

- Permission is granted for your request in both print and electronic formats, and translations.
- If figures and/or tables were requested, they may be adapted or used in part.
- Please print this page for your records and send a copy of it to your publisher/graduate school.
- Appropriate credit for the requested material should be given as follows: "Reprinted (adapted) with permission from (COMPLETE REFERENCE CITATION). Copyright (YEAR) American Chemical Society." Insert appropriate information in place of the capitalized words.
- One-time permission is granted only for the use specified in your request. No additional uses are granted (such as derivative works or other editions). For any other uses, please submit a new request.

If credit is given to another source for the material you requested, permission must be obtained from that source.

BACK CLOSE WINDOW

Title: Identifying the missing link in catalyst transfer polymerization
Author: Weiying He et al
Publication: Nature Communications
Publisher: Springer Nature
Date: Sep 24, 2018

Creative Commons

Title: Recent Advances, Design Guidelines, and Prospects of All-Polymer Solar Cells

Author: Changyeon Lee, Seungjin Lee, Geon-U Kim, et al

Publication: Chemical Reviews

Publisher: American Chemical Society

Date: Jul 1, 2019

PERMISSION/LICENSE IS GRANTED FOR YOUR ORDER AT NO CHARGE

This type of permission/license, instead of the standard Terms & Conditions, is sent to you because no fee is being charged for your order. Please note the following:

- Permission is granted for your request in both print and electronic formats, and translations.
- If figures and/or tables were requested, they may be adapted or used in part.
- Please print this page for your records and send a copy of it to your publisher/graduate school.
- Appropriate credit for the requested material should be given as follows: "Reprinted (adapted) with permission from (COMPLETE REFERENCE CITATION). Copyright (YEAR) American Chemical Society." Insert appropriate information in place of the capitalized words.
- One-time permission is granted only for the use specified in your request. No additional uses are granted (such as derivative works or other editions). For any other uses, please submit a new request.

If credit is given to another source for the material you requested, permission must be obtained from that source.

BACK CLOSE WINDOW

Title: Conjugated Polymer Synthesis via Catalyst-Transfer Polycondensation (CTP): Mechanism, Scope, and Applications

Author: Zachary J. Bryan, Anne J. McNeil

Publication: Macromolecules

Publisher: American Chemical Society

Date: Nov 1, 2013

PERMISSION/LICENSE IS GRANTED FOR YOUR ORDER AT NO CHARGE

This type of permission/license, instead of the standard Terms & Conditions, is sent to you because no fee is being charged for your order. Please note the following:

- Permission is granted for your request in both print and electronic formats, and translations.
- If figures and/or tables were requested, they may be adapted or used in part.
- Please print this page for your records and send a copy of it to your publisher/graduate school.
- Appropriate credit for the requested material should be given as follows: "Reprinted (adapted) with permission from (COMPLETE REFERENCE CITATION). Copyright (YEAR) American Chemical Society." Insert appropriate information in place of the capitalized words.
- One-time permission is granted only for the use specified in your request. No additional uses are granted (such as derivative works or other editions). For any other uses, please submit a new request.

If credit is given to another source for the material you requested, permission must be obtained from that source.

BACK CLOSE WINDOW

Title:	Chain-Growth Polymerization for the Synthesis of Polyfluorene via Suzuki–Miyaura Coupling Reaction from an Externally Added Initiator Unit
Author:	Akihiro Yokoyama, Hirofumi Suzuki, Yasuhiro Kubota, et al
Publication:	Journal of the American Chemical Society
Publisher:	American Chemical Society
Date:	Jun 1, 2007

PERMISSION/LICENSE IS GRANTED FOR YOUR ORDER AT NO CHARGE

This type of permission/license, instead of the standard Terms & Conditions, is sent to you because no fee is being charged for your order. Please note the following:

- Permission is granted for your request in both print and electronic formats, and translations.
- If figures and/or tables were requested, they may be adapted or used in part.
- Please print this page for your records and send a copy of it to your publisher/graduate school.
- Appropriate credit for the requested material should be given as follows: "Reprinted (adapted) with permission from (COMPLETE REFERENCE CITATION). Copyright (YEAR) American Chemical Society." Insert appropriate information in place of the capitalized words.
- One-time permission is granted only for the use specified in your request. No additional uses are granted (such as derivative works or other editions). For any other uses, please submit a new request.

If credit is given to another source for the material you requested, permission must be obtained from that source.

BACK CLOSE WINDOW

Title: Catalyst-Transfer Suzuki–Miyaura Coupling Polymerization for Precision Synthesis of Poly(p-phenylene)

Author: Tsutomu Yokozawa, Haruhiko Kohno, Yoshihiro Ohta, et al

Publication: Macromolecules

Publisher: American Chemical Society

Date: Sep 1, 2010

PERMISSION/LICENSE IS GRANTED FOR YOUR ORDER AT NO CHARGE

This type of permission/license, instead of the standard Terms & Conditions, is sent to you because no fee is being charged for your order. Please note the following:

- Permission is granted for your request in both print and electronic formats, and translations.
- If figures and/or tables were requested, they may be adapted or used in part.
- Please print this page for your records and send a copy of it to your publisher/graduate school.
- Appropriate credit for the requested material should be given as follows: "Reprinted (adapted) with permission from (COMPLETE REFERENCE CITATION). Copyright (YEAR) American Chemical Society." Insert appropriate information in place of the capitalized words.
- One-time permission is granted only for the use specified in your request. No additional uses are granted (such as derivative works or other editions). For any other uses, please submit a new request.

If credit is given to another source for the material you requested, permission must be obtained from that source.

BACK CLOSE WINDOW

Copyright Clearance Center

Confirmation Number: 11851604
Order Date: 09/16/2019

Customer Information

Customer: Chunwa Kei
Account Number: 3001518768
Organization: Northern Illinois University
Email: z1860314@students.niu.edu
Phone: +1 (857) 308-8333
Payment Method: Invoice

This is not an invoice

Order Details

Chemical communications

Billing Status: **N/A**

Order detail ID:	72011427
ISSN:	1364-548X
Publication Type:	e-Journal
Volume:	
Issue:	
Start page:	
Publisher:	ROYAL SOCIETY OF CHEMISTRY
Author/Editor:	Royal Society of Chemistry (Great Britain)

Permission Status: **Granted**

Permission type: Republish or display content
Type of use: Thesis/Dissertation
Order License Id: 4671000776923
Order ref number: 1

Requestor type	Academic institution
Format	Print, Electronic
Portion	image/photo
Number of images/photos requested	1
The requesting person/organization	Chunwa Kei
Title or numeric reference of the portion(s)	Fig. 1.
Title of the article or chapter the portion is from	Accessing Conjugated Polymers with Precisely Controlled Heterobisfunctional Chain Ends via Post-Polymerization Modification of the OTf Group and Controlled Pd(0)/t-bu3P-Catalyzed Suzuki- Cross-Coupling Polymerization
Editor of portion(s)	N/A
Author of portion(s)	N/A
Volume of serial or monograph	51
Page range of portion	14869
Publication date of portion	August 2015
Rights for	Main product
Duration of use	Life of current edition

Title: A Rational Design of Highly Controlled Suzuki–Miyaura Catalyst-Transfer Polycondensation for Precision Synthesis of Polythiophenes and Their Block Copolymers: Marriage of Palladacycle Precatalysts with MIDA-Boronates

Author: Kyeong-Bae Seo, In-Hwan Lee, Jaeho Lee, et al

Publication: Journal of the American Chemical Society

Publisher: American Chemical Society

Date: Mar 1, 2018

PERMISSION/LICENSE IS GRANTED FOR YOUR ORDER AT NO CHARGE

This type of permission/license, instead of the standard Terms & Conditions, is sent to you because no fee is being charged for your order. Please note the following:

- Permission is granted for your request in both print and electronic formats, and translations.
- If figures and/or tables were requested, they may be adapted or used in part.
- Please print this page for your records and send a copy of it to your publisher/graduate school.
- Appropriate credit for the requested material should be given as follows: "Reprinted (adapted) with permission from (COMPLETE REFERENCE CITATION). Copyright (YEAR) American Chemical Society." Insert appropriate information in place of the capitalized words.
- One-time permission is granted only for the use specified in your request. No additional uses are granted (such as derivative works or other editions). For any other uses, please submit a new request.

If credit is given to another source for the material you requested, permission must be obtained from that source.

APPENDIX B: Nuclear Magnetic Resonance Spectroscopy

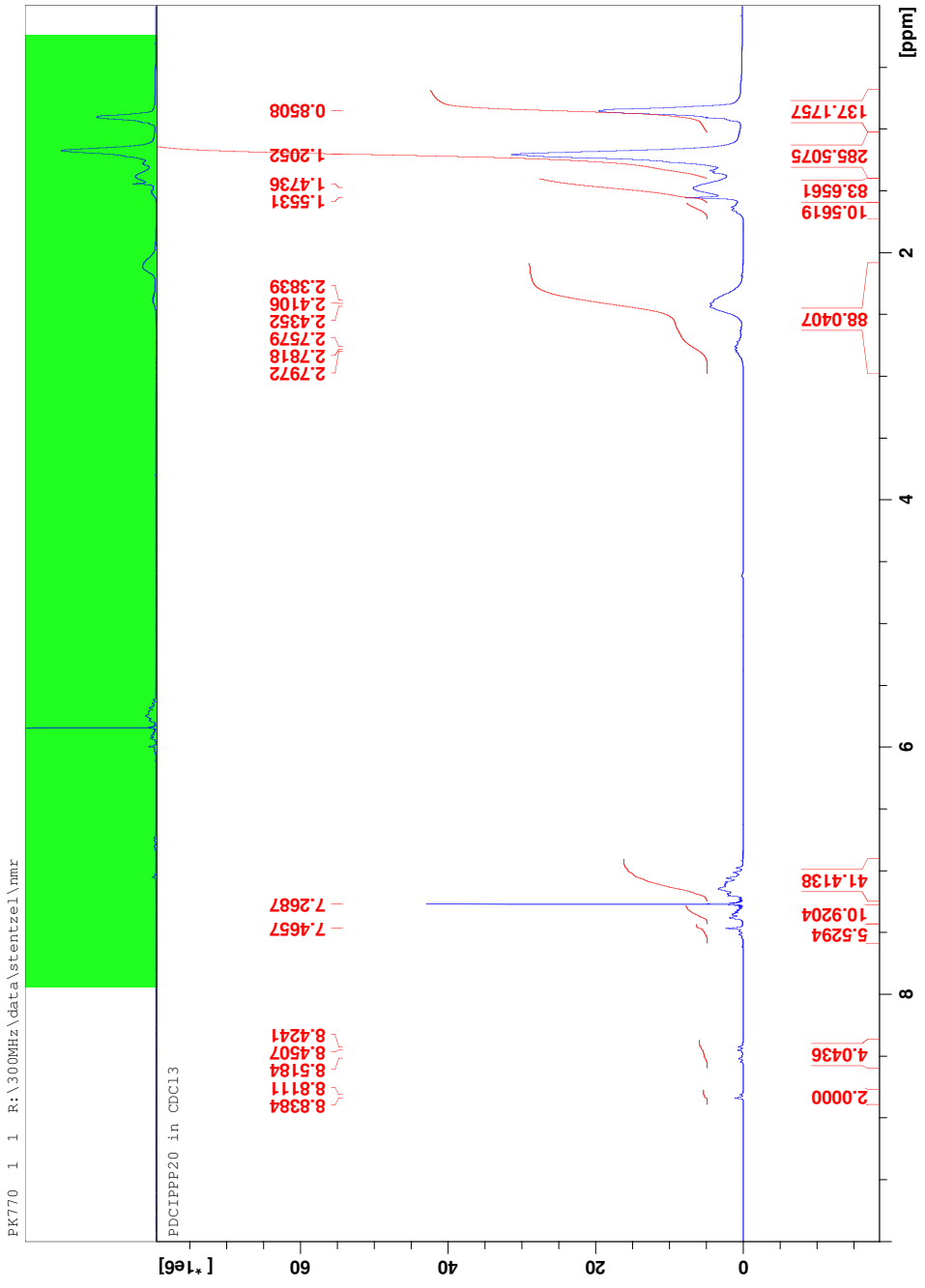

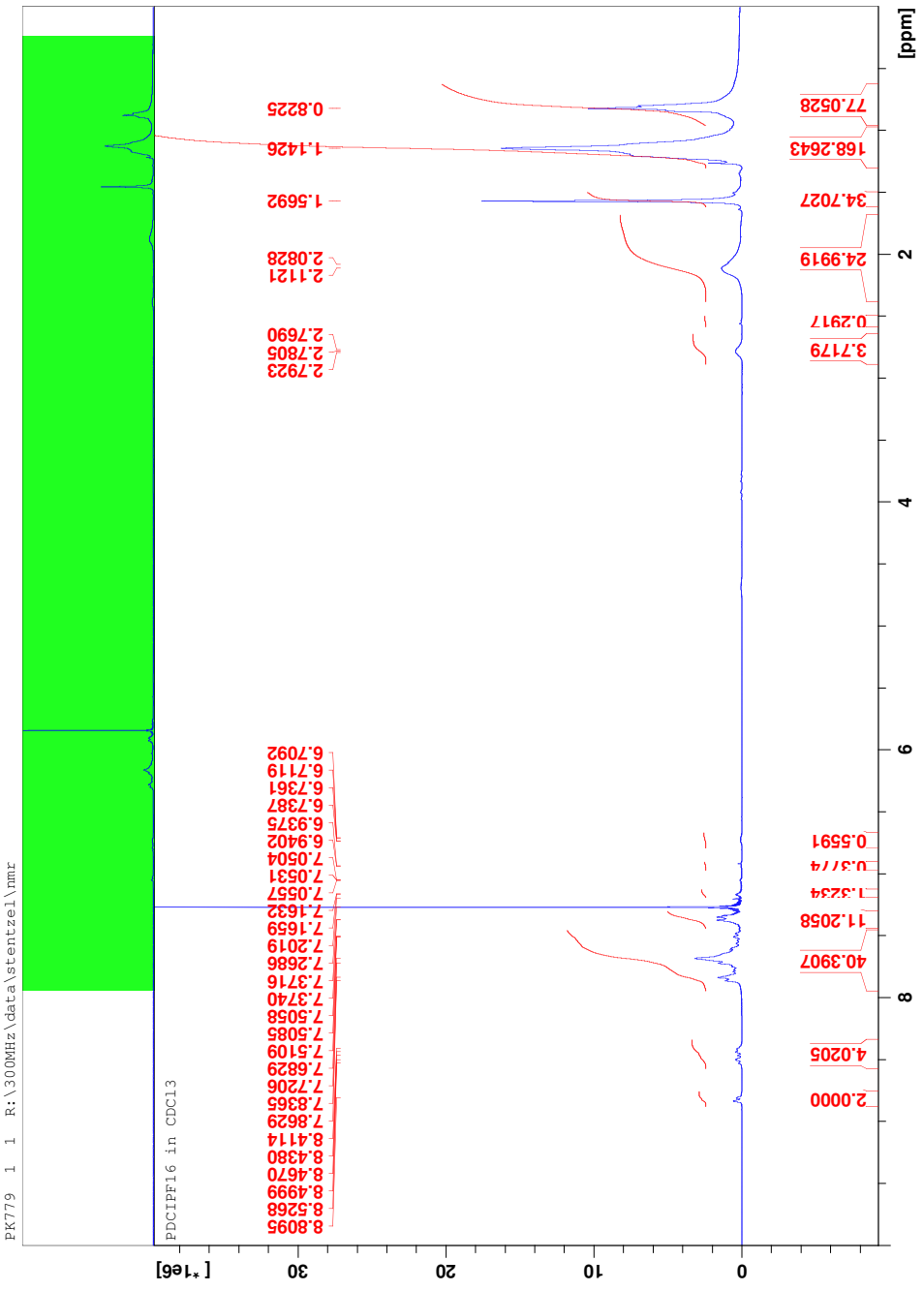
PK779 1 1 R:\300MHz\data\stentzel\nmr
PDCIPF16 in CDC13
8.8095
8.5268
8.4999
8.4670
8.4380
8.4114
7.8629
7.8365
7.7206
7.6829
7.5109
7.5085
7.5058
7.3740
7.3716
7.2686
7.2019
7.1659
7.1632
7.0557
7.0531
7.0504
6.9402
6.9375
6.7387
6.7361
6.7119
6.7092
2.7923
2.7805
2.7690
2.1121
2.0828
1.5692
1.1426
0.8225
0.5591
0.3774
1.3234
11.2058
40.3907
4.0205
2.0000
3.7179
0.2917
24.9919
34.7027
168.2643
77.0528
[ppm]
[*1e6]

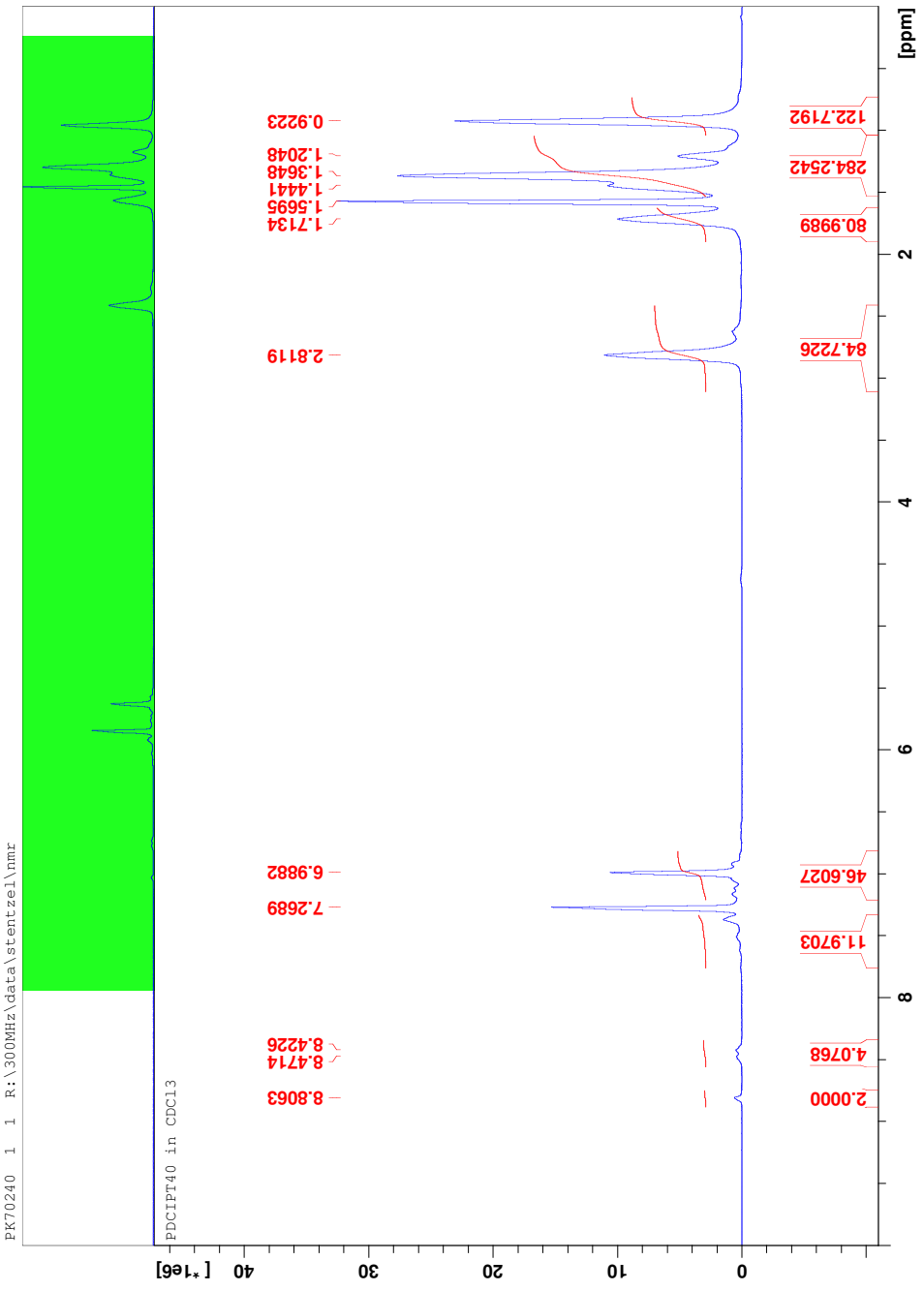
PK70240 1 1 R:\300MHz\data\stentzel\nmr
PDCIPT40 in CDC13
[*1e6]
40
30
20
10
0
[ppm]
8
6
4
2
8.8063
8.4714
8.4226
7.2689
6.9882
2.8119
1.7134
1.5695
1.4441
1.3648
1.2048
0.9223
2.0000
4.0768
11.9703
46.6027
84.7226
80.9989
284.2542
122.7192

LIST OF REFERENCES

Al-Mudhaffer, M. F.; Griggith, M. J.; Feron, K.; Nicolaidis, N. C.; Cooling, N. A.; Zhou, X.; Holdsworth, J.; Belcher, W. J.; Dastoor, P. C. The Origin of Performance Limitations in Miniemulsion Nanoparticulate Organic Photovoltaic Devices. *Sol. Energy Mater. Sol. Cells* **2018**, 175, 77-88.

Allison, L. K.; Andrew, T. L. A Wearable All-Fabric Thermoelectric Generator. *Adv. Mater. Technol.* **2019**, 1800615.

Almyahi, F.; Andersen, T. R.; Cooling, N.; Holmes, N. P.; Fahy, A.; Barr, M. G.; Kilcoyne, D.; Belcher, W.; Dastoor, P. C. Optimization, Characterization and Upscaling of Aqueous Solar Nanoparticle Inks for Organic Photovoltaics Using Low-Cost Donor:Acceptor Blend. *Org. Electron.* **2018**, 52, 71-78.

Amatore, C.; Jutand A.; Le Duc, G. Mechanistic Origin of Antagonist Effects of Usual Anionic Bases (OH^-, CO_3^{2-}) as Modulated by Their Countercations (Na^+, Cs^+, K^+) in Palladium-Catalyzed Suzuki-Miyaura Reactions. *Chem. Eur. J.* **2012**, 18, 6616-6625.

Amatore, C.; Jutand, A.; Duc, G. L. Kinetic Data for the Transmetalation/Reductive Elimination in Palladium-Catalyzed Suzuki-Miyaura Reactions: Unexpected Triple Role of Hydroxide Ions Used as Base. *Chem. Eur. J.* **2011**, 17, 2492-2503.

Amatore, C.; Le Duc, G.; Jutand, A. Mechanism of Palladium-Catalyzed Suzuki-Miyaura Reactions: Multiple and Antagonistic Roles of Anionic "Bases" and Their Countercations. *Chem. Eur. J.* **2013**, 19, 10082-10093.

Ansari, M. A.; Mohiuddin, S.; Kandemirli, F.; Malik, M. I. Synthesis Characterization of Poly(3-hexylthiophene): Improvement of Regioregularity and Energy Band Gap. *RSC Adv.* **2018**, 8, 8319-8328.

Aplan, M. P.; Gomez, E. D. Recent Developments in Chain-Growth Polymerizations of Conjugated Polymers. *Ind. Eng. Chem. Res.* **2017**, 56, 7888-7901.

Arias, A. C.; MacKenzie, J. D.; Stevenson, R.; Halls, J. J. M.; Inbasekaran, M.; Woo, E. P.; Richards, D.; Friend, R. H. Photovoltaic Performance and Morphology of Polyfluorene Blends: A Combined Microscopic and Photovoltaic Investigation. *Macromolecules* **2001**, 34, 6005-6013.

Baker, M. A.; Ayuso-Carrillo, J.; Koos, M. R. M.; Macmillan, S. N.; varni, A. J.; Gil, R. R.; Noonan, K. J. T. A Robust Nickel Catalyst with an Unsymmetrical Propyl-Bridged Diphosphine Ligand for Catalyst-Transfer Polymerization. *Polym. J.* **2019**,

Bang, J. H.; Suslick, K. S. Applications of Ultrasound to the Synthesis of Nanostructure Materials. *Adv. Mater.* **2010**, 22, 1039-1059.

Bässler, H. Charge Transport in Disordered Organic Photoconductors. *Phys. Stat. Sol.* **1993**, 175, 15-36.

Bässler, H. Charge Transport in Disordered Organic Photoconductors. *Phys. Stat. Sol.* **1993**, 175, 15.

Bässler, H.; Brandl, V.; Deussen, M.; Göbel, E. O.; Kersting, R.; Kurz, H.; Lemmer, U.; Mahrt, R. F.; Ochse, A. Excitation Dynamics in Conjugated Polymers. *Pure & Appl. Chem.* **1995**, 67, 377-385.

Bässler, H.; Schweitzer, B. Site-Selective Fluorescence Spectroscopy of Conjugated Polymers and Oligomers. *Acc. Chem. Res.* **1999**, 32, 173-182.

Beaupré, S.; Boudreault, P. T.; Leclerc, M. Solar-Energy Production and Energy-Efficient Lighting: Photovoltaic Devices and White-Light-Emitting Diodes Using Poly(2,7-fluorene), Poly(2,7-carbazole), and poly(2,7-dibenzosilole) Derivatives. *Adv. Mater*. **2010**, 22, E6-E27.

Becker, K.; Lupton, J. M. Efficient Light Harvesting in Dye-Endcapped Conjugated Polymers Probed by Single Molecule Spectroscopy. *J. Am. Chem. Soc.* **2006**, 128, 6468-6479.

Beers, K. L.; Gaynor, S. G.; Matyjaszewski, K.; Sheiko, S. S.; Möller, M. The Synthesis of Densely Grafted Copolymers by Atom Transfer Radical Polymerization. *Macromolecules* **1998**, 31, 9413-9415.

Bouffard, Swager, T. M. Fluorescent Conjugated Polymers That Incorporate Substituted 2,1,3-Benzooxadiazole and 2,1,3-Benzothiadiazole Units. *Macromolecules* **2008**, 41, 5559-5562.

Bryan, Z. J.; McNeil, A. J. Conjugated Polymer Synthesis via Catalyst-Transfer Polycondensation (CTP): Mechanism, Scope, and Applications. *Macromolecules* **2013**, 46, 8395-8405.

Bryan, Z. J.; McNeil, A. J. Controlled Synthesis of Fully π-Conjugated Donor–Acceptor Block Copolymers Using a Ni(II) Diimine Catalyst. *Macromolecules* **2015**, 48, 7385-7395.

Bryan, Z.; McNeil, A. J. Conjugated Polymer Synthesis via Catalyst-Transfer Polycondensation (CTP): Mechanism, Scope, and Applications. *Macromolecules* **2013**, 8395-8405.

Burnett, E. K.; Ai, Q.; Cherniawski, B. P.; Parkin, S. R.; Risko, C.; Briseno, A. L. Even-Odd Alkyl Chain-Length Alternation Regulates Oligothiophene Crystal Structure. *Chem. Mater.* **2019**, 31, 6900-6907.

Burroughes, J. H.; Bradley, D. D. C.; Brown, A. R.; Marks, R. N; Mackay, K; Friend, R. H.; Burns, P. L.; Holmes, A. B. Light-Emitting Diodes Based on Conjugated Polymers. *Nature* **1990**, 347, 539-541.

Butcher, J. A.; Chambers, J. Q.; Pagni, R. M. Synthesis of Highly Conducting Films of Derivatives of Polyacetylene, $(CH)_x$. *J. Am. Chem. Soc.* **1978**, 100, 1013-1015.

Byun, H. Y.; Chung, I. J.; Shim, H.-K.; Kim, C. Y. Optoelectronic and Photophysical Properties of Polyfluorene Blends as Side-Chain Length and Shape. *Macromolecules* **2004**, 37, 6945-6953.

Carrillo, J. A.; Ingleson, M. J.; Turner, M. L. Thienyl MIDA Boronate Esters as Highly Effective Monomers for Suzuki-Miyaura Polymerization Reactions. *Macromolecules* **2015**, 48, 979-986.

Carrillo, J. A.; Ingleson, M. J.; Turner, M. L. Thienyl MIDA Boronate Esters as Highly Effective Monomers for Suzuki-Miyaura Polymerization Reactions. *Macromolecules* **2014**, 48, 979-986.

Carrow, B. P.; Hartwig, J. F. Distinguishing Between Pathways for Transmetalation in Suzuki-Miyaura Reactions. *J. Am. Chem. Soc.* **2011**, 133, 2116-2119.

Chavez, C. A.; Choi, J.; Nesterov, E. E. One-Step Simple Preparation of Catalytic Initiators for Catalyst-Transfer Kumada Polymerization: Synthesis of Defect-Free Polythiophenes. *Macromolecules* **2014**, 47, 506-516.

Chen, S.; Liu, Y.; Qiu, W.; Sun, X.; Ma, Y.; Zhu, D. Oligothiophene-Functionalized Perylene Bisimide System: Synthesis, Characterization, and Electrochemical Polymerization Properties. *Chem. Mater.* **2005**, 17, 2208-2215.

Chen, S.; Slattum, P.; Wang, C.; Zang, L. Self-Assembly of Perylene Imide Molecules into 1D Nanostructure: Methods, Morphologies, and Applications. *Chem. Rev.* **2015**, 11967-11998.

Chen, Z.; Yan, L.; Rech, J. J.; Hu, J.; Zhang, Q.; You, W. Green-Solvent-Processed Conjugated Polymers for Organic Solar Cells: The Impact of Oligoethylene Glycol Side Chains. *ACS Appl. Polym. Mater.* **2019**, 1, 804-814.

Cherniawski, B. P.; Lopez, S. A.; Burnett, E. K.; Yavuz, I.; Zhang, I.; Parkin, S. R.; Houk, K. N.; Briseno, A. L. The Effect of Hexyl Side Chains on Molecular Conformations, Crystal Packing, and Charge Transport of Oligothiophenes. *J. Mater. Chem. C.* **2017**, 5, 582-588.

Cho, J.; Yu, S. H.; Chung, D. S. Environmentally Benign Fabrication Processes for High-Performance Polymeric Semiconductors. *J. Mater. Chem. C.* **2017**, 5, 2745-2757.

Coakley, K. M.; McGehee, M. D. Conjugated Polymer Photovoltaic Cells. *Chem. Mater.* **2004**, 16, 4533-542.

Colberts, F. J. M.; Wienk, M. M.; Janssen,m R. A. J. Aqueous Nanoparticle Polymer Solar Cells: Effects of Surfactant Concentration and Processing on Device Performance. *ACS Appl. Mater. Interfaces* **2017**, 9, 13380-13389.

Cornil, J.; Beljonne, D.; Calbert, J.-P.; Brèdas, J.-L. Interchain Interactions in Organic π-Conjugated Materials: Impact on Electronic Structure, Optical Response, and Charge Transport. *Adv. Mater.* **2001**, 13, 1053-1067.

Cox, P. A.; Leach, A. G.; Campbell, A. D.; Lloyd-Jones, G. C. Protodeboronation of Heteroaromatic, Vinyl and Cyclopropyl Boronic Acids: pH-Rate Profiles, Autocatalysis, and Disproportionation. *J. Am. Chem. Soc.* **2016**, 128, 9145-9157.

Cox, P. A.; Reid, M.; Leach, A. G.; Campbell, A. D.; King, E. J. Lloyd-Jones, G. C. Base-Catalyzed Aryl-$B(OH)_2$ Protodeboronation Revisited: From Concerted Proton Transfer to Liberation of a Transient Aryl Anion. *J. Am. Chem. Soc.* **2017**, 13156-13165.

Cullen, A. T.; Price, A. D. Digital Light Processing for the Fabrication of 3D Intrinsically Conductive Polymer Structure. *Synth. Met.* **2018**, 235, 34.

Eede, M.-P. V. D.; Winter, J. D.; Gerbaux, P.; Koeckelberghs, G. Controlled Polymerization of a Cyclopentadithiophene-Phenylene Alternating Copolymer. *Macromolecules* **2018**, 51, 9043-9051.

Eede, M.-P. V. D.; Winter, J. D.; Gerbaux, P.; Teyssandier, J.; Feyter, S. D.; Goethem, C. V.; Vankelecom, I. F. J.; Koeckelberghs, G. Controlled Synthesis and Supramolecular Organization of Conjugated Star-Shaped Polymers. *Macromolecules* **2018**, 51, 8689-8697.

Ego, C.; Marsitzky, D.; Becker, S.; Zhang, J.; Grimsdale, A. C.; Müllen, K.; MacKenzie, J. D.; Silva, C.; Friend, R. H. Attaching Perylene Dyes to Polyfluorene: Three Simple, Efficient Methods for Facile Color Tuning of Light-Emitting Polymers. *J. Am. Chem. Soc.* **2003**, 125, 437-443.

Faure, S.; Stern, C.; Guilard, R.; Harvey, P. D. Role of the Spacer in the Singlet-Singlet Energy Transfer Mechanism (Föster vs Dexter) in Cofacial Bisporphyrins. *J. Am. Chem. Soc.* **2004**, 126, 1253-1261.

Feng, C.; Li, Y.; Yang, D.; Hu, J.; Zhang, X.; Huang, X. Well-Defined Graft Copolymers: From Controlled Synthesis to Multipurpose Applications. *Chem. Soc. Rev.* **2011**, 40, 1282-1295.

Ferron, T.; Waldrip, M.; Pope, M.; Collins, B. A. Increased Charge Transfer State Separation via Reduced Mixed Phase Interface In Polymer Solar Cells. *J. Mater. Chem. A.* **2019**, 7, 4536-4545.

Fichou, D. Structural Order in Conjugated Oligothiophenes and Its Implications on Opto-Electronic Devices. *J. Mater. Chem.* **2000**, 10, 571-588.

Friend, R. H.; Gymer, R. W.; Holmes, A. B.; Burroughes J. H.; Marks, R. N.; Taliani, C.; Bradley, D. D. C.; Dos Santos, D. A.; Brédas, J. L.; Lögdlund, M.; Salaneck, W. R. Electroluminescence in conjugated polymers. *Nature* **1999**, 397, 121-128.

Fukumoto, H.; Nakajima, H.; Kojima, T.; Yamamoto, T. Preparation and Chemical Properties of π-Conjugated Polymers Containing Indigo Unit in the Main Chain. *Materials* **2014**, 7, 2030-2043.

Gärtner, S.; Christmann, M.; Sankaran, S.; Röhm, H.; Prinz, E.-M.; Penth, F.; Pütz, A.; Türeli, A. E.; Penth, B.; Baumstümmler, B.; Colsmann, A. Eco-Friendly Fabrication of 4% Efficient Organic Solar Cells from Surfactant-Free P3HT:ICBA Nanoparticle Dispersions. *Adv. Mater.* **2014**, 26, 6653-6657.

Gonzalez, J. A.; Ogba, O. M.; Morehouse, G. F.; Rosson, N.; Houk, K. N.; Leach, A. G.; Cheong, P. H.-Y.; Burke, M. D.; Lloyd-Jones, G. C. MIDA Boronates are Hydrolysed Fast and Slow by Two Different Mechanisms. *Nat. Chem.* **2016**, 8, 1067-1075.

Grisorio, R.; Suranna, G. P. Catalyst-Transfer Polymerization of Arylamines by the Buchwald-Hartwig Cross-Coupling. *Polym. Chem.* **2019**, 10, 1947-1955.

Grisorio, R.; Suranna, G. P. Intramolecular Catalyst-Transfer Polymerization of Conjugated Monomers: From Lessons Learned to Future Challenges. *Polym. Chem.* **2015**, 6, 7781-7795.

Grubbs, R. B.; Grubbs, R. H. 50th Anniversary Perspective: Living Polymerization-Emphasizing the Molecule in Macromolecules. *Macromolecules* **2017**, 6979-6997.

Guo, Z.; Zhang, X.; Wang, Y.; Li, Z. Supramolecular Self-Assembly of Perylene Bisimide Derivatives Assisted by Various Groups. *Langmuir* **2019**, 35, 342-358.

Hadjichristidis, N; Pitskalis, M; Pispas, S.; Iatrou, H. Polymers with Complex Architecture by Living Anionic Polymerization. *Chem. Rev.* **2001**, 101, 3747-3792.

Handa, N. V.; Mendoza, K. D.; Shirtcliff, L. D. Syntheses and Properties of 1,6 and 1,7 Perylene Diimides and Tetracarboxylic Dianhydrides. *Org. Lett.* **2011**, 17, 4724-4727.
He, W.; Patrick, B. O.; Kennepohl, P. Identifying the Missing Link in Catalyst-Transfer Polymerization. *Nat. Commun.* **2018**, 9, 3866.

Heeger, A. J. Nobel Lecture: Semiconducting and Metallic Polymers: The Fourth Generation of Polymeric Materials. *Rev. Mod. Phys.* **2001**, 73, 681.

Henson, Z. B.; Müllen, K.; Bazan, G. C. Design Strategies for Organic Semiconductors Beyond the Molecular Formula. *Nat. Chem.* **2012**, 699-704.

Herrera, M.; Abdul-Moqueet, M.; Mahmoud, M. A. Conjugated Polymer Nanoparticles Having Modified Band Gaps Assembled into Nano- and Micropatterned Organic Light-Emitting Diodes. *ACS Appl. Nano Mater.* **2019**, 2, 577-585.
Hirao, A.; Goseki, R.; Ishizone, T. Advances in Living Anionic Polymerization: From Functional Monomers, Polymerization Systems, to Macromolecular Architectures. *Macromolecules* **2014**, 47, 1883-1905

Holliday, S.; Li, Y.; Luscombe, C. K.; Recent Advances in High Performance Donor-Acceptor Polymers for Organic Photovoltaics. *Prog. Polym. Sci.* **2017**, 70, 34-51.

Howes, P.; Green, M.; Bowers, A.; Parker, D.; Varma, G.; Kallumadil, M.; Hughes, M.; Warley, A.; Brain, A.; Botnar, R. Magnetic Conjugated Polymer Nanoparticles as Bimodal Imaging Agents. *J. Am. Chem. Soc.* **2010**, 132, 9833-9842.

Hu, J.; Ku, K.; Shen, L.; Wu, Q.; He, G.; Wang, J.-Y.; Pei, J.; Xia, J.; Sfeir, M. Y. New Insights Into the Design of Conjugated Polymers for Intramolecular Singlet Fission. *Nat. Commun.* **2018**, 9, 2999.

Isz, S.; Weissbuch, I.; Kjaer, K.; Bouwman, W. G.; Als-Nielsen, J.; Palacin, S.; Ruaudel-Teixier, A.; Leiserowitz, L.; Lahav, M. Crystalline Mono- and Multilayer Self-Assemblies of Oligothiophene at the Air-Water Interface. *Chem. Eur. J.* **1997**, 3, 6.

Jagadesan, P.; Schanze, K. S. Poly(phenylene ethynylene) Conjugated Polyelectrolytes Synthesized via Chain-Growth Polymerization. *Macromolecules* **2019**, 52, 3845-3851.

Jager, E. W. H.; Inganäs, O.; Lundström, I. Microrobots for Micrometer-Size Objects in Aqueous Media: Potential Tools for Single-Cell Manipulation. *Science* **2000**, 288, 2335.

Jana. B.; Ghosh, A.; Patra, A. Photon Harvesting in Conjugated Polymer-Based Functional Nanoparticles. *J. Phys. Chem. Lett.* **2017**, 8, 4608-4620.

Jindal, A; Kotani, H.; Kushida, S.; Saeki, A.; Kojima, T.; Yamamoto, Y. Significant Enhancement of Hole Transport Ability in Conjugated Polymer/Fullerene Bulk Heterojunction Microspheres. *ACS Appl. Polym. Mater.* **2019**, 1, 118-123.

Junnila, S.; Houbenov, N.; Karatzas, A.; Hadjichristidis, N.; Hirao, A.; Iatrou, H.; Ikkala O. Side-Chain-Controlled Self-Assembly of Polystyrene-Polypeptide Miktoarm Star Copolymers. *Macromolecules* **2012**, 45, 2850-2856.

Kamigawara, T.; Sugita, H.; Mikami, K.; Ohta, Y.; Yokozawa, T. Intramolecular Transfer of Pd Catalyst on Carbon-Carbon Triple Bond and Nitrogen-Nitrogen Double Bond in Suzuki-Miyaura Coupling Reaction *Catalysis* **2017**, 7, 195.

Kasai, Y.; Tamai, Y.; Ohkita, H.; Benten, H.; Ito S. Ultrafast Singlet Fission in a Push-Pull Low-Bandgap Polymer Film. *J. Am. Chem. Soc.* **2015**, 15980-15983.

Kertesz, M.; Choi, C. H.; Yang, S. Conjugated Polymers and Aromaticity. *Chem. Rev.* **2009**, 105, 3448-3481.

Kim, N.-K.; Jang, S.-Y.; Pace, G.; Caironi, M.; Park, W.-T.; Khim, D.; Kim, J.; Kim, D.-Y.; Noh, Y.-Y. High-Performance Organic Field-Effect Transistors with Directionally Aligned Conjugated Polymer Film Deposited from Pre-Aggregated Solution. *Chem. Mater.* **2015**, 27, 8345-8353.

Kiriy, A.; Senkovskyy, V.; Sommer, M. Kumada Catalyst-Transfer Polycondensation: Mechanism, Opportunities, and Challenges. *Macromol. Rapid Commun.* **2011**,32, 1503-1517.
Konkolewicz, D.; Monteriro, M. J.; Perrier, S. Dendritic and Hyperbranched Polymers from Macromolecular Units: Elegant Approaches to the Synthesis of Functional Polymers. *Macromolecules* **2011**, 44, 7067-7087.

Kosaka, K.; Ohta, Y.; Yokozawa, T. Influence of the Boron Moiety and Water on Suzuki-Miyaura Catalyst-Transfer Condensation Polymerization. *Macromol. Rapid Commun.* **2015**, 36, 373-377.

Kosaka, K.; Uchida, T.; Mikami, K.; Ohta, Y.; Yokozawa, T. AmPhos Pd-Catalyzed Suzuki-Miyaura Catalyst-Transfer Condensation Polymerization: Narrower Dispersity by Mixing the Catalyst and Base Prior to Polymerization. *Macromolecules* **2018**, 51, 364-369.

Kuivila H. G.; Reuwer, J. F.; Mangravite, J. A. Electrophilic Displacement Reactions. *Can. J. Chem.* **1963**, 41, 3081-3090.

Landfester, K. Miniemulsion Polymerization and the Structure of Polymer and Hybrid Nanoparticles. *Angew. Chem. Int. Ed.* **2009**, 48, 4488-4507.

Lee, C.; Lee, S.; Kim, G.-U.; Lee, W.; Kim, B. Recent Advances, Design Guidelines, and Prospects of All-Polymer Solar Cells. *Chem. Rev.* **2019**, 119, 8028-8086.

Lee, J.-H.; Chen, C.-H.; Lee, P.-H.; Lin, H.-Y.; Leung, M.-K.; Chiu, T.-L.; Lin, C.-F. Blue Organic Light-Emitting Diodes: Current Status, Challenges, and Future Outlook. *J. Mater. Chem. C.* **2019**, 5874-5888.

Lee, S. J.; Lee, J. M.; Cheong, I. W.; Lee, H.; Kim, J. H. A Facile Route of Polythiophene Nanoparticles via Fe^{3+}-Catalyzed Oxidative Polymerization in Aqueous Medium. *J. Polym. Sci. Part A: Polym. Chem.* **2008**, 46, 2097-2108.

Lee, S. M.; Park, K. H.; Jung. S.; Park. H.; Yang, C. Stepwise heating in Stille Polycondensation Toward No Batch-To-Batch Variations in Polymer Solar Cell Performance. *Nat. Commun*. **2018**, 9, 1867.

Leone, A. K.; McNeil, A. J. Matchmaking in Catalyst-Transfer Polycondensation: Optimizing Catalysts based on Mechanistic Insight. *Acc. Chem. Res.* **2016**, 49, 2822-2831.

Leone, A. K.; Mueller, E. A.; McNeil, A. J. The History of Palladium-Catalyzed Cross-Coupling Should Inspire the Future of Catalyst-Transfer Polymerization. *J. Am. Chem. Soc.* **2018**, 140, 15126-15139.

Leone, A. K.; Souther, K. D.; Vitek, A. K.; LaPointe, A. M.; Coates, G. W.; Zimmerman, P. M.; McNeil, A. J. Mechanistic Insight into Thiophene Catalyst-Transfer Polymerization Mediated by Nickel Diimine Catalsyt. *Macromolecules* **2017**, 9121-9127.

Levitsky, I. A.; Kim, J.; Swager, T. M. Energy Migration in a Poly(phenylene ethynylene): Determination of Interpolymer Transport in Anisotropic Langmuir-Blodgett Films. *J. Am. Chem. Soc.* **1999**, 121, 1466-1472.

Li-Destri, G.; Tuccitto, N.; Livio, P. A.; Messina, G. M. L.; Pithan, L.; Marletta, G. Energy-Sustained Reversible Nanoscale Order and Conductivity Increase in Polymer Thin Films. *Polymer* **2018**, 153, 344-353.

Li, S.; Ye, L.; Zhao, W.; Yan, H.; Yang, B.; Liu, D.; Li, W.; Ade, H.; Hou, J. A Wide Band Gap Polymer with a Deep Highest Occupied Molecular Orbital Level Enables 14.2% Efficiency in Polymer Solar Cells. *J. Am. Chem. Soc.* **2018**, 140, 7159-7167.

Li, Z.; Gelbaum, C.; Campbell, Z. S.; Gould, P. C.; Fisk, J. S.; Holden, B.; Jaganathan, A.; Whiteker, G. T.; Pollet, P.; Liotta, C. L. Pd-Catalyzed Suzuki Coupling Reactions of Aryl Halides Containing Basic Nitrogen Centers with Aryl Boronic Acids in Water in the Absence of Added Base. *New J. Chem.* **2017**, 41, 15420-15432.

Li, Z.; Gelbaum, C.; Fisk, J. S.; Holden, B.; Jaganathan, A.; Whiteker, G. T.; Pollet, P.; Liotta, C. L. Aqueous Suzuki Coupling Reactions of Basic Nitrogen-Containing Substrates in the Absence of Added Base and Ligand: Observation of High Yields under Acidic Conditions. *J. Org. Chem.* **2016**, 81, 8520-8529.

Liang, Y.; Xu, Z.; Xia, J.; Tsai, S.-T.; Wu, Y.; Li, G.; Ray, C.; Yu, L. For the Bright Future-Bulk Heterojunction Polymer Solar Cells with Power Conversion Efficiency of 7.4%. *Adv. Mater.* **2010**, 22, E135-E138.

Liang, Z.; Zhang, Y.; Souri, M.; Luo, X.; Boehm, A. M.; Li, R.; Zhang, Y.; Wang, R.; Kim, D.-Y.; Mei, J.; Marder, S. R.; Graham, K. R. Influence of Dopant Size and Electron Affinity on the Electrical Conductivity and Thermoelectric Properties of a Series of Conjugated Polymers. *J. Mater. Chem. A.* **2018**, 6, 16495-16505.

Liao, Y.; Wang, H.; Zhu, M.; Thomas, A. Efficient Supercapacitor Energy Storage Using Conjugated Microporous Polymer Networks Synthesized from Buchwald-Hartwig Coupling. *Adv. Mater.* **2018**, 30, 1705710.

Lin, J.; Liu, B.; Yu, M.; Wang, X.; Lin, Z.; Zhang, X.; Sun, C.; Cabanillas-Gonzalez, J.; Xie, L.; Liu, F.; Ou, C.; Bai, L.; Han, Y.; Xu, M.; Zhu, W.; Smith, T. A.; Stavrinou, P. N.; Bradley D. D. C.; Huang, W. Ultrastable Supramolecular Self-Encapsulated Wide-Bandgap Conjugated Polymers for Large-Area and Flexible Electroluminescent Devices. *Adv. Mater.* **2019**, 1804811.

London, A. E.; Chen, H.; Sabuj, M. A.; Tropp, J.; Saghayezhian, M.; Eedugurala, N.; Zhang, B. A.; Liu, Y.; Gu, X.; Wong, B. M.; Rai, N.; Bowman, M. K.; Azoulay, J. D. A High-Spin Ground-State Donor-Acceptor Conjugated Polymer. *Sci. Adv.* **2019**, 5, eaav2336.

London, A. E.; Chen, H.; Sabuj, M. A.; Tropp, J.; Saghayezhian, M.; Eedugurala, N.; Zhang, B. A.; Liu, Y.; Gu, X.; Wong, B. M.; Rai, N.; Bowman, M. K.; Azoulay, J. D. A High-Spin Ground-State Donor-Acceptor Conjugated Polymer. *Sci. Adv.* **2019**, 5:eaav2336.

Love, B. E.; Jones, E. G. The Use of Salicylaldehyde Phenylhydrazone as an Indicator for Titration of Organometallic Reagents. *J. Org. Chem.* **1999**, 64, 3755-3756.

Lu, L.; Zheng, T.; Wu, Q.; Schneider, A. M.; Zhao, D.; Yu, L. Recent Advances in Bulk Heterojunction Polymer Solar Cells. *Chem*. *Rev.* **2015**, 115-12666-12731.

Lutz, J. P.; Hannigan, M. D.; McNeil, A. J. Polymers Synthesized via Catalyst-Transfer and Their Applications. *Coord. Chem. Rev.* **2018**, 376, 225-247.

MacDiarmid, A. G. Nobel Lecture: "Synthetic Metals": A Novel Role for Organic Polymers. *Rev. Mod. Phys.* **2001**, 73, 701.

Marks, M.; Holmes, N. P.; Sharma, A.; Pan, X.; Chowdhury, R.; Barr, M. G.; Fenn, C.; Griffith, M. J.; Feron, K.; Kilcoyne, A. L. D.; Lewis, D. A.; Andersson, M. R.; Belcher, W. J.; Dastoor, P. C. Building Intermixed Donor-Acceptor Architectures for Water-Processable Organic Photovoltaics. *Phys. Chem. Chem. Phys.* **2019**, 21, 5705-5715.

Marty, R. et al. Hierarchically Structured Microfibers of "Single Stack" Perylene Bisimide and Quaterthiophene Nanowires. *ACS Nano* **2013**, 7, 8498-8508.

McQuade, D. T.; Pullen, A. E.; Swager, T. M. Conjugated Polymer-Based Chemical Sensors. *Chem. Rev.* **2000**, 100, 2537-2574.

Menon, A.; Dong, H.; Niazimbetova, Z. I.; Rothberg, L. J.; Galvin, M. E. Polydispersity Effects on Conjugated Polymer Light-Emitting Diodes. *Chem. Mater.* **2002**, 14, 3668-3675.

Mo, Z.; Lee, K. B.; Kobayashi, M.; Heeger, A. J.; Wudl, F. X-ray Scattering from Poly(thiophene): Crystallinity and Crystallographic Structure. *Macromolecules* **1985**, 18, 1972-1977.

Murphy, C. B.; Zhang, Y.; Troxler, T.; Ferry, V.; Martin, J. J.; Jones, W. E. Probing Förster and Dexter Energy-Transfer Mechanisms in Fluorescent Conjugated Polymer Chemosensors. *J. Phys. Chem. B* **2004**, 108, 1537-1543.

Nguyen, T.-Q.; Doan, V.; Schwartz, B. J. Conjugated Polymer Aggregates in Solution: Control of Interchain Interactions. *J. Chem. Phys.* **1999**, 110, 4068-4078.

Nguyen, T.-Q.; Wu, J.; Doan, V.; Schwartz, B. J.; Tolbert, S. H. Control of Energy Transfer in Oriented Conjugated Polymer-Mesoporous Silica Composites. *Science* **2000**, 288, 652-656.

Nojima, M.; Kamigawara, T.; Ohta, Y.; Yokozawa, T. Catalyst-Transfer Suzuki-Miyaura Condensation Polymerization of Stilbene Monomer: Different Polymerization Behavior

Depending on Halide and Aryl Group of Aryl Group of ArPd(^{t}Bu$_3$P)X Initiator *J. Polym. Sci. A.* **2019**, 57, 297-304.

Ozel, I. O.; Ozel, T.; Demir, H. V.; Tuncel, D. Non-Radiative Resonance Energy Transfer in Bi-Polymer Nanoparticles of Fluorescent Conjugated Polymers. *Opt. Express* **2010**, 670-672.

Park, E.-J.; Erdem, T.; Ibrahimova, V.; Nizamoglu, S.; Demir, H. V.; Tuncel, D. White-Emitting Conjugated Polymer Nanoparticles With Cross-Linked Shell for Mechanical Stability and Controllable Photomertric Properties in Color-Conversion LED Applications. *ACS Nano* **2011**, 4, 2483-2492.

Parrenin, L.; Laurans, G.; Pavlopoulou, E.; Fleury, G.; Pecastaings, G.; Brochon, C.; Vignau, L.; Hadziioannou, G.; Cloutet, E. Photoactive Donor-Acceptor Composite Nanoparticles Dispersed in Water. *Langmuir* **2017**, 33, 1507-1515.

Patil, A. O.; Wudl, I. F.; Heeger, A. J. Water-Soluble Conducting Polymers. *J. Am. Chem. Soc.* **1987**, 109, 1858-1859.

Pecher, J.; Mecking, S. Nanoparticles of Conjugated Polymers. *Chem. Rev.* **2010**, 110, 6260-6279.

Pinder, K. L. Activity of Water in Solution with Tetrahydrofuran. *J. Chem. Eng. Data* **1973**, 18, 275-277.

Ramanan, C.; Smeigh, A. L.; Anthony, J. E.; Marks, T. J.; Wasielewski, M. R. Competition between Singlet Fission and Charge Separation in Solution-Processed Blend Films of 6,13-Bis(triisopropylsilylethynyl)pentacene with Sterically-Encumbered Perylene-3,4:9,10-bis(dicarboximide)s. *J. Am. Chem. Soc.* **2012**, 134, 386-397.

Rana, S.; Elci, S. G.; Mout, R.; Singla, A. K.; Yazdani, M.; Bender, M.; Bajaj, A.; Saha, K.; Bunz, U. H. F.; Jirik, F. R.; Rotello, V. M. Ratiometric Array of Conjugated Polymers-Fluorescent Protein Provides a Robust Mammalian Cell Sensor. *J. Am. Chem. Soc.* **2016**, 138, 4522-4529.

Remmers, M.; Müller, B.; Martin, K.; Räder, H.-J. Poly(*p*-phenylene)s: Synthesis, Optical Properties, and Quantitative Analysis with HPLC and MALDI-TOF Mass Spectrometry. *Macromolecules* **1999**, 32, 1073-1079.

Rentsch, S.; Yang, J. P., Paa, W.; Birckner, E.; Schiedt, J.; Weinkauf, R. Size Dependence of Triplet and Singlet States of α-Oligothiophenes. *Phys. Chem. Chem. Phys.* **1999**, 1, 1707-1714.

Sahoo, D et al. Hierarchical Self-Organization of Perylene Bisimides into Supramolecular Spheres and Periodic Arrays Thereof. *J. Am. Chem. Soc.* **2016**, 138, 14798-14807.

Scherf. U.; List, E. J. Semiconducting Polyfluorenes – Towards Reliable Structure-Property Relationships. *Adv. Mater.* **2002**, 14, 477-487.

Schon, T. B.; McAllister, B. T.; Li, P.-F.; Seferos, D. S.; The Rise of Organic Electrode Materials for Energy Storage. *Chem. Soc. Rev.* **2016**, 45, 6345-6404.

Sengupta, S.; Dubey, R. K.; Hoek, R.-W. M.; van Eeden, S.-P. P.; Gunbas, D. D.; Grozema, F. C.; Sudholter, E.-J. R.; Jager, W. F. Synthesis of Regioisomerically Pure 1,7-Dibromoperylene-3,4,9,10-tetracarboxylic Acid Derivatives. *J. Org. Chem.* **2014**, 79, 6655-6662.

Seo, K.-B.; Lee, I. H.; Lee, J.; Choi, I.; Choi. T.-L A Rational Design of Highly Controlled Suzuki-Miyaura Catalyst-Transfer Polycondensation for Precision Synthesis of Polythiophenes and Their Block Copolymers: Marriage of Palladacycle Precatalysts with MIDA-Boronates. *J. Am. Chem. Soc.* **2018**, 140, 4335-4343.

Sheina, E. E.; Liu, J. S.; Iovu, M. C.; Laird, D. W.; McCullough, R. D. Chain-Growth Mechanism for Regioregular Nickel-Initiated Cross-Coupling Polymerizations. *Macromolecules* **2004**, 37, 3526-3528.

Shirakawa, H. Nobel Lecture: The Discovery of Polyacetylene Film-The Dawning of an Era of Conducting Polymers. *Rev. Mod. Phys.* **2001**, 73, 713.

Shirakawa, H.; Louis, E. J.; MacDiarmid, A. G.; Chiang, C. K.; Heeger, A. J. Synthesis of Electrically Conducting Organic Polymers: Halogen Derivatives of Polyacetylene, $(CH)_x$. *J. Chem. Soc., Chem. Commun.* **1977**, 578-580.

Shirakawa, H.; Louis, E. J.; Park, Y. W.; Heeger, A. J. Electrical Conductivity in Doped Polyacetylene. *Phys. Rev. Lett.* **1978**, 40, 1472.

Smith, M. B.; Michi, J. Singlet Fission. *Chem. Rev.* **2010**, 110, 6891-6939.

Steverlynck, J.; De Cattelle, A.; De Winter, J.; Gerbaux, P.; Koeckelberghs, G. Energy Transfer in Poly(3-hexylthiophene)-*g*-Polyfluorene graft copolymers. *J. Polym. Sci. Part A Polym. Chem.* **2016**, 54, 1252-1258.

Sui, A.; Shi, X.; Tian, H.; Gend, Y.; Wang. Suzuki-Miyaura Catalyst-Transfer Polycondensation with $Pd(IPr)(OAc)_2$ as the catalyst for the controlled synthesis of polyfluorenes and polythiophenes. *Polym. Chem.* **2014**, 5, 7072-7080.

Sun, B.; Sun, M.-J.; Gu, Z.; Shen, Q.-D.; Jiang, S.-J.; Xu, Y.; Wang, Y. Conjugated Polymer Fluorescence Probe for Intracellular Imaging of Magnetic Nanoparticles. *Macromolecules* **2010**, 43, 10348-10354.

Suslick, K. S. Sonochemistry. *Science* **1990**, 247, 1439-1445.

Suslick, K. S.; Hyeon, T.; Fang, M. Nanostructured Materials Generated by High-Intensity Ultrasound: Sonochemical Synthesis and Catalytic Studies. *Chem. Mater.* **1996**, 8, 2172-2179.

Swager, T. M. 50th Anniversary Perspective: Conducting/Semiconducting Conjugated Polymers. A Personal Perspective on the Past and the Future. *Macromolecules* **2017**, 50, 4867-4886.

Swager, T. M.; Gil, C. J.; Wrighton, M. S. Fluorescence Studies of Poly(*p*-phenyleneethynlene)s: The Effect of Anthracene Substitution. *J. Phys. Chem.* **1995**, 99, 4886-4893.

Tang, S.-J.; Liu, Z.; Qian, Y.-J.; Shi, K.; Sun. Y.; Wu, C.; Gong, Q.; Xiao, Y.-F. A Tunable Optofluidic Microlaser in a Photostable Conjugated Polymer *Adv. Mater.* **2018**, 30, 1804556.

Theander, M.; Inganäs, O. Photophysics of Substituted Polythiophenes *J. Phys. Chem. B.* **1999**, 103, 7771-7780.

Thienpoint, H.; Rikken, G. L. J. A.; Meijer, E. W. Saturation of the Hyperpolarizability of Oligothiophenes *Phys. Rev. Lett.* **1990**, 65, 2141-2144.

Tretiak, S.; Saxena, A.; Martin, R. L. Bishop, A. R. Interchain Electronic Excitations in Poly(phenylenevinylene) (PPV) Aggregates. *J. Phys. Chem. B* **2000**, 104, 7029-7037.

Tuncel, D.; Demir, H. V. Conjugated Polymer Nanoparticles. *Nanoscale* **2010**, 2, 484-494.

Uenishi, J.-C.; Beau, J.-M.; Armstrong, R. W.; Kishi, Y. Dramatic Rate Enhancement of Suzuki Diene Synthesis: Its Application to Palytoxin Synthesis. *J. Am. Chem. Soc.* **1987**, 109, 4756-4758.

Vazaios, A.; Lohse, D. J.; Hadjichristidis, N. Linear and Star Block Copolymers of Styrenic Macromonomers by Anionic Polymerization. *Macromolecules* **2005**, 38, 5468-5474.

Verheyen, L.; Janssens, K.; Marinelli, M.; Salatelli, E.; Koeckelberghs, G. Rational Design of Poly(fluorene)-*b*-poly(thiophene) Block Copolymers to Obtain a Unique Aggregation Behavior. *Macromolecules* **2019**, 52, 6578-6584.

Verheyen, L.; Leysen, P.; Eede, M.-P. V. D.; Ceunen, W.; Hardeman, T.; Koeckelberghs, G. Advances in the Controlled Polymerization of Conjugated Polymers. *Polymer* **2017**, 108, 521-546.

Vohra, V. Can Polymer Solar Cells Open the Path to Sustainable and Efficient Photovoltaic Windows Fabrication? *Chem. Rec.* **2019**, 19, 1166-1178.

Wang, C.-H.; Nesterov, E. E. Amplifying Fluorescent Conjugated Polymer Sensor for Singlet Oxygen Detection. *Chem. Commun.* **2019**, 55, 8955-8958.

Wasserberg, D.; Marsal, P.; Meskers, S. C. J.; Janssen, R. A. J.; Beljonne, D. Phosphorescence and Triplet State Energy of Oligothiophenes. *J. Phys. Chem. B* **2005**, 109, 4410-4415.

Wilot, P.; Govaerts, S.; Koeckelberghs, G. The Controlled Polymerization of Poly(cyclopentadithiophenes)s and Their All-Conjugated Block Copolymers *Macromolecules* **2013**, 46, 8888-8895.

Wu, C.; Szymanski, C.; McNeill, J. Preparation and Encapsulation of Highly Fluorescent Conjugated Polymer Nanoparticles. *Langmuir* **2006**, 22, 2956-2960.

Wu, C.; Zheng, Y.; Szymanski, C.; McNeill, J. Energy Transfer in a Nanoscale Multichromophoric System: Fluorescent Dye-Doped Conjugated Polymer Nanoparticles. *J. Phys. Chem. C* **2008**, 112, 1772-1781.

Würthner, F.; Stepanenko, V.; Chen, Z.; Saha-Moller, C. R.; Kochner, N.; Stalke, D. Preparation and characterization of regioisomerically pure 1,7-disubstituted perylene bisimide dyes. *J. Org. Chem.* **2004**, 69, 7933-7939.

Xi, Y.; Li, D. S.; Newbloom, G. M.; Tatum, W. K.; O'Donnell, M.; Luscombe, C. K.; Pozzo, L. D. Sonocrystallization of Conjugated Polymers with Ultrasound Fields. *Soft Matter* **2018**, 4, 4963-4976.

Xia, J.; Sanders, S. N.; Cheng, W.; Low, J. Z.; Liu, J.; Campos, L. M.; Sun, T. Singlet Fission: Progress and Prospects in Solar Cells. *Adv. Mater.* **2017**, 29, 1601652.

Xie, C.; Heumüller, T.; Gruber, W.; Tang, X.; Classen, A.; Schuldes, I.; Bidwell, M.; Späth, A.; Fink, R.; Unruh, T.; McCulloch, I.; Li, N.; Brabec, C. J. Overcoming Efficiency and Stability Limits in Water-Processing Nanoparticular Organic Photovoltaics by Minimizing Microstructure Defects. *Nat. Commun.* **2018**, 5335.

Xie, J.; Gu, P.; Zhang, Q. Nanostructured Conjugated Polymers: Toward High-Performance Organic Electrodes for Rechargeable Batteries. *ACS Energy Lett.* **2017**, 2, 1985-1996.

Xiong, S.; Hu. L.; Hu. L.; Sun, L.; Qin, F.; Liu, X.; Fahlman, M.; Zhou, Y. 12.5% Flexible Nonfullerene Solar Cells by Passivating the Chemical Interaction Between the Active Layer and Polymer Interfacial Layer. *Adv. Mater.* **2019**, 31, 1806616.

Xu, H.; Zeiger, B. W.; Suslick, K. S. Sonochemical Synthesis of Nanomaterials. *Chem. Soc. Rev.* **2013**, 42, 2555.

Xu, S.; Wang, G.; Biswal, B. P.; Addicoat, M.; Paasch, S.; Sheng, W.; Zhuang, X.; Brunner, E.; Heine, T.; Berger, R.; Feng, X. A Nitrogen-Rich 2D sp^2-Carbon-Linked Conjugated Polymer Framework as a High-Performance Cathode for Lithium-Ion Batteries. *Angew. Chem. Int. Ed.* **2019**, 58, 849-853.

Yan, M. Y.; Rothberg, L. J.; Papadimitrakopoulos, F.; Galvin, M. E.; Miller, T. M. Defect Quenching of Conjugated Polymer Luminescence. *Phys. Rev. Lett.* **1994**, 73, 744-747.

Yan, M.; Rothberg, L. J.; Kwock, E. W.; Miller, T. M. Interchain Excitations in Conjugated Polymers. *Phys. Rev. Lett.* **1995**, 75, 1992-1995.

Yan, T.; Song, W.; Huang, J.; Peng, R.; Huang, L.; Ge, Z. 16.67% Rigid and 14.06% Flexible Organic Solar Cells Enabled by Ternary Heterojunction Strategy. *Adv. Mater.* **2019**, 1902210.

Yokoyama, A.; Miyakoshi, R.; Yokozawa, T. Chain-Growth Polymerization for Poly(3-hexylthiophene) with a Defined Molecular Weight and a Low Polydispersity. *Macromolecules* **2004**, 37, 1169-1171.

Yokoyama, A.; Suzuki, H.; Kubota, Y.; Ohuchi, K.; Higashimura, H.; Yokozawa. Chain-Growth Polymerization for the Synthesis of Polyfluorene via Suzuki-Miyaura Coupling Reaction from an Externally Added Initiator Unit. *J. Am. Chem. Soc.* **2007**, 129, 7236-7237.

Yokozawa, T.; Harada, N.; Sugita, H.; Ohta, Y. Intramolecular Catalyst Transfer on a Variety of Functional Groups Between Benzene Rings in a Suzuki-Miyaura Coupling Reaction. *Chem. Eur. J.* **2019**, 25, 10059-10062.

Yokozawa, T.; Kohno, H.; Ohta, Y.; Yokoyama, A. Catalyst-Transfer Suzuki-Miyaura Coupling Polymerization for Precision Synthesis of Poly(*p*-phenylene). *Macromolecules* **2010**, 43, 7095-7100.

Yokozawa, T.; Ohta, Y. Scope of Controlled Synthesis via Chain-Growth Condensation Polymerization: From Aromatic Polyamides to π-Conjugated Polymers. *Chem. Commun.* **2013**, 49, 8281-8310.

Yokozawa, T.; Ohta, Y. Transformation of Step-Growth Polymerization into Living Chain-Growth Polymerization. *Chem. Rev.* **2016**, 116, 1950-1968.

Yokozawa, Y.; Yokoyama, A. Chain-Growth Condensation Polymerization for the Synthesis of Well-Defined Condensation Polymers and π-Conjugated Polymers. *Chem. Rev.* **2009**, 109, 5595-5619.

Yumusak, C.; Sariciftci, N. S. Organic Electrochemical Light-Emitting Field Effect Transistors. *Appl. Phys. Lett.* **2010**, 97, 033302.

Zhang, H.-H.; Hu, Q.-S.; Hong, K. Accessing Conjugated Polymers with Precisely Controlled Heterobisfunctional Chain Ends via Post-Polymerization Modification of the OTf Group and Controlled Pd(0)/*t*-Bu_3P-Catalyzed Suzuki-Cross-Coupling Polymerization. *Chem. Commun.* **2015**, 51, 14869-14872.

Zhang, H.-H.; Ma, C.; Bonnesen, P. V.; Zhu, J.; Sumpter, B. G.; Carrillo, J.-M. Y.; Yin, P.; Wang, Y.; Li, A.-P.; Hong, K. Helical Poly(5-alkyl-2,3-thiophenes)s: Controlled Synthesis and Structure Characterization *Macromolecules* **2016**, 49, 4691-4698.

Zhang, H.-H.; Xing, C.-H.; Hu, Q.-H. Controlled Pd(0)/*t*-Bu_3-P-Catalyzed Suzuki Cross-Coupling Polymerization of AB-Type Monomers with PhPd(*t*-Bu_3P)I or $Pd_2(dba)_3$/*t*-Bu_3-P/ArI as the Initiator. *J. Am. Chem. Soc.* **2012**, 134, 13156-13159.

Zhao, C.; Nagura, K.; Takeuchi, M; Sugiyasu, K. Twisting Poly(3-substituted thiophene)s: Cyclopolymerization of Gemini Thiophene Monomers Through Catalyst-Transfer Polycondensation. *Polym. J.* **2017**, 49, 133-139.

Zhou, X.; Belcher, W.; Dastoor, P. Solar Paint: From Synthesis to Printing. *Polymers* **2014**, 6, 2832-2844.

Zotti, G.; Schiavon, G.; Zecchin, S.; Morin, J.-F.; Leclerc, M. Electrochemical, Conductive, and Magnetic Properties of 2,7-Carbazole-Based Conjugated Polymers. *Macromolecules* **2002**, 35, 2122-2128.

VITA

Peter Kei was born in 1988 in Hong Kong. He moved to the U.S. in 1996 and grew up in Quincy, MA. After graduating from North Quincy High School, he obtained his Associates in Science Degree at Quincy College. In 2010, he enrolled in Bridgewater State University as a Biochemistry major. There, he began his research career in the laboratory of Prof. Stephen A. Waratuke, conducting multistep synthesis of asymmetric carbamate ligands and investigated titanium catalyzed hydroamination reactions using them. After graduating with a Bachelor of Science, Peter moved to Baton Rouge in 2014 to join the laboratory of Prof. Evgueni Nesterov. Soon after, Peter received an Honorable Mention by the National Science Foundation Graduate Research Fellowship Program. He also received U.S. Department of Energy Office of Science Graduate Student Research Award, which supported his studies at Oak Ridge National Laboratory in 2017. In 2018, Peter moved along with the laboratory of Prof. Evgueni Nesterov to Northern Illinois University. His research contributions include development of controlled polymerizations for the preparation of well-defined conjugated polymer architectures. Peter is a candidate for the Doctor of Philosophy in Chemistry. His dissertation is entitled: “Hierarchical Conjugated Polymer Systems Prepared by Controlled Chain-Growth Polymerization”.